1121

TRANSPORTATION RESEARCH RECORD

Effects of Temperature and Water on Pavement Performance

TRANSPORTATION RESEARCH BOARD
NATIONAL RESEARCH COUNCIL

Transportation Research Record 1121
Price $13.00
Editor: Elizabeth W. Kaplan
Typesetter: Joan G. Zubal

mode
1 highway transportation

subject areas
24 pavement design and performance
34 maintenance

Transportation Research Board publications are available by ordering directly from TRB. They may also be obtained on a regular basis through organizational or individual affiliation with TRB; affiliates or library subscribers are eligible for substantial discounts. For further information, write to the Transportation Research Board, National Research Council, 2101 Constitution Avenue, N.W., Washington, D.C. 20418.

Printed in the United States of America

Library of Congress Cataloging-in-Publication Data
National Research Council. Transportation Research Board.

Effects of temperature and water on pavement performance.

p. cm.—(Transportation research record, ISSN 0361-1981 ; 1121)
Reports prepared for the 66th Annual Meeting of the Transportation Research Board.
ISBN 0-309-04501-0
1. Pavements—Performance—Congresses. I. National Research Council (U.S.). Transportation Research Board. Meeting (66th : 1987 : Washington, D.C.) II. Series.
TE7.H5 no. 1121
[TE250]
380.5 s—dc 19
[625.28] 87-34964
CIP

Sponsorship of Transportation Research Record 1121

GROUP 2—DESIGN AND CONSTRUCTION OF TRANSPORTATION FACILITIES
David S. Gedney, Harland Bartholomew & Associates, chairman

Pavement Management Section
R. G. Hicks, Oregon State University, chairman

Committee on Strength and Deformation Characteristics of Pavement Sections
J. Brent Rauhut, Brent Rauhut Engineering, Inc., chairman
Joseph H. Amend III, Gilbert Y. Baladi, Richard D. Barksdale, Stephen F. Brown, Albert J. Bush III, George R. Cochran, Billy G. Connor, Amir N. Hanna, R. G. Hicks, Ignat V. Kalcheff, William J. Kenis, Thomas W. Kennedy, Erland Lukanen, Robert L. Lytton, Michael S. Mamlouk, Edwin C. Novak, Jr., Lutfi Raad, Quentin L. Robnett, Byron E. Ruth, Gary Wayne Sharpe, James F. Shook, Roger E. Smith, R. N. Stubstad, Marshall R. Thompson, Ulian I. Tufektchiev, Thomas D. White

Soil Mechanics Section
Raymond A. Forsyth, California Department of Transportation, chairman

Committee on Subsurface Drainage
Gary L. Hoffman, Pennsylvania Department of Transportation, chairman
Robin Bresley, George R. Cochran, Barry J. Dempsey, Gregory A. Dolson, Ervin L. Dukatz, Jr., Wilbur M. Haas, Donald J. Janssen, Larry Lockett, Donald C. Long, Robert H. Manz, Vernon J. Marks, Charles D. Mills, Lyle K. Moulton, Edwin C. Novak, Jr., Willard G. Puffer, Georges Raimbault, Hallas H. Ridgeway, Emile A. Samara, L. David Suits, William D. Trolinger, Walter C. Waidelich, David C. Wyant, Thomas F. Zimmie

Geology and Properties of Earth Materials Section
Wilbur M. Haas, Michigan Technological University, chairman

Committee on Environmental Factors Except Frost
Malcolm L. Steinberg, Texas State Department of Highways and Public Transportation, chairman
S. S. Bandyopadhyay, Warren T. Bennett, Michael L. Bunting, Fu Hua Chen, Barry J. Dempsey, Donald G. Fohs, Donald J. Janssen, Badru M. Kiggundu, Amos Komornik, C. William Lovell, Robert L. Lytton, Said Ossama Mazen, R. Gordon McKeen, James B. Nevels, Jr., Zvi Ofer, Thomas M. Petry, Rogel H. Prysock, Albert C. Ruckman, Larry A. Scofield, Joe P. Sheffield, Shiraz D. Tayabji, T. Paul Teng, John L. Walkinshaw, William G. Weber, Jr., Gdalyah Wiseman

George (Pat) W. Ring III, Transportation Research Board staff

Sponsorship is indicated by a footnote at the end of each paper. The organizational units, officers, and members are as of December 31, 1986.

NOTICE: The Transportation Research Board does not endorse products or manufacturers. Trade and manufacturers' names appear in this Record because they are considered essential to its object.

Transportation Research Record 1121

The **Transportation Research Record** series consists of collections of papers on a given subject. Most of the papers in a Transportation Research Record were originally prepared for presentation at a TRB Annual Meeting. All papers (both Annual Meeting papers and those submitted solely for publication) have been reviewed and accepted for publication by TRB's peer review process according to procedures approved by a Report Review Committee consisting of members of the National Academy of Sciences, the National Academy of Engineering, and the Institute of Medicine.

Transportation Research Records are issued irregularly; approximately 50 are released each year. Each is classified according to the modes and subject areas dealt with in the individual papers it contains. TRB publications are available on direct order from TRB, or they may be obtained on a regular basis through organizational or individual affiliation with TRB. Affiliates or library subscribers are eligible for substantial discounts. For further information, write to the Transportation Research Board, National Research Council, 2101 Constitution Avenue, N.W., Washington, D.C. 20418.

Contents

Foreword

This Record contains 12 research papers that address the effects of water and temperature on the performance of pavements. The papers are of interest to both researchers and practicing engineers.

Badu-Tweneboah, Tia, and Ruth present methods for determining moduli of asphalt concrete from dynamic indirect tensile tests on either cores or compacted specimens. Input to the relationships includes the viscosity of asphalt (at various temperatures) as obtained from Schweyer constant stress rheometer tests. Reliability of the method is good below 7.0 percent air void content and for low binder viscosities.

Temperature gradients in a portland cement concrete pavement were measured and recorded over a 9-month period by Richardson and Armaghani. An analysis of resulting compressive and tensile stresses showed that temperature gradients probably have little effect on the performance of concrete pavement (related to cracking) in Florida.

Thompson, Dempsey, Hill, and Vogel modeled pavement temperatures with a climatic-materials-structural computer program using material thermal properties, air temperatures, solar radiation, and wind velocities. A climatic data base, which can be used in pavement analysis and design, was developed for Illinois. The method can be used by other states to establish climatic data bases.

Pavement temperatures on a full-scale concrete test road were collected for 3 years in Florida by Armaghani, Larsen, and Smith. Related vertical and horizontal displacements were also measured. The basic data collected provide an understanding of the response of concrete pavements to temperature.

Hudson and Flanagan summarize the results of a study of pavements at 14 locations in five states. Visual condition surveys of trafficked and untrafficked sections indicate that traffic loading is more damaging than environment and is proportionally more damaging in harsh environments.

Moisture measurements in concrete pavements by Janssen showed that only the top 2 in. (or less) becomes dry. On the basis of computer modeling Janssen believes that the resulting moisture gradient can promote shallow hairline cracks to a depth of 3/4 in.

A study by Saraf, Chou, and McCullough of rigid pavement condition evaluations made over a 10-year period shows that the average rate of failures per mile is highly related to the amount of rainfall. In areas with 10 in. of annual rainfall, pavements showed an almost zero rate of failure development, and those in areas with 52 in. of annual rainfall developed failures at a rate of one failure per mile per year. Rainfall effects were much less for pavements built on subgrades with little clay. The authors recommend modifications to rigid pavement designs in Texas to accommodate the effect of rainfall on performance.

Thom and Brown report on repeated load triaxial tests on limestone. Wet aggregates accumulated permanent deformation 10 times faster than dry aggregates. Saturated undrained (low-permeability) aggregates demonstrated immense weakening under loading.

T. F. Fwa describes water-induced flexible pavement problems in Singapore and Malaysia. The problems include localized pavement structure softening, heaving of the pavement surface, separation of pavement layers, and undulations of the surface. Preventive methods are recommended because repair of these types of distress is usually costly and elaborate.

The effect of the depth to water below the bottom of a pavement base was studied by Elfino and Davidson in Florida. They conclude that soil type, as well as depth to the water table, is an important factor that should be considered in the design of high-water clearances of pavements.

Forsyth, Wells, and Woodstrom report on the performance of pavements with subsurface drainage. Concrete pavements designed and constructed with an open-graded two-layer drainage system exhibited no cracking after 5 to 10 years of service, and concrete pavements with

retrofit edge drains exhibited reduced rates of cracking and faulting. Economic analysis indicates a 40 percent lower annual cost for concrete pavements and a 20 percent lower annual cost for asphalt pavements built with good subsurface drainage. The paper includes descriptions of the subsurface drainage systems currently used in California.

The results of a national questionnaire on the use of subsurface drainage systems are summarized by James Baldwin. Thickness and location of drainage layers, aggregate gradations, aggregate fracture, compaction of the drainage layer, stabilization of the drainage layer, permeability, structural value, protection from intrusion, and outlet systems are among the items addressed in the review of 24 responses from agencies reported to be using the free-draining concept.

Procedures for Estimation of Asphalt Concrete Pavement Moduli at In Situ Temperatures

KWASI BADU-TWENEBOAH, MANG TIA, AND BYRON E. RUTH

Methods to supplement conventional elastic layer analysis of nondestructive test (NDT) measurements are needed to improve the ability to evaluate layer moduli. In particular, the determination of asphalt concrete moduli (E_1) for thin pavements often results in substantial errors in the values of E_1 and E_2 using iteration techniques in computer programs (e.g., ELSYM-5, ISSEM-4). The development and predictive reliability of two methods of E_1 determinations are presented for the purpose of improving the analysis techniques used in pavement evaluation studies. The methods are classified as direct and indirect even though both methods are based on E_1-values from dynamic indirect tension testing of asphalt concrete specimens (cores or compacted samples). The direct method requires the development of an E_1-temperature relationship using E_1-values from the indirect tension test, which is conducted at different temperatures. The indirect method is based on a previously developed relationship between E_1 and constant power viscosity (η_j) of the asphalt as obtained from Schweyer constant stress rheometer tests. Cores or cut samples from the pavement are separated into individual layers and the asphalt is recovered using reflux and Abson methods. Asphalt viscosity (η_j) determinations from tests at different temperatures are used in a regression analysis to develop an η_j versus temperature (°K) relationship. Pavement temperature recorded at the time of NDT measurements is used to determine a corresponding η_j from the relationship. E_1 is then predicted from the developed equations using this η_j-value. The reliability of the E_1 predictions is appraised by comparing layer moduli from BISAR simulation of Dynaflect-measured deflection basins and ISSEM-4 predictions of falling weight deflectometer deflection basins. Comments are made on the effects of air void content and mix characteristics.

The analysis of nondestructive test (NDT) measurements for evaluation of the structural characteristics of flexible pavement systems is often complicated by temperature differences, variations in underlying support caused by moisture content changes, the number and relative stiffness of layers being considered in the analysis, and the approach followed in determining layer moduli. Iteration of layer moduli in elastic layer computer programs can yield erroneous results even though the predicted deflection basin is essentially the same as that measured by NDT equipment (e.g., Dynaflect, Road Rater, falling weight deflectometer). Therefore, it is desirable to develop procedures that provide layer moduli independent of other pavement layers. These moduli can be used in multilayer analyses to minimize the number of variables in the iteration. For example, the fifth Dynaflect sensor deflection response can be used for estimation of subgrade or foundation modulus.

Department of Civil Engineering, University of Florida, Gainesville, Fla. 32611.

Two methods for the determination of asphalt concrete modulus (E_1) are presented. The direct method involved the dynamic indirect tension testing of cores or laboratory-compacted specimens using a bonded strain gauge for horizontal strain measurements. The results of tests at different temperatures provided modulus values from which a modulus-temperature relationship was developed for prediction of modulus at the pavement temperature or temperatures encountered during nondestructive testing.

A comprehensive laboratory study was performed using the direct method and constant power viscosity (η_j) tests on asphalt recovered from the test specimens. The resilient modulus and viscosity data obtained from these tests were used to develop relationships between E_1 and η_j. This provided the basis for development of the indirect method for estimation of E_1.

The indirect method requires: *(a)* the recovery of asphalt from each layer of asphalt concrete; *(b)* viscosity testing of the recovered asphalt at different test temperatures; *(c)* regression analysis of the data to establish an η_j versus temperature relationship; and *(d)* prediction of E_1 using the η_j-values computed at temperatures corresponding to those of the pavement during nondestructive pavement evaluation tests.

DEVELOPMENT OF RESILIENT MODULUS TESTING PROCEDURES

The resilient modulus of asphalt concrete mixtures can be determined using compression, flexural, or different indirect tension test methods. Difficulty is encountered with both the interpretation of test data and the reliability of test procedures for providing realistic values of moduli for use in elastic layered stress analysis computer programs.

The compression test is usually performed in an unconfined or triaxial mode using test specimens that have a length-to-diameter ratio of 2. This requires special emphasis on the compaction equipment and procedures used to produce the test specimen. Conventional test specimens are 4 in. in diameter and only 2½ in. thick. It appears to be more rational to evaluate tensile properties because both elastic and inelastic behavior affect elastic response and contribute to cracking (fracture) of pavements subjected to tensile stresses.

The flexural test has similar drawbacks. Furthermore, the nonuniform stressing condition throughout the depth of the specimen makes it more susceptible to variation in test results. Even though the viscosity of the binder is the same at the test temperature, test specimens prepared with a highly shear susceptible binder will not yield the same response or resilient moduli as specimens that contain a low shear susceptible asphalt. This condition has also been observed in dynamic indirect tensile tests using the measured diametral deformation for resilient modulus evaluation. In these tests highly shear susceptible asphalts respond more elastically with fewer delayed elastic effects *(1)*. This produces noticeably higher resilient modulus values for mixtures that contain highly shear susceptible asphalts (e.g., steep roofing) than are obtained with conventional paving asphalt. This difference in response and the variation in temperature susceptibility of asphalts suggests that it is not possible to adjust NDT measurements for temperature without performing tests either on the mix or on the asphalt binder.

Experience with the dynamic indirect tension test with both diametral deformation measurements and bonded strain gauges has indicated that more precise and consistent strain measurements are obtained with bonded strain gauges. At low temperatures, where the specimens behave as brittle elastic materials, both methods should yield the same results provided the precision of the measurement methods is about equal. However, at warmer temperatures the viscosity and elastic behavior of the asphalt binder interact with loading time, rest time, and specimen geometry to inhibit the accurate determination of resilient moduli using the diametral equations that are based on elastic response:

$$E_R = \frac{\sigma_{xx}(1 + 3\upsilon)}{\varepsilon_{xx}} \quad (1)$$

where

E_R = resilient modulus (psi),
σ_{xx} = computed tensile stress (psi),
ε_{xx} = computed strain from diametral measurements, and
υ = Poisson's ratio.

DIRECT METHOD FOR DETERMINATION OF E_1

The test procedure that has evolved from prior experimentation requires the use of an indirect tension testing device equipped with 0.5-in.-wide loading strips that are curved to fit 4.0-in.-diameter test specimens. The device was installed in an environmental chamber set under the crosshead of an MTS closed-loop testing machine. Temperature control was achieved using a dummy specimen with thermistors or thermocouples installed on its surface and interior to provide direct temperature measurements for manual adjustment of the servo-valve for the liquid nitrogen cooling medium. Instrumented test specimens are placed in the chamber along with the dummy specimen and cooled to the specified temperature or temperatures. After the specimen was preconditioned, 20 cycles of loading are usually applied at each of five or more stress levels. A 0.1-sec haversine loading followed by a 0.4-sec rest period is conventionally used in the resilient modulus test.

Test specimens are either compacted in the laboratory to a thickness of 2.50 in., or 4.0-in.-diameter cores are cut from the pavement and trimmed with a masonry saw to a thickness of from 2 to 3 in. It is essential that cores be obtained perpendicular to the pavement so that asphalt concrete layers are normal to the core surface for easy separation by sawing. Also, care must be taken to obtain a uniform cut surface on the core. Surface irregularities will result in excessive stress concentrations when the specimen is loaded between the curved loading strips. One major problem is how to accommodate multiple thin lifts without inducing excessive testing error. Combined lifts of the same asphalt concrete can be cut to 2 or more in. in thickness for testing. Specimens as thin as 1.5 in. can be used if they are within the paving layer. In all cases in which sample size is inadequate there is a greater chance for test discrepancies to occur. The other procedure is to use asphalt viscosity values for asphalt extracted from each layer for computation of moduli using the indirect method.

The preparation of cores for installation of a 0.5-in.-long strain gauge requires the removal of dust from a cut surface before gauge installation. In the case of laboratory-compacted specimens, precooled specimens should be sandblasted or sandpapered on their flat face until clean aggregate is exposed. Strain gauges are epoxied horizontally along or parallel to the x-x axis (within $\pm$ 0.3 in.) and the gauge is centered about the vertical loading axis (y-y). The lead wires from strain gauges are connected to a strain bridge balance, and the output is connected to a strip chart or x-y recorder with a time base for recording the dynamic strain response. A quarter bridge configuration can be used with good results or, if the effect of temperature variation is questioned, a half bridge setup using an unloaded instrumented specimen for temperature compensation may be employed.

Testing may start at 25°C (77°F) provided the asphalt binder is sufficiently hard as encountered with pavement cores from old pavements or laboratory specimens prepared with at least an AC-20 or harder grade asphalt cement. If the specimen has insufficient compacted density or too soft a binder, or both, the stiffness of the strain gauge will be excessive and prevent development of realistic strains. When the stiffness of the asphalt is less than the gauge stiffness, the gauge prevents the full development of strains in its vicinity. This is comparable to strain gauge slippage due to inadequate curing of the epoxy on an elastic material (e.g., steel).

The first step before dynamic testing is to precondition the specimen. This is accomplished by applying a constant low stress for sufficient time to accumulate about 150-μin. of creep strain and then allowing time for strain recovery before the dynamic tests are begun. It is best to precondition and test at warm temperatures before testing at low temperatures. Preconditioning at low temperatures to this strain level could result in damage to the specimen and initiation of fracture.

Stress levels must be selected to prevent excessive creep accumulation or damage to the test specimen. For example, stresses of 2, 4, 6, 8, and 10 psi may be selected for 25°C tests and stresses of as much as 200 psi for tests conducted at 0°C or -5°C. Generally speaking, stress levels should not exceed 50 percent of the failure stress from standard indirect tension tests (at 2 in./min).

Resilient moduli are computed for each stress level and each test temperature using the total resilient strain and the computed stress:

$$\sigma_x = \frac{2P}{\pi l d} \tag{2}$$

$$E_R = \frac{\sigma_x}{\varepsilon_x} \tag{3}$$

where

σ_x = indirect tensile stress (psi),
P = applied load (lb),
l = thickness of specimen (in.),
d = diameter of specimen (in.),
ε_x = measured horizontal strain, and
E_R = resilient modulus (psi).

Specimens properly preconditioned and tested without overstressing will yield almost identical E_R-values for the different stress levels at a given temperature. Usually the mean of four or more E_R-values is considered representative of the resilient modulus at a given test temperature.

Test temperatures of -5°C, +5°C, 15°C, 25°C, and sometimes higher are often used for resilient modulus testing to represent Florida's lower temperature range. The test results can be plotted on log-log graph paper, and regression analyses can be performed for prediction of E_R within and above the test temperature range as shown in Figure 1. Obviously, for colder climates additional tests may be derived at lower temperatures to aid in low-temperature pavement response evaluation or predictions using elastic layer computer programs.

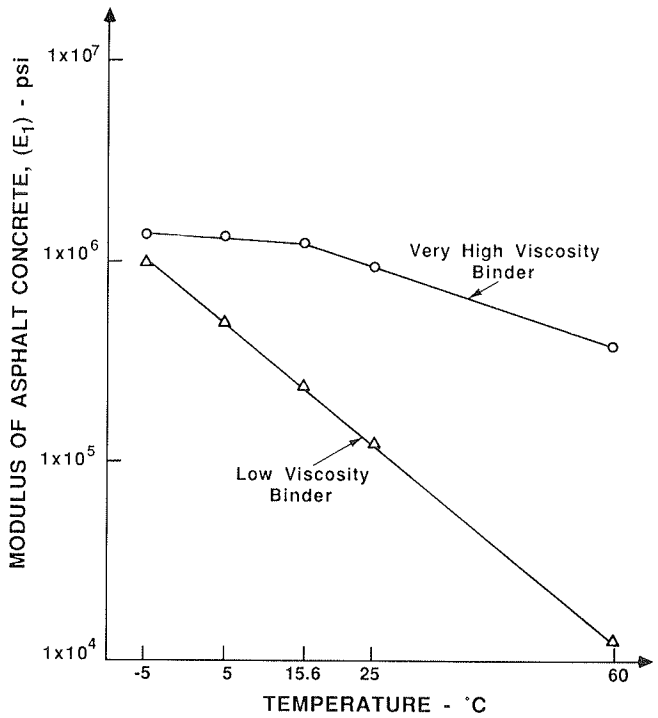

FIGURE 1 E_1**-temperature relationships.**

INDIRECT METHOD FOR DETERMINATION OF E_1

In many instances asphalt concrete pavements have multiple thin lifts or inadequate total thickness for resilient modulus testing using the direct method. Consequently, relationships previously developed from a laboratory test program can be used to predict E_1 for dense-graded mixtures using the viscosity of the binder *(2)*. The relationship was originally developed using a variety of asphalts to prepare test specimens for the previously described dynamic indirect tension tests. After testing, the asphalts were recovered and tested at different temperatures using the Schweyer constant stress rheometer *(3)*. Relationships between E_R and constant power viscosity (η_j) were developed and subsequently used for the prediction of E_1 when the viscosity of asphalts recovered from pavements was known.

The indirect method requires that cut or cored samples be obtained from the pavement section being evaluated. These samples are separated according to each layer or type of asphalt concrete, then heated and broken down for extraction using Method B (reflux) of ASTM D 2172, "Quantitative Extraction of Bitumen from Bituminous Paving Mixtures." The asphalt is recovered using the Abson method (ASTM D 1856). The recovered asphalt is poured into sample tubes with attached capillary tube for viscosity determination at different shear stresses and test temperatures. Background and basic information on the use of the Schweyer constant stress rheometer are available elsewhere *(3–5)*. Details of the physical characteristics, operation, and computational methods of the Schweyer constant stress rheometer are presented in Tia and Ruth *(6)*. Also, Roque et al. *(7)* provide additional information on the relationships between mix properties and asphalt viscosity.

One of the most important aspects of the determination of asphalt viscosity is the asphalt's shear susceptibility at each test temperature. A slight error in the shear susceptibility (slope of Log shear stress versus Log shear rate relationship) may result in errors in viscosity values. The use of constant shear rate (e.g., 1.0- or 0.05-sec^{-1}) viscosity calculations for low-temperature tests will almost always produce problems in developing a good viscosity-temperature relationship. The constant power approach (100 watts/m^3) gives a viscosity (η_j) that has shear stresses and shear rates close to or within the range of those measured. Consequently, errors in shear susceptibility are minimized by using the constant power viscosity.

Basic viscosity calculations using the Schweyer rheometer include

$$\eta_{1.0} = \frac{\tau' \times G}{(\dot{\gamma}' \times R)^c} \tag{4}$$

where

$\eta_{1.0}$ = apparent viscosity at a shear rate of 1.0 sec^{-1} (Pa-sec),
τ' = uncorrected shear stress (Pa),
$\dot{\gamma}'$ = uncorrected shear rate (sec),
G = geometric correction factor,
R = Rabinowich correction = $0.75 - \frac{0.25}{C}$, and
C = shear susceptibility factor (complex flow).

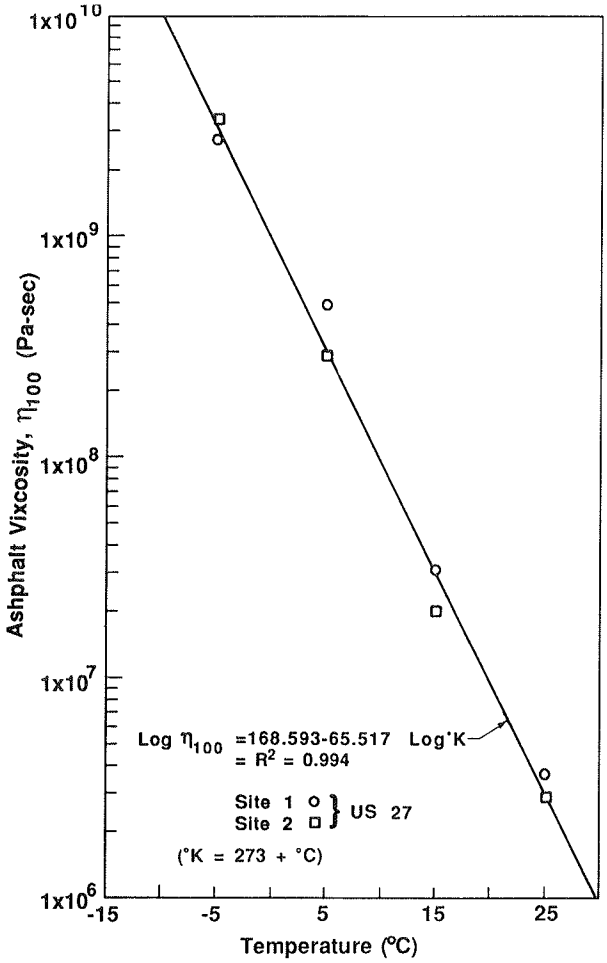

FIGURE 2 Low-temperature asphalt rheology.

To convert $\eta_{1.0}$ to a constant power corresponding to $j = \tau_j \dot{\gamma}_j = 100$ watts/m^3,

$$\eta_j = \eta_{100} = \eta_{1.0}\left(\frac{100}{\eta_{1.0}}\right) \exp\,(c_{-1}/c_{+1}) \qquad (5)$$

The viscosity-temperature relationship may be established by regression analyses of test results and plotted as shown in Figure 2. Usually four to six temperature levels are used to establish the viscosity-temperature relationships. Often it is possible to incorporate the absolute viscosity at 60°C (140°F) in the regression analysis provided the trend is not excessively altered. In this case two sample sites were selected from the pavement of US-27, which had been evaluated by Dynaflect. If the Dynaflect tests had been performed at a temperature of 10°C (50°F), the viscosity (η_{100}) would be determined using the regression equation

$$\text{Log } \eta_{100} = 168.593 - 65.517 \text{ Log (°K)} \qquad (6)$$

where

°K = 273 + °C,
n = 8, and
R^2 = 0.994,

which would yield a constant power viscosity of 9.11×10^7 Pa-sec.

The resilient modulus of the asphalt concrete pavement layer (E_1) can then be computed using one of two equations selected on the basis of viscosity *(2)*:

For $\eta_{100} \leq 9.19 \times 10^8$ Pa-sec,

$$\text{Log } E_1 = 7.18659 + 0.30677 \text{ Log } (\eta_{100}) \qquad (7)$$

For $\eta_{100} > 9.19 \times 10^8$ Pa-sec,

$$\text{Log } E_1 = 9.51354 + 0.04716 \text{ Log } (\eta_{100}) \qquad (8)$$

These equations were originally developed using data derived from mixtures prepared with a Pennsylvania aggregate blend with five different asphalts and a Florida aggregate blend using nine different asphalts that were tested at five stress levels and four different temperatures *(2)*. In this case Equation 7 is used to compute E_1. This gives a value for E_1 equal to 4.25 $\times 10^9$ Pa-sec or 616,000 psi. Figure 3 shows a comparison of

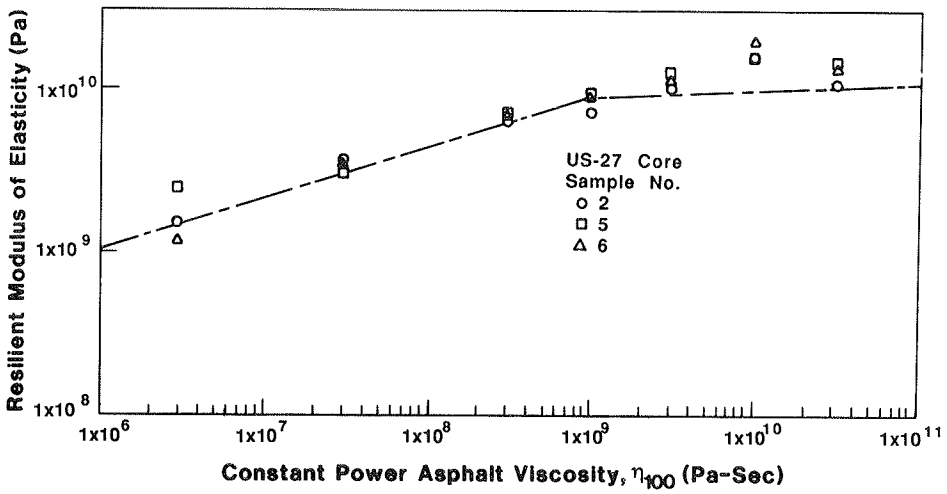

FIGURE 3 Resilient modulus–asphalt viscosity relationship and comparison.

relationships of Equations 7 and 8 with E_1-values obtained by the direct method of testing.

Care should be exercised in the use of Equation 8 because this is an approximation of the extension of Equation 7 to simulate a curved relation that attains maximum E_1-values in the range of from 2×10^{10} to 5×10^{10} Pa. Therefore, predicted E_1-values in excess of 5×10^{10} should be questioned or considered in error. The majority of test results indicates that maximum E_1-values are generally less than 3×10^{10} Pa.

The preceding indirect method for estimation of E_1 has worked exceedingly well for dense-graded mixtures with air void contents within the 3 to 7 percent range. Higher air void contents result in a reduction in measured E_1-values. Southgate *(8)* developed a relationship between modulus ratio and air void content. Dynamic flexural tests conducted by Ruth and Maxfield *(9)* provided results almost identical to Southgate's relationship. These relationships, shown in Figure 4, indicate an 11.0 percent reduction in E_1 for each 1.0 percent increase in air void content over 4.0 percent but not in excess of 9.0 percent. At low temperatures (high asphalt viscosity) the effect is considerably less because the asphalt binder properties influence E_1 more than compacted density or air void content. The reverse is true at extremely warm pavement temperatures.

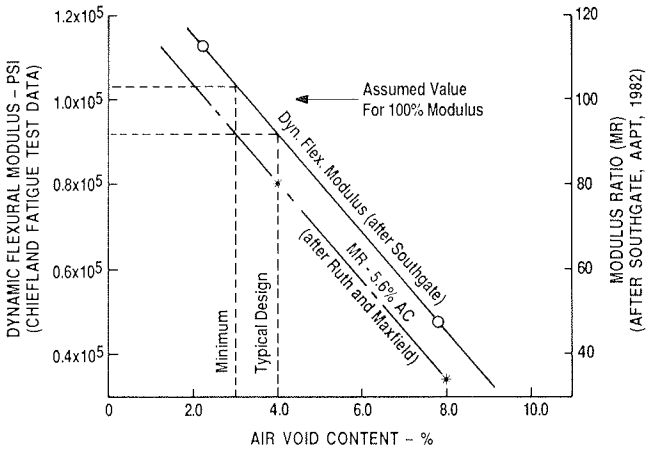

FIGURE 4 Effect of air void content on modulus.

RELIABILITY OF PREDICTED E_1-VALUES

The reliability of the indirect method of estimating E_1 is quite good according to comparisons of predicted and measured values determined by the dynamic indirect tension test using bonded strain gauges. The most prevalent predictive error occurs at higher-than-normal air void contents (> 7.0 percent) when the viscosity of the binder is low.

Another indicator of reliability is if predicted E_1-values can be used with E_2-, E_3-, and E_4-values as input in an elastic multilayer computer program (e.g., BISAR) to predict Dynaflect deflection basins without further adjustment of E_1. Of nine test road sites given in Table 1, only SR 26B required a significant change in E_1 to achieve simulation of pavement response as measured by Dynaflect. Also, the results of ISSEM-4 *(10)* predictions of E_1 using falling weight deflectometer deflection basins are given in Table 1. The predicted E_1-values were used as seed moduli in the ISSEM-4 analysis.

CONCLUSIONS

The need for methods to evaluate the moduli of pavement layers without excessive extrapolation error is most apparent when NDT data and iteration methods are used to solve for the moduli of three- or four-layer systems. This is particularly true when the asphalt concrete modulus (E_1), which is affected by temperature, layer thickness (t_1), and the stiffness of underlying pavement layers, is considered. Two methods of providing a more direct approach for the estimation of E_1 have been presented:

TABLE 1 COMPARISON OF PREDICTED AND TUNED ASPHALT CONCRETE MODULI

Test Road	Thickness of AC (in.)	Pavement Temp. °F	Asphalt Concrete Modulus (E_1), psi		
			Predicted[a]	Tuned w/ BISAR[b]	ISSEM-4[c]
SR 24	2.5	55	338,260	338,260	338,000
SR 26A	8.0	81	171,250	171,500	174,000
SR 26B	8.0	59	406,493	360,000	360,000
SR 26C	6.5	82	171,250	171,500	171,000
US 301	4.0	69	256,640	250,000	250,000
US 441	3.0	79	289,580	290,000	290,000
I-10 A	8.0	104	60,776	65,000	-
I-10 B	7.0	88	113,182	113,000	113,000
I-10 C	5.5	106	66,888	67,000	67,400

(a) Predicted from recovered asphalt viscosity-temperature relationship and E_1 prediction equations.

(b) Layer moduli obtained when BISAR predicted deflection basins match those measured by Dynaflect.

(c) Layer moduli obtained from ISSEM-4 using initial estimates of layer moduli (seed moduli) for the four layer system as input into the program. ISSEM-4 iterates layer moduli to achieve a close match of the deflection basin measured by the Falling Weight Deflectometer.

1. The first method involves the direct measurement of horizontal strain in the dynamic indirect tension test and computation of E_1 using only the computed stress (σ_{xx}), measured total resilient strain (ε_x), and Equation 3. This method is only limited by specimen size and a sufficiently high binder viscosity. Otherwise, reproducible test results and reliable E_1-values are obtained for most mixtures.

2. The second method is considered an indirect estimate of E_1 because recovered asphalt viscosity has been related to E_1-values obtained from direct measurement (first method). The major advantage to the use of the indirect method is its adaptability to thin asphalt concrete pavements or thin lifts where direct measurement on samples is not feasible.

The prediction accuracy of both methods is considered to be quite good on the basis of results of BISAR simulation of Dynaflect response and ISSEM-4 predictions of falling weight deflectometer measurements using these E_1-values.

ACKNOWLEDGMENTS

The authors wish to extend their appreciation to the Florida Department of Transportation (FDOT) for their sponsorship of research projects from which the data and the stipulated procedures were developed for inclusion in this technical paper. In particular, the technical assistance of numerous FDOT personnel at the Bureau of Materials and Research is gratefully acknowledged.

REFERENCES

1. B. E. Ruth, H. E. Schweyer, A. S. Davis, and J. D. Maxfield. Asphalt Viscosity: An Indicator of Low Temperature Fracture Strain in Asphalt Mixtures. *Proceedings of the Association of Asphalt Paving Technologists*, Vol. 48, 1979, pp. 221–237.
2. B. E. Ruth, A. K. Bloy, and A. A. Avital. Prediction of Pavement Cracking at Low Temperatures. *Proceedings of the Association of Asphalt Paving Technologists*, Vol. 51, 1982, pp. 53–90.
3. H. E. Schweyer, L. L. Smith, and G. W. Fish. A Constant Stress Rheometer for Asphalt Cements. *Proceedings of the Association of Asphalt Paving Technologists*, Vol. 45, 1976, pp. 53–72.
4. H. E. Schweyer and F. Y. Kafka. Constant Stress Rheology of Asphalt Cements. *Industrial and Engineering Chemical Fundamentals*, Vol. 15, May 1976, pp. 138–144.
5. H. E. Schweyer, R. L. Baxley, and A. M. Burns. In *Low-Temperature Rheology of Asphalt Cements—Rheological Background*, Special Technical Publication 628. ASTM, Philadelphia, Pa., 1977, pp. 5–42.
6. M. Tia and B. E. Ruth. Basic Rheology and Rheological Concepts Established by H. E. Schweyer. In *Asphalt Rheology Relationship to Mixture*, Special Technical Publication 941, ASTM, Philadelphia, Pa., April 1987, pp. 118–145.
7. R. Roque, M. Tia, and B. E. Ruth. Asphalt Rheology To Define the Properties of Asphalt Concrete Mixtures and the Performance of Pavements. In *Asphalt Rheology Relationship to Mixture*, Special Technical Publication 941, ASTM, Philadelphia, Pa., April 1987, pp. 3–27.
8. H. F. Southgate. Effects of Construction Variations Upon Dynamic Moduli of Asphalt Concrete. *Proceedings of the Association of Asphalt Paving Technologists*, Vol. 51, 1982, pp. 484–493.
9. B. E. Ruth and J. D. Maxfield. *Fatigue of Asphalt Concrete*. Final Report, Project 245-D54. Department of Civil Engineering, University of Florida, Gainesville, Nov. 1977.
10. J. Sharma and R. N. Stubstad. Evaluation of Pavement in Florida by Using the Falling-Weight Deflectometer. In *Transportation Research Record 755*, TRB, National Research Council, Washington, D.C., 1980, pp. 42–48.

Publication of this paper sponsored by Committee on Strength and Deformation Characteristics of Pavement Sections.

Stress Caused by Temperature Gradient in Portland Cement Concrete Pavements

JOSEPH M. RICHARDSON AND JAMSHID M. ARMAGHANI

Concern has been expressed in Florida that, because of a nonlinear temperature gradient in a portland cement concrete (PCC) pavement, internal stresses could be developed such that the life of the pavement would be seriously reduced. A research program was undertaken by the Florida Department of Transportation to determine the actual temperature gradient in a PCC pavement. For a period of 9 months, hourly temperatures were recorded from a 9-in.-thick test pavement in Gainesville, Florida. The temperature data were analyzed to determine what curve best fit the data and what were the actual maximum compressive and tensile stresses caused by the nonlinearity of the temperature gradient. These results were compared with those obtained from the AASHO Test Road and with Bergstrom's prediction method. The results indicated that the nonlinearity of the temperature gradient in a PCC pavement did not have a significant impact on its performance.

Fluctuations in air temperature and in the intensity of solar radiation cause stresses in a concrete pavement. Recently a new portland cement concrete (PCC) pavement in Florida experienced premature cracking. It was hypothesized that a stress that would significantly contribute to the failure of the pavement could be generated by the nonlinearity of the temperature gradient. To evaluate this hypothesis it was decided to examine historical temperature data (1983 and 1984) from a test road that was constructed in Gainesville, Florida. The test road had a pavement thickness of 9 in., which was the same as that of the distressed pavement.

Concrete is sensitive to volumetric change caused by thermal fluctuation. A model must be assumed in order to isolate the stress due to the nonlinearity of a temperature gradient. Bergstrom *(1)* presented this method in 1950. It is assumed that pavement temperature is increased by some amount above that which would correspond to zero stress (Figure 1*a*). The energy that increases the temperature of the pavement is applied only to the surface of the pavement through the air and solar radiation. This causes a temperature gradient in the pavement. If the displacements of the pavement (axial and curling) are completely prevented, an axial compressive stress across the whole cross section is generated. This total stress is found by integrating across the section and dividing by the depth of the pavement (Figure 1*b*). When this axial stress is subtracted from the total stress, the resulting stress will cause a curling bending moment in the pavement. This moment can be calculated by taking the stresses about any convenient point (i.e., the bottom of the pavement). This moment will result in a curling stress distribution as shown in Figure 1*c*. When both the axial and the curling stresses are subtracted from the total temperature stress, the resulting stress is that caused by the nonlinearity of the temperature gradient of the pavement (Figure 1*d*). A linear temperature gradient would result in zero stresses in Figure 1*d*. Even though this nonlinear temperature stress was determined assuming complete restraint of the pavement, it exists whether the pavement is restrained or not.

J. M. Richardson, Civil Engineering Department, McNeese State University, Lake Charles, La. 70609. J. M. Armaghani, Bureau of Materials and Research, Florida Department of Transportation, P.O. Box 1029, Gainesville, Fla. 32602.

TESTING PROCEDURES

The Gainesville, Florida, test road (Figure 2) consists of six slabs, each 12 ft wide and 20 ft long, made of PCC placed on undisturbed soil. The road does not support any vehicular traffic. The compressive strength of the concrete in the pavement averages about 5,000 psi. Five thermocouples were implanted in the center of Slab 4 to measure the temperature of the concrete (fresh and hardened). The thermocouples were spaced at 1, 2.5, 4.5, 6.5, and 8 in. below the surface of the pavement. No temperature measurements were made at the top and bottom of the pavement. The thermocouples were secured to a 1/4-in. wooden dowel imbedded in the fresh concrete and connected to a Fluke programmable data logger. The data logger was programmed to take temperature measurements from all five sensors at 1-hr intervals. In some cases, measurements were made at 30- and 15-min intervals. With some discontinuities, measurements were taken from November 1983 through August 1984 in conjunction with other ongoing research. Temperature measurements at only three levels have been continued to the present. The months of December 1983 and November 1984 were almost continuously monitored with at least hourly measurements.

METHOD OF ANALYSIS

The temperature data were analyzed in a three-step procedure. In the first step, the objective was to identify the time intervals that created the maximum tensile and compressive stresses caused by a nonlinear temperature gradient so that further analysis could be focused on only these incidents. The second step was to determine what form of equation best fit the experimental temperature data. The third and final step was to conduct stress analyses on the critical days with the best-fit equation to determine the nonlinear temperature stresses.

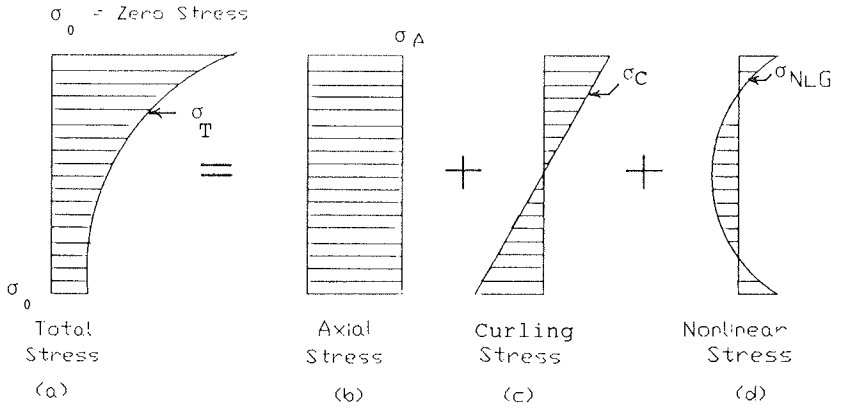

FIGURE 1 Typical temperature stresses in concrete pavements.

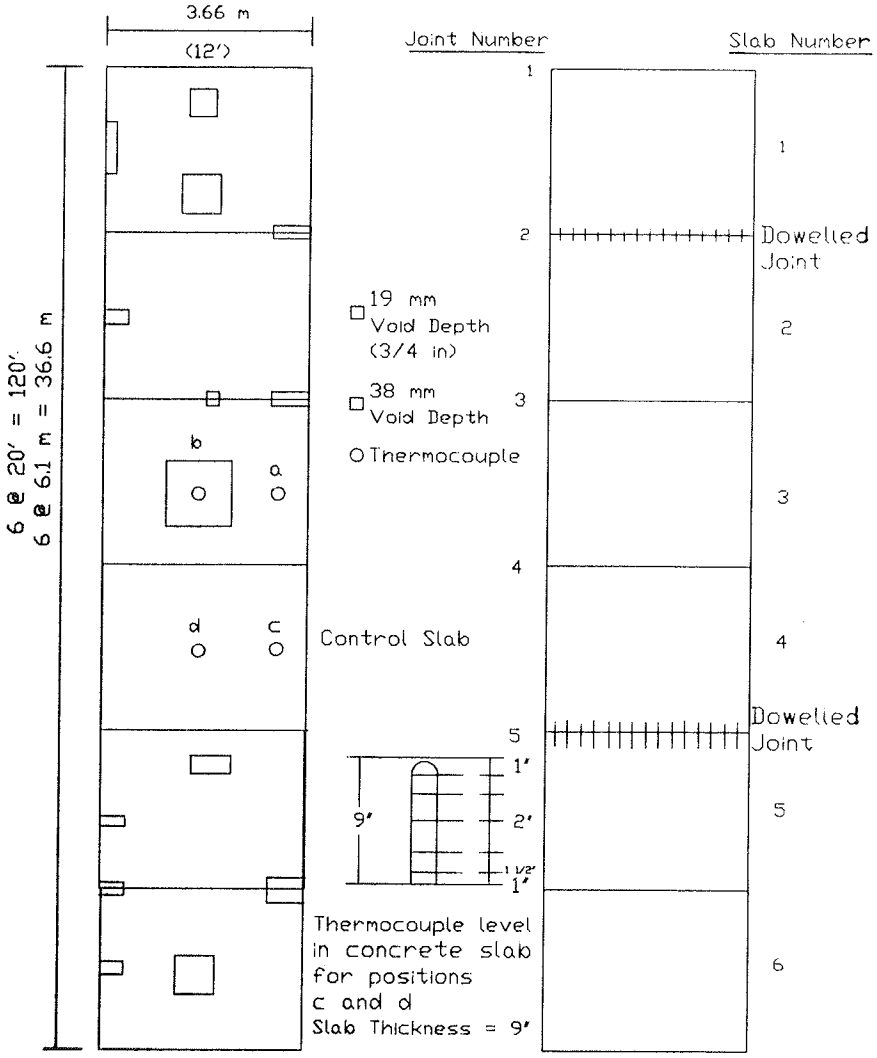

FIGURE 2 Details of test road.

FORTRAN ANALYSIS

Because five temperature thermocouples were used, the method that was used to first examine the data was to assume a linear temperature gradient between sensor locations. The temperature gradient for the top 1 in. of pavement was found by extending the line connecting the temperatures taken at the 1- and the 2.5-in. levels below the pavement surface. The bottom 1 in. of pavement was assumed to be at the same temperature as the sensor located 8 in. below the surface of the pavement. A FORTRAN program was written that first divided the pavement into 90 levels and then determined the area for each section and summed to give the total area. This number was multiplied by the coefficient of thermal expansion (assumed to be 6×10^{-6} degrees Fahrenheit) and Young's modulus of elasticity (assumed to be 3.5×10^6 psi) to give the

total force on the cross section. Dividing this total by the depth of the pavement (9 in.) and a strip of the pavement 1 in. wide gave the axial stress above some predetermined temperature of zero stress. This was assumed to be zero degree (°F) for convenience in calculations, but any temperature is acceptable because the magnitude of the axial and curling stress is not the subject of this study.

The next step was to determine the curling stress of the pavement. This was done by taking the moments of the areas of the 90 levels that remained after the axial stress was subtracted from the total stress at each level. This stress had to conform to the double triangular stress areas shown in Figure 1*c*. Subtracting the curling stress plus the axial stress from the total stress yielded the stresses that were caused by a nonlinear temperature gradient. The value of this method is that it does not require an assumed equation to examine the thousands of individual time intervals observed.

SAS ANALYSIS

When the day and times of maximum stresses (top, bottom, and midway in the pavement) had been determined, the corresponding temperature gradients were analyzed using linear regression to see what equation would give the best fit. The following models (equations) were tested: parabolic parallel to the thickness, parabolic parallel to the temperature, semilog, log-log, semilog with axes reversed, and the Gompertz growth equation. This analysis was accomplished using SAS Version 5 *(2)*. The parabolic model parallel to the temperature axis gave the best fit at all of the time intervals examined. The model was next fitted to 325 time intervals. The curve fit was extremely good. Using the correlation coefficient (R^2) as the measure of the goodness of fit, it was found that 255 time intervals had R^2 greater than 0.99 (1.0 is a perfect fit). Forty-nine time intervals had a fit between 0.95 and 0.99, and 18 time intervals had a fit between 0.90 and 0.95. The three remaining intervals had R^2 of 0.85, 0.84, and 0.75.

DISCUSSION OF RESULTS

The parabolic model parallel to the temperature axis is

$$t = A + By + Cy^2 \quad (1)$$

where

t = temperature (°F),
y = location above the bottom of the pavement (in.), and
A, B, C = factors fitted by linear regression.

Representative values of A, B, C, and R^2 for August 14, 1984, are given in the following table.

Hour	*A*	*B*	*C*	R^2
Midnight	96.09	0.1841	–0.11789	0.9993
4:00 a.m.	93.24	–0.2906	–0.0819	0.9990
8:00 a.m.	90.71	–0.5673	–0.0426	0.9990
Noon	91.98	–0.8172	0.3125	0.9984
4:00 p.m.	98.32	0.8178	0.2250	0.9999
8:00 p.m.	99.87	1.2641	–0.1593	0.9747

The temperature in Equation 1 is related to stress by assuming a temperature for zero stress, as was done previously, and then subtracting this temperature from the derived temperature and, finally, multiplying by the coefficient of thermal expansion and the modulus of elasticity:

$$\sigma_T = E \alpha t \quad (2)$$

where α is the coefficient of thermal expansion and E is the modulus of elasticity.

The axial stress at any level in a 9-in. pavement can be found to be

$$\sigma_A = E \alpha (A + 4.5B + 27C) \quad (3)$$

By finding the moment by double integration, the curling stress (if fully restrained) can be found to be

$$\sigma_C = E \alpha [(y - 4.5) B + 9 (y - 4.5)C] \quad (4)$$

Subtracting σ_A plus σ_C from σ_T yields the stress due to the nonlinearity of the temperature gradient:

$$\sigma_{NL} = E \alpha C(y^2 - 9y + 13.5) \quad (5)$$

This result is not unexpected because the only nonlinear term in the parabolic equation is y^2 and C is only associated with this term.

Using the fitted parabolic equations, the maximum compressive stress (Figure 3) due to a nonlinear temperature gradient was found to be 113 psi on August 14, 1984, at 1:00 p.m. eastern daylight time (EDT) [12 noon eastern standard time (EST)]. An examination of all of the data revealed that the maximum nonlinear compressive stress occurred at about 12 noon EST throughout the year.

Levels of stress near the maximum occurred throughout the testing period. Representative stresses (psi) are given in the following table.

Date	*Stress (psi)*
December 23	60
January 1	100
February 1	107
March 13	104
April 2	91
July 25	109

The maximum tensile stress due to the nonlinearity of a temperature gradient (Figure 4) of 113 psi occurred on August 15 at 8:00 p.m. EDT. The maximum nonlinear tensile and compressive stresses occurred in both the top and the bottom of the pavement. Unlike the time of occurrence of the maximum nonlinear compressive stress, that of the maximum nonlinear tensile stress varied throughout the test period. In December 1983 it occurred about midnight and became progressively earlier in the evening until it reached 8:00 p.m. EDT on August 5, 1984.

The maximum tensile stress is much higher than that measured at other times. Representative values are given in the following table.

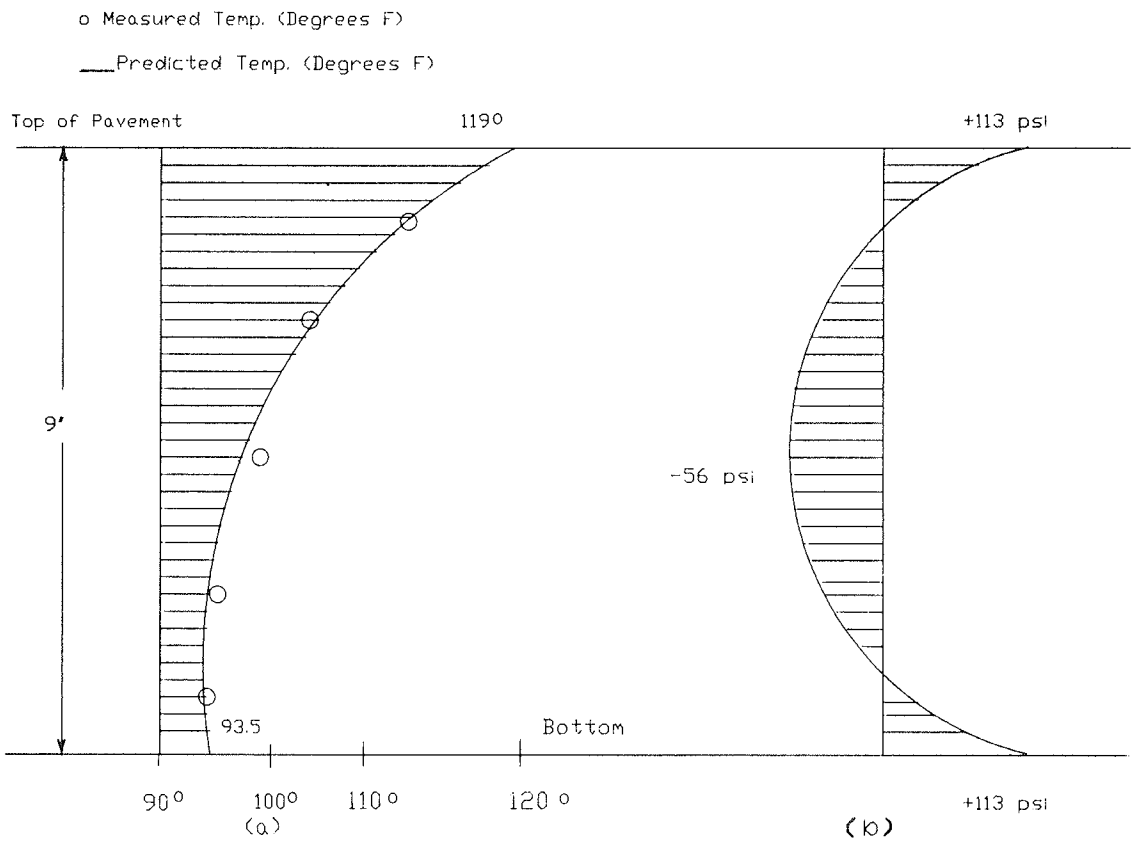

FIGURE 3 Temperature gradient and nonlinear temperature stresses on August 14, 1984, at 1:00 p.m. EDT.

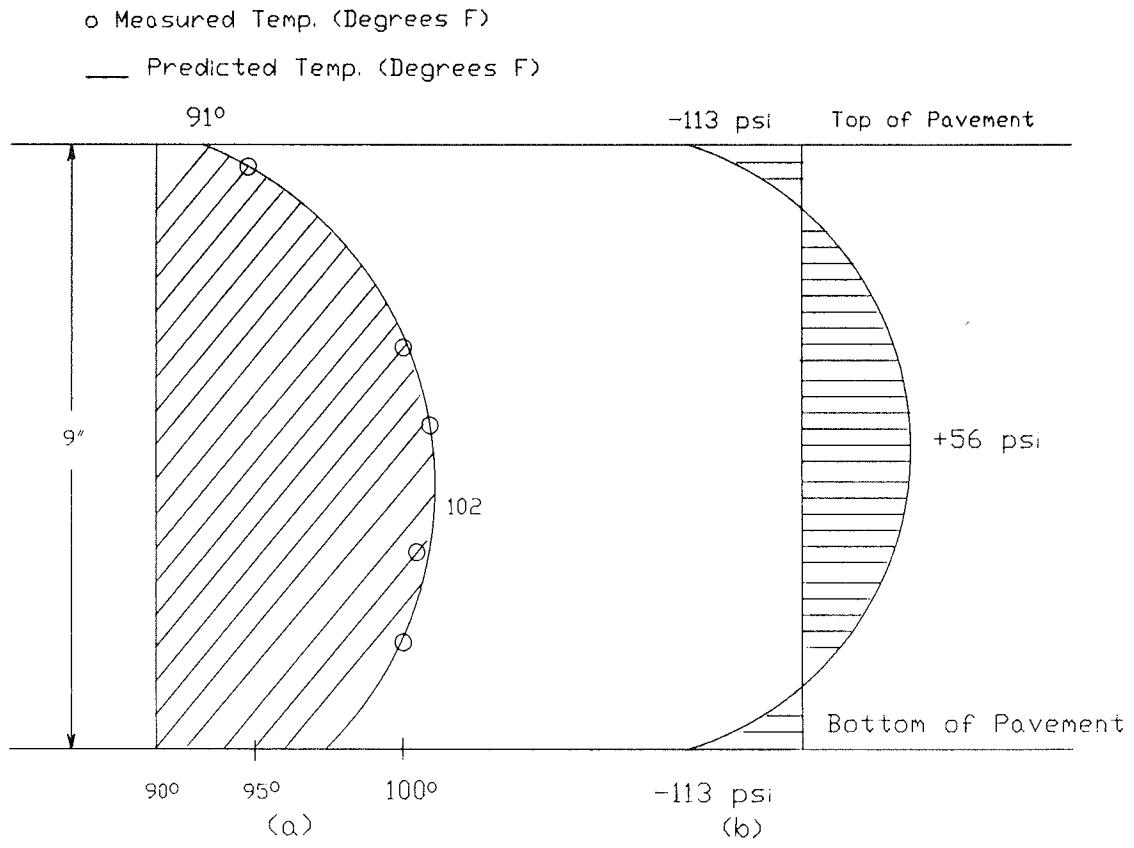

FIGURE 4 Temperature gradient and nonlinear temperature stresses on August 15, 1984, at 8:00 p.m. EDT.

Date	*Maximum Tensile Stress (psi)*
December 23	37
January 30	30
February 6	43
March 14	58
April 2	40
July 25	53

The highest tensile stress on a previous day (August 14) was 56 psi. The reason for the high tensile stress on August 15 is the rapid cooling of the surface of the pavement, which was probably caused by an evening thunderstorm, just before 6:00 p.m. EDT. The temperatures were recorded automatically so that no one was present at 6:00 p.m., but at 5:00 p.m. the sky was reported as being heavily overcast.

That the maximum nonlinear tensile and compressive stresses have the same value is purely coincidental. Bergstrom's *(1)* analysis using the same modulus of elasticity, coefficient of thermal expansion, and temperature difference between the top and bottom of the pavement produced a compressive strength of 63 psi. Bergstrom used an exponential (semilog) model that did not provide a good fit to the test road data.

During July 1986 an additional temperature sensor, insulated from incident solar radiation, was placed on the surface of the pavement. On July 9, 1986, at 12:00 noon EDT the temperature at the 1 in. below the surface level reached 116°F while the surface had a temperature of 122°F. This differential between the surface and 1 in. below the surface is what had been predicted by the model. This is additional confirmation of the validity of the parabolic model.

Figures 5 and 6 are plots of the air temperature, the temperature 1 in. from the top, 1 in. from the bottom, and in the middle of the pavement for August 14, 1984, and August 15, 1984, respectively. During the night, concrete temperatures varied closely with variations in air temperature, but during the daylight hours incident solar radiation on the surface of the pavement played a much larger part than did air temperature, as shown by the rapid rise in the temperature of the top of the pavement. This may be primarily a phenomenon of more southerly regions because Bergstrom *(1)* reported that in Sweden concrete temperatures varied with air temperatures. The area of maximum nonlinear tensile stress is clearly defined by the region in which the temperature at the middle of the pavement exceeds those at the top and the bottom in Figure 6. The area of maximum nonlinear compressive stress is not clearly defined and cannot be determined from Figure 5.

Figure 7 is a plot of the temperature gradients at 4-hr time intervals on August 14, 1984. The curves are quite similar to those found in the AASHO Road Test *(3)*.

The assumed value of 6×10^{-6} degrees Fahrenheit for the coefficient of thermal expansion is probably high for concrete made with porous Florida coarse aggregates. Initial findings from ongoing research have indicated a value of less than 4×10^{-6} degrees Fahrenheit. The assumed modulus of elasticity has been shown to be approximately correct for concrete of 5,000-psi compressive strength manufactured in Florida. If the lower value is used, the maximum nonlinear stresses would be +75 psi.

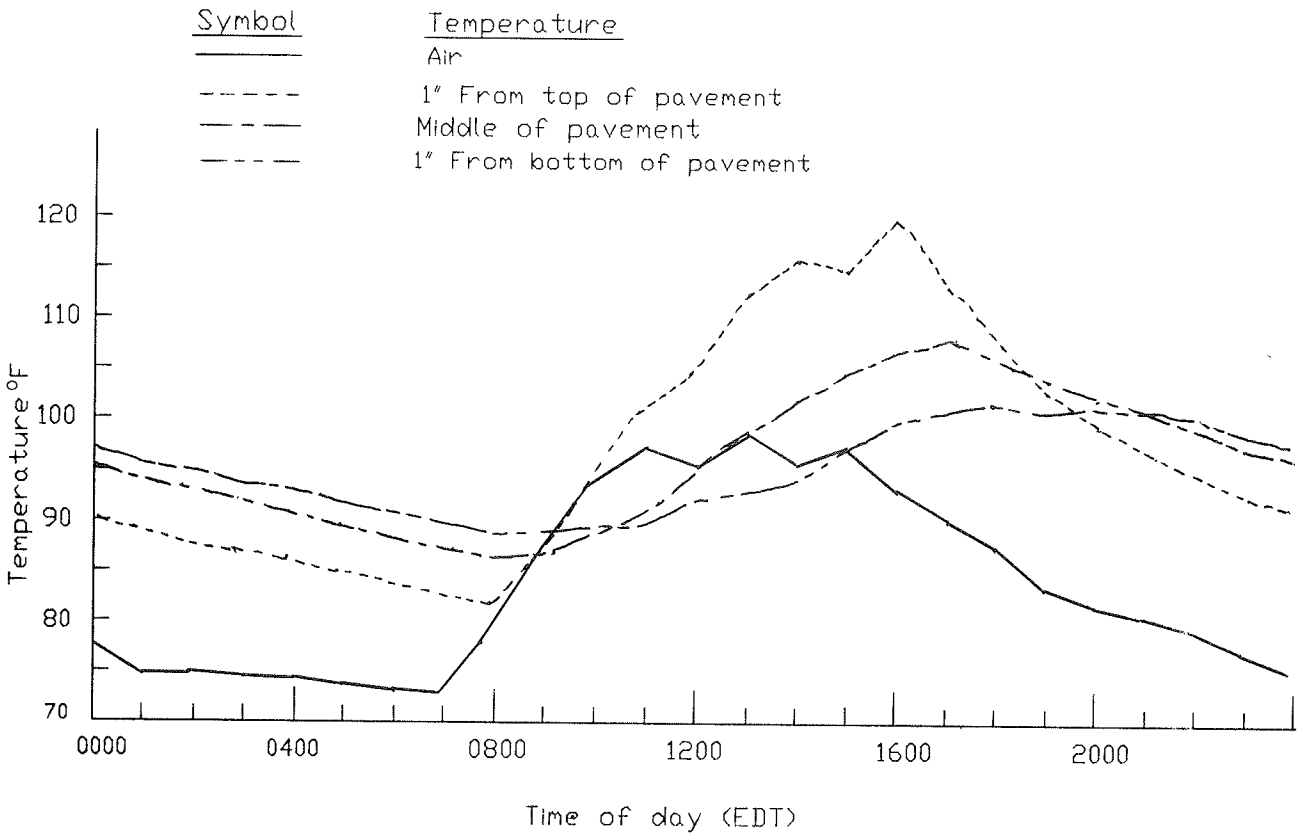

FIGURE 5 Temperature distribution for August 14, 1984.

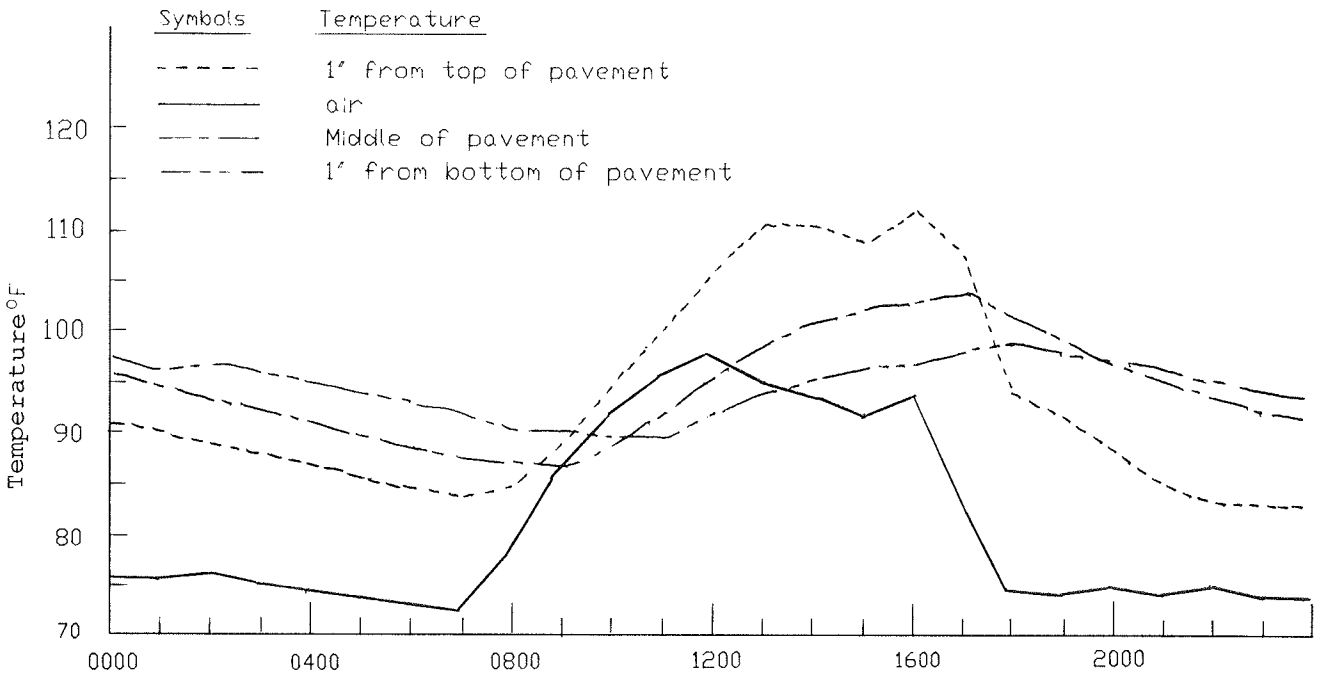

FIGURE 6 Temperature distribution for August 15, 1984.

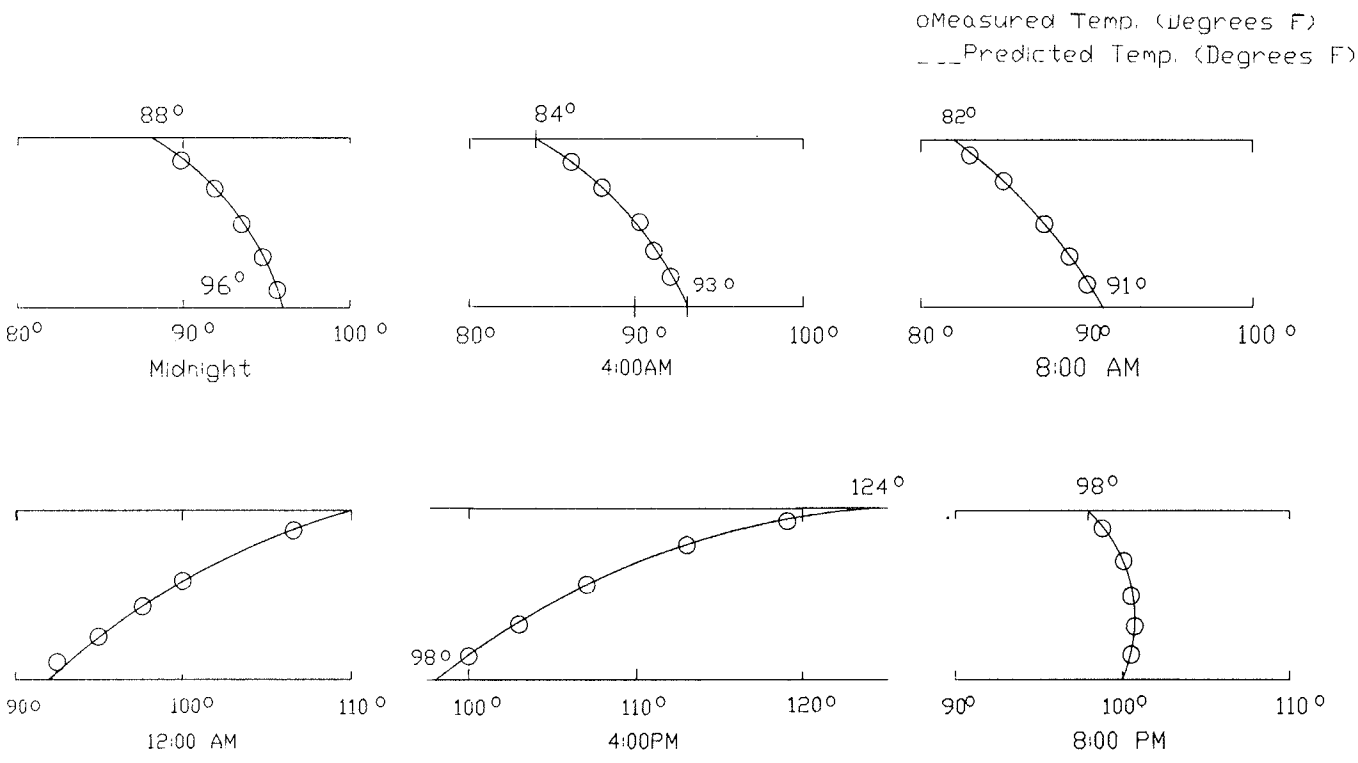

FIGURE 7 Temperature gradient at 4-hr intervals for August 14, 1984.

CONCLUSIONS

The following conclusions were drawn:

1. The maximum compressive stress due to the nonlinearity of the temperature gradient, and which is independent of the slab restraints, was found to be 113 psi and to occur at 1:00 p.m. EDT. This stress is not significant compared with the 5,000-psi compressive strength of the concrete. In addition, this stress occurs in the top and bottom of pavement and actually aids in the carrying of loads that cause flexural stresses in the pavement.

2. The maximum tensile stress due to the nonlinearity of the temperature gradient was found to be 113 psi and to occur at 6:00 p.m. EDT. The flexural strength (modulus of rupture = R) of a beam cut from the section of highway experiencing the premature failure was 671 psi with a corresponding core

Characterizing Temperature Effects for Pavement Analysis and Design

M. R. THOMPSON, B. J. DEMPSEY, H. HILL, AND J. VOGEL

Pavement temperatures can be accurately quantified utilizing the Climatic-Materials-Structural (CMS) computer model developed at the University of Illinois. Required CMS inputs (for temperature modeling) are *(a)* thermal properties of materials and soils, *(b)* air temperature data, *(c)* solar radiation data, and *(d)* wind velocity data. In this paper the development and use of a comprehensive Illinois Climatic Data Base for Pavements are presented. Air temperature data are summarized on a weekly basis and solar radiation and wind velocity data are presented in the form of a monthly state map. Illustrative, applications-oriented examples are presented for *(a)* strength–degree-day curing relations for pozzolanic stabilized base materials, *(b)* asphalt concrete moduli–pavement temperature effects, and *(c)* temperature gradients in portland cement concrete slabs. The emphasis here is on the concepts and techniques used to establish the Illinois Climatic Data Base for Pavements. The illustrative information demonstrates the versatility and usefulness of the climatic data base and heat-transfer model procedures in pavement analysis and design. The procedures and techniques described can be used to establish a climatic data base for other states or locations. The climatic data base and heat-transfer model approach is recommended for quantifying temperature effects in flexible and rigid pavement analysis and design.

Pavement temperature is an important consideration in pavement analysis and design. Examples of significant temperature effects follow. Strength development in pozzolanic stabilized base (PSB) materials is dependent on available degree-days of curing (degree-days based on pavement temperatures above 40°F). Figure 1 shows compressive strength–degree-day relations for typical lime-flyash and cement-flyash mixtures. Freeze-thaw action affects decreases in the strength of stabilized base material. Residual strength after cyclic or freeze-thaw action is primarily controlled by the cured stabilized material strength before freeze-thaw *(1)*, as shown in Figure 2. Asphalt concrete (AC) moduli are temperature dependent. Figure 3 shows AC moduli–temperature relations for a proposed full-depth AC thickness design procedure *(2)*. Temperature gradients in portland cement concrete (PCC) pavements are important in considering "slab-curling" effects. Large curling stresses and loss of support develop from PCC slab temperature gradients. PCC slab gradients show large daily and seasonal variability.

It is apparent that pavement temperature is an extremely important factor in pavement analysis and design. Current research at the University of Illinois is focused on the mechanistic analysis and design of flexible and rigid pavements. To facilitate the appropriate consideration of pavement temperature effects, an Illinois Climatic Data Base was developed. In this paper are described the data base and how it can be used with a previously developed heat-transfer model to characterize important pavement temperature effects.

M. R. Thompson, B. J. Dempsey, and H. Hill, Department of Civil Engineering, University of Illinois at Urbana-Champaign, Urbana, Ill. 61801. J. Vogel, Climate Information Unit, Illinois State Water Survey, Mail Code 674, Champaign, Ill. 61801.

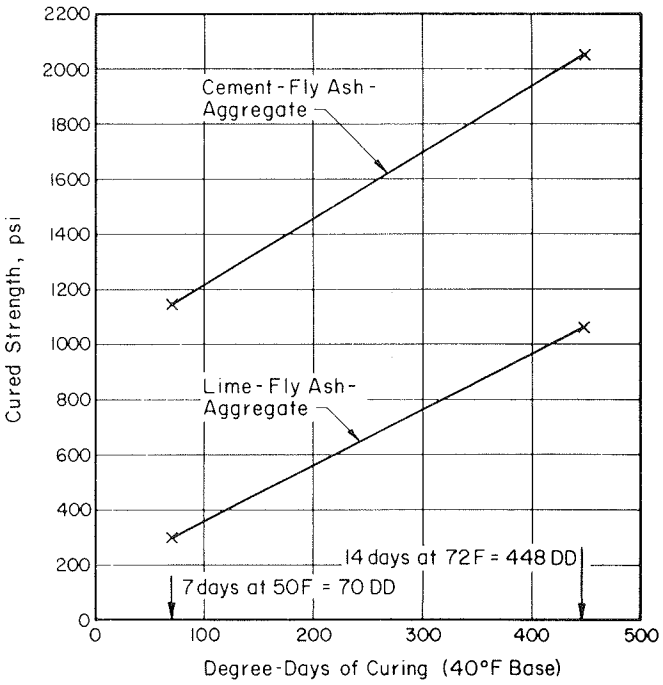

FIGURE 1 Strength–degree-day relations for PSB materials.

HEAT-TRANSFER MODEL

The heat-transfer model used in this study was originally developed at the University of Illinois *(3)* and is used in the Climatic-Materials-Structural (CMS) program *(4)*, which can be run on an IBM PC-AT computer. The heat-transfer model uses a finite-difference solution to the one-dimensional, Fourier heat-transfer equation for transient heat flow to compute pavement temperatures as a function of time. Energy balance procedures developed by Scott *(5–7)* and Berg *(8)* are used to relate the pavement surface temperatures to climatic parameters. Further details concerning the program are available in Dempsey et al *(3)*.

compressive strength (f_c') of 5,330 psi ($R = 9.17 \sqrt{f_c'}$). The nonlinear temperature stress is thus 17 percent of the flexural strength. This stress is not in itself sufficient to cause a pavement to crack or fail. The nonlinear temperature stress is independent of the compressive strength of the concrete. At the design strength of the concrete (3,000 psi) and using the previously derived relationship for the modulus of rupture, the nonlinear temperature stress would be 22 percent of the flexural strength. At an early curing time when the flexural strength is low, this stress may be more critical.

It should be cautioned that these results are only applicable to the conditions that obtained on the test road at Gainesville, Florida. Their extension to other climates, thicknesses of pavements, coarse aggregates, and base materials is not advisable until further research has been conducted.

ACKNOWLEDGMENTS

This research has been conducted by the Florida Department of Transportation's Bureau of Materials and Research. The technical assistance and suggestions of T. J. Larsen are gratefully acknowledged. The cooperation and effort of C. R. Davis are highly appreciated.

REFERENCES

1. K. C. Bergstrom. Temperature Stresses in Concrete Pavements. *Proceedings of the Swedish Cement and Concrete Institute*, No. 14, Stockholm, 1950.
2. *SAS User's Guide: Statistics.* SAS Institute, Cary, N.C., 1982.
3. *Special Report 61E: The AASHO Road Test, Report 5: Pavement Research.* HRB, National Research Council, Washington, D.C., 1962.

Publication of this paper sponsored by Committee on Strength and Deformation Characteristics of Pavement Sections.

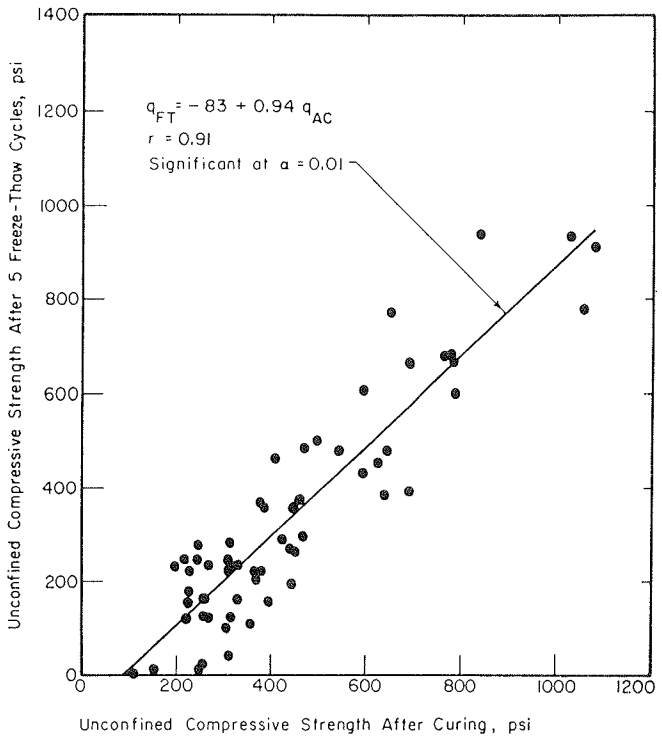

FIGURE 2 Freeze-thaw strength: cured strength relation for stabilized materials.

Inputs to the heat-transfer model are climatic data and thermal properties of the paving materials and soils. The climatic data inputs are maximum and minimum daily air temperature, percent sunshine, and wind speed. Thermal property inputs are thermal conductivity, heat capacity, and latent heat of fusion. The model recognizes three sets of thermal properties depending on whether the material is in an unfrozen, freezing, or frozen condition. The procedures for determining the thermal properties of pavement materials have been described in detail elsewhere *(3, 9)*. The methods developed by Kersten *(10)* are well suited for determining the thermal properties of the base, subbase, and subgrade soils.

The climatic data inputs are not readily available in a suitable format. To facilitate the application of the heat-transfer model to various pavement-related problems, a comprehensive climatic data base was recently developed for Illinois as part of the University of Illinois–Illinois Department of Transportation Highway Planning and Research Program.

CLIMATIC DATA BASE

Temperature

Historical temperature data for the following 23 weather stations in and adjacent to Illinois were obtained from the National Oceanographic and Atmospheric Administration (NOAA).

Anna	LaHarpe
Belleville	Moline
Cairo	Mt. Vernon
Carbondale	Ottawa
Charleston	Peoria
Chicago	Quincy
Decatur	Rockford
Effingham	Springfield
Fairfield	St. Louis
Freeport	Urbana
Harrisburg	Whitehall
Kankakee	

The lengths of the records varied from 15 to 93 years, and all but one were 63 years or longer. After extensive interactions with Illinois State Water Survey climatologists and careful consideration of the nature of pavement temperature problems, it was concluded that a weekly analysis of temperature data was adequate. Average and standard deviation values for the

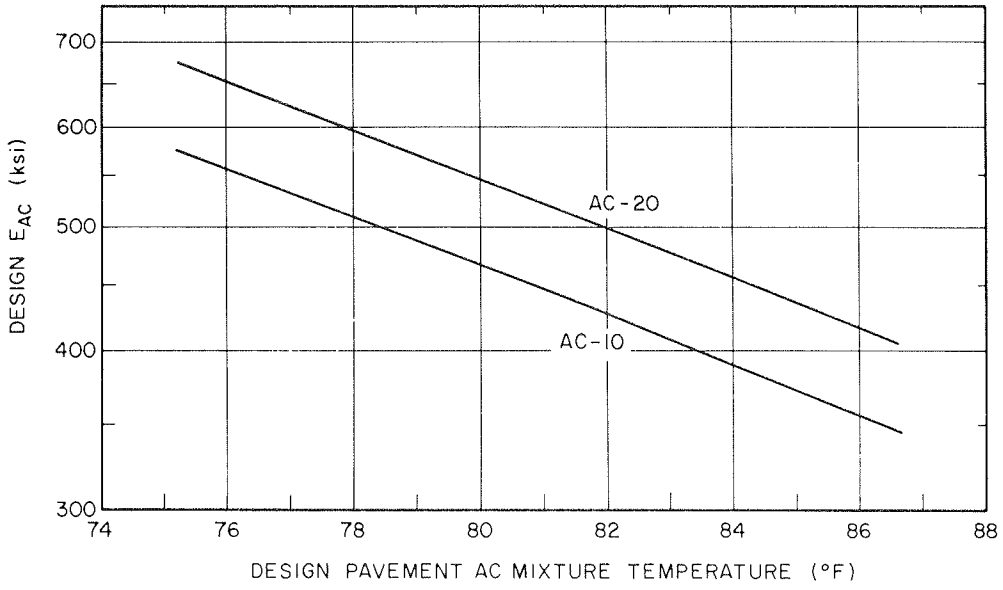

FIGURE 3 Asphalt concrete modulus-temperature relations.

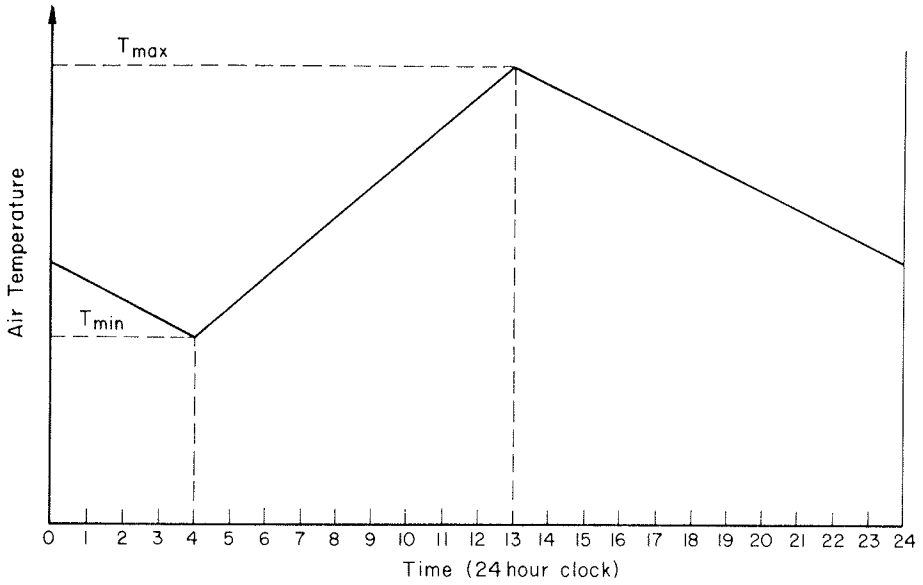

FIGURE 4 Diurnal temperature relation for heat-transfer model.

daily high, daily low, and daily mean temperatures were calculated using the NOAA data and a special computer program developed by the Illinois State Water Survey. Diurnal effects (which vary throughout the year) are considered by assuming that the maximum temperature occurs at 1:00 p.m. and the minimum temperature occurs at 4:00 a.m. as shown in Figure 4. Seven repetitions of the diurnal temperature cycle constitute a week's input to the heat-transfer model.

Percent Sunshine

NOAA data tapes for selected weather stations, in and adjacent to Illinois, were analyzed on a monthly basis to establish "percent sunshine" information. Percent sunshine data are available for only major weather stations. As much as possible, long-term records (37 to 89 years) were used. Comparisons were made for 20-year periods to ensure the continuity of the data set. The percent sunshine data are presented for each month in terms of isolines of percent sunshine on a map of Illinois, as shown in Figure 5. Typical standard deviations for the monthly percent sunshine data are from 6 to 13 percent.

Average Wind Speed

Average daily wind speed data (1965–1974, 20- to 25-ft recorder heights) for available National Weather Service stations in and around Illinois were evaluated by Illinois State Water Survey climatologists to establish average wind speeds for each month. The data are presented as isolines of average wind speed on a map of Illinois, as shown in Figure 6. Average monthly wind speed data do not vary by more than about 2 to 3 mph for various Illinois locations or months of the year. Heat-transfer model temperature calculations are not particularly sensitive to such small variations.

Combined Climatic Data Base

The most detailed available information is the temperature data for the 23 Illinois locations. Temperature data are much more variable (relatively) than either percent sunshine or wind speed.

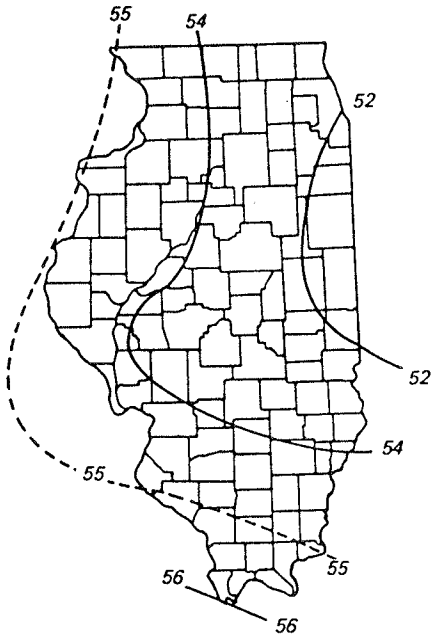

FIGURE 5 Percent sunshine data for March.

Thus most temperature-related pavement considerations are primarily controlled by air temperature inputs. Percent sunshine and wind speed data for each station were determined from the appropriate monthly maps for each location and added to the temperature data base (weekly values). The combined climatic data base was stored on floppy discs to facilitate data input for heat-transfer model calculations. A typical climatic data summary for Urbana, Illinois, is given in Table 1.

APPLICATIONS

Pozzolanic Stabilized Base Strength Development

Barenberg and Thompson *(11)* recommend using strength–degree-day (DD) relations for predicting the strength of

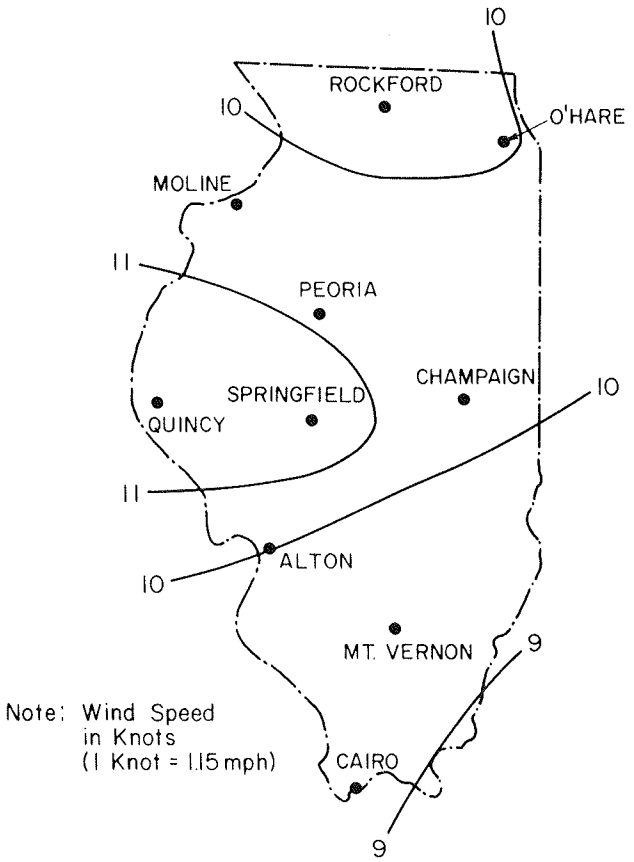

FIGURE 6 Wind speed data for March.

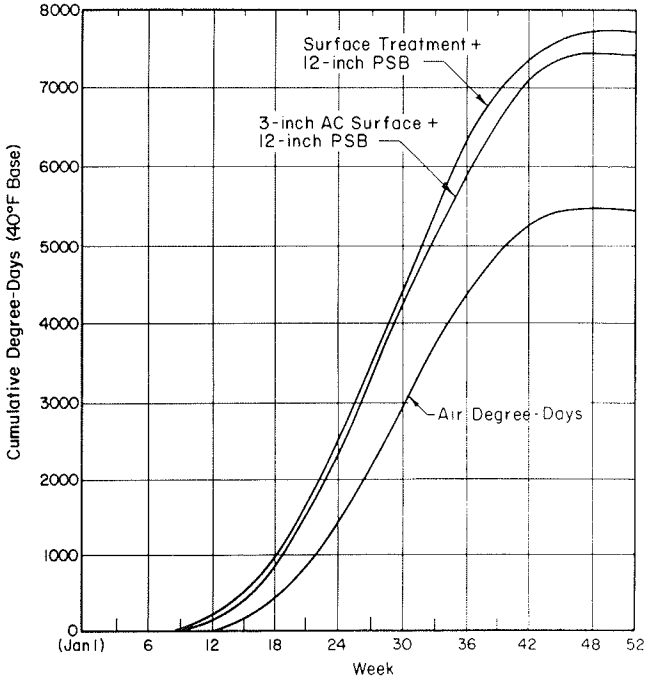

FIGURE 7 Degree-day–time data for Urbana, Illinois.

pozzolanic stabilized base (PSB) materials (DD based on 40°F reference temperature). The Illinois Department of Transportation uses strength-DD concepts for establishing late season (fall) construction cutoff dates for pozzolanic stabilized base materials.

A critical input to predicting PSB strength development in the field is the available DD during the curing period. The heat-transfer model has been previously used for DD calculations. PSB materials strength-DD relations vary depending on the flyash and activator (lime, cement, cement kiln dust, lime kiln dust) incorporated in the mixture. PSB mixture proportions also influence the strength-DD relation. Figure 1 data are for identical PSB mixes (3.5 percent activator, 9 percent flyash, 87.5 percent aggregate) with either lime or cement used as the activator. Two typical PSB pavements (3-in. AC surface + 12-in. PSB; bituminous surface treatment + 12-in. PSB; thermal properties given in Table 2) were evaluated for three Illinois locations (Rockford, Urbana, Cairo) that cover extremes of temperature in Illinois. Cumulative PSB layer DD-time relations for Urbana are shown in Figure 7. Air DD (40°F base) data are also shown. It is obvious that PSB DDs are responding primarily to air DDs. Statistical analyses of the middepth average PSB temperature and the air temperature indicated the PSB layer temperature can be accurately predicted from air temperature. The regression equations are

For 3-in. AC surface

$$T_{mix} = 2.9 + 1.08\,AT$$

$$R^2 = 0.996,\ SEE = 1.2$$

For bituminous surface treatment

$$T_{mix} = 1.15\,AT - 0.8$$

$$R^2 = 0.996,\ SEE = 1.4$$

T_{mix} is temperature (°F) at middepth of 12-in. stabilized base layer and AT is average air temperature (°F).

The stabilized layer temperatures predicted from air temperature can be used to calculate pavement DD. The air temperature DD procedure was compared with the heat-transfer model data. The maximum error in cumulative DD (for a year of data) was about 1.5 percent. The effect of depth within the stabilized layer on cumulative DD is negligible (approximately 1 DD/week per inch of depth). The equations are considered quite adequate for routine strength-DD predictions. The air DD procedure expedites the development of DD information for a particular location because the only needed climatic inputs are readily available average air temperature data.

AC Pavement Temperature

Figure 3 shows the large effect of temperature on AC modulus. The Shell *(12)* and the Asphalt Institute *(13)* pavement design procedures include procedures for estimating AC modulus–temperature relations. For given mixture and loading conditions, the AC temperature is the primary factor controlling modulus. Thus good AC pavement temperature input data are essential in flexible pavement analysis and design.

TABLE 1 CLIMATIC DATA BASE FOR URBANA, ILLINOIS

WEEK*	LOW TEMP. (F) AVERAGE	LOW TEMP. (F) STNDEV	HIGH TEMP. (F) AVERAGE	HIGH TEMP. (F) STNDEV	MEAN TEMP. (F) AVERAGE	MEAN TEMP. (F) STNDEV	SUN (%)	WIND (MPH)
1	26.28	7.16	43.26	8.61	34.77	7.66	52.0	11.5
2	28.78	6.12	46.25	7.99	37.51	6.82	52.0	11.5
3	30.87	6.90	49.32	8.83	40.10	7.66	52.0	11.5
4	33.55	6.51	52.96	8.82	43.25	7.47	52.0	11.5
5	35.75	5.74	55.47	7.95	45.61	6.57	56.0	12.1
6	37.51	5.00	57.99	7.12	47.75	5.78	56.0	12.1
7	40.93	6.05	62.18	7.59	51.56	6.66	56.0	12.1
8	43.77	5.51	64.96	6.42	54.36	5.69	56.0	12.1
9	45.72	5.48	67.24	6.96	56.48	5.94	62.0	12.1
10	47.90	5.71	69.48	7.33	58.69	6.29	62.0	12.1
11	49.38	4.51	70.57	5.74	59.97	4.86	62.0	12.1
12	52.58	5.50	74.39	6.47	63.49	5.71	62.0	12.1
13	54.72	5.66	76.31	5.96	65.52	5.53	62.0	12.1
14	57.87	4.90	79.31	6.10	68.59	5.28	69.0	12.7
15	59.18	4.50	80.88	5.42	70.03	4.57	69.0	12.7
16	60.57	4.27	82.48	5.06	71.52	4.36	69.0	12.7
17	62.52	4.70	83.87	5.17	73.20	4.70	69.0	12.7
18	63.37	4.18	85.13	4.73	74.25	4.27	74.0	10.4
19	63.55	4.46	85.64	4.54	74.60	4.15	74.0	10.4
20	64.60	3.83	86.54	4.37	75.57	3.80	74.0	10.4
21	64.76	3.70	86.35	4.23	75.55	3.62	74.0	10.4
22	64.58	4.24	86.30	4.51	75.44	4.13	69.0	09.2
23	63.74	4.21	85.42	4.44	74.58	3.94	69.0	09.2
24	63.02	3.91	84.44	4.36	73.73	3.75	69.0	09.2
25	62.26	4.38	83.44	4.15	72.85	3.96	69.0	09.2
26	60.65	4.58	83.09	4.54	71.87	4.23	69.0	09.2
27	60.26	5.20	82.21	5.22	71.24	4.78	66.0	08.1
28	58.18	4.79	81.01	5.56	69.59	4.84	66.0	08.1
29	55.46	5.49	78.22	5.89	66.84	5.34	66.0	08.1
30	52.47	5.58	75.47	5.70	63.97	5.15	66.0	08.1
31	49.04	5.72	72.69	5.93	60.87	5.30	64.0	07.5
32	47.03	6.12	69.92	6.20	58.48	5.74	64.0	07.5
33	45.30	5.57	67.95	6.90	56.62	5.89	64.0	07.5
34	41.90	6.55	63.48	7.94	52.69	6.86	64.0	07.5
35	39.24	6.07	59.85	7.97	49.55	6.64	64.0	07.5
36	36.90	6.02	56.12	6.82	46.51	6.03	50.0	08.6
37	33.90	5.88	51.83	6.98	42.87	6.12	50.0	08.6
38	32.55	7.02	50.10	7.56	41.33	6.90	50.0	08.6
39	28.15	5.83	44.10	6.46	36.13	5.85	50.0	08.6
40	26.28	7.35	42.07	7.85	34.17	7.39	41.0	10.4
41	24.00	8.22	39.14	8.21	31.57	8.02	41.0	10.4
42	21.12	9.13	36.14	8.46	28.63	8.60	41.0	10.4
43	21.57	8.35	36.14	7.66	28.85	7.80	41.0	10.4
44	20.08	8.05	35.53	7.12	27.80	7.32	45.0	11.5
45	18.18	9.37	33.78	8.66	25.98	8.83	45.0	11.5
46	17.90	9.79	33.48	9.13	25.69	9.33	45.0	11.5
47	19.08	9.32	35.01	8.42	27.05	8.71	45.0	11.5
48	16.84	10.41	33.32	9.65	25.08	9.85	45.0	11.5
49	17.50	9.75	33.59	8.38	25.55	8.87	49.0	11.5
50	19.17	10.03	35.25	9.11	27.21	9.40	49.0	11.5
51	21.37	8.27	37.86	7.84	29.61	7.82	49.0	11.5
52	23.87	7.43	39.98	7.90	31.93	7.48	49.0	11.5
53	23.87	7.43	39.98	7.90	31.93	7.48	49.0	11.5

*NOTE: WEEK 1 BEGINS MARCH FIRST

TABLE 2 THERMAL PROPERTIES OF MATERIALS

Material	Density (pcf)	Moisture Content (%)	Thermal Conductivity (BTU/Hr-Ft-°F) Unfrozen	Thermal Conductivity (BTU/Hr-Ft-°F) Freezing	Thermal Conductivity (BTU/Hr-Ft-°F) Frozen	Heat Capacity (BTU/lb-°F) Unfrozen	Heat Capacity (BTU/lb-°F) Freezing	Heat Capacity (BTU/lb-°F) Frozen
Asphalt concrete	148	2.0	0.7	0.7	0.7	0.22	1.44	0.22
Stabilized base	146	9.4	1.92	2.22	2.52	0.24	6.19	0.19
Portland cement concrete	150	3.0	1.25	1.29	1.33	0.22	2.16	0.22
Cohesive subgrade	129	17.0	0.92	1.02	1.13	0.29	10.49	0.22

TABLE 3 PAVEMENT TEMPERATURE AND *MMAT* FOR 12-IN. FULL-DEPTH AC PAVEMENT (°F)

	JAN.	FEB.	MARCH	APRIL	MAY	JUNE	JULY	AUG.	SEPT.	OCT.	NOV.	DEC.
ROCKFORD, IL												
MMAT*	21.0	24.6	35.6	48.5	59.4	69.1	74.0	71.9	64.2	52.3	38.4	26.0
1.5 in	25.1	29.2	41.5	56.7	69.5	80.3	85.5	82.3	72.1	57.5	42.3	29.5
Temp @ 6.0 in	27.8	29.9	40.5	54.8	67.2	77.8	83.3	81.1	72.3	58.7	44.4	32.0
10.5 in	30.3	30.7	39.7	53.1	65.0	75.3	81.2	79.9	72.3	59.8	46.4	34.3
URBANA, IL												
MMAT*	26.1	28.8	39.5	51.4	61.8	71.3	75.2	73.2	66.7	55.0	41.2	30.1
1.5 in	29.7	33.5	45.7	59.7	71.9	81.9	85.8	82.8	74.9	61.1	45.7	33.5
Temp @ 6.0 in	31.4	33.9	44.7	57.8	69.6	79.4	83.8	81.6	74.8	62.1	47.6	35.7
10.5 in	33.1	34.4	43.9	56.1	67.4	77.0	81.7	80.6	72 3	63.0	49.5	37.7
CAIRO, IL												
MMAT*	35.9	39.2	48.4	59.4	68.3	77.0	80.5	78.6	72.2	61.2	48.7	38.9
1.5 in	39.3	43.9	54.7	68.0	81.7	88.4	92.2	89.5	80.9	67.4	53.2	42.4
Temp @ 6.0 in	40.1	43.8	53.4	65.9	76.6	85.7	89.9	88.0	80.5	68.1	54.7	44.1
10.5 in	40.9	43.7	52.2	63.8	74.2	83.1	87.6	86.5	80.0	68.7	56.1	45.6

* MMAT - Mean Monthly Air Temperature

A typical 12-in. full-depth AC pavement (see Table 2 for material thermal properties) was analyzed for Rockford, Urbana, and Cairo, Illinois. Average monthly AC temperatures for 1.5-, 6-, and 10.5-in. depths in the full-depth section are summarized in Table 3. Mean monthly air temperature (*MMAT*) data are also included in Table 3 for comparison purposes. Linear regression analyses indicated that AC pavement temperature could be accurately predicted from air temperature data. The regression equations (developed from the combined data base for Rockford, Urbana, and Cairo) are

For 1.5-in. depth

$$T_{AC} = 1.15\ MMAT - 0.6$$
$$R^2 = 0.996,\ SEE = 1.4$$

For 6-in. depth

$$T_{AC} = 1.08\ MMAT + 2.9$$
$$R^2 = 0.999,\ SEE = 0.8$$

For 10.5-in. depth

$$T_{AC} = 1.0\ MMAT + 6.3$$
$$R^2 = 0.994,\ SEE = 1.5$$

where T_{AC} is AC mixture temperature (°F) and *MMAT* is mean monthly air temperature (°F); the average air temperature for a shorter time period, perhaps a week, would also be suitable.

Note the consistent progression (with depth) of the *MMAT* coefficients and the intercepts for the regression equations. The coefficient decreases and the intercept increases with depth. An equation that includes a depth parameter was developed:

$$T_{AC} = (0.76\ Z - 1.7) + (1.18 - 0.017\ Z)\ MMAT$$

where Z is depth from AC pavement surface in inches.

A comparison of the Shell *MMAT*–pavement temperature relation and the heat-transfer model data is shown in Figure 8.

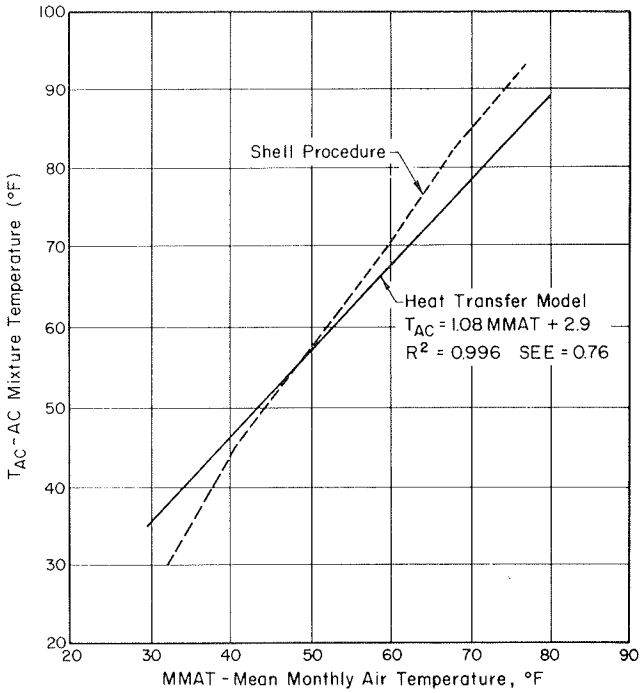

FIGURE 8 Comparison of Shell and heat-transfer model predictions.

The Shell-predicted pavement temperatures are in general larger, particularly at higher *MMAT*.

The Asphalt Institute procedure *(13)* based on Witczak's study *(14)* for estimating AC pavement temperatures is

$$MMPT = MMAT\ \ 1 + \left(1\ \ \frac{1}{z+4}\right) - \frac{34}{z+4} + 6$$

where

MMPT = mean monthly pavement temperature (°F),
MMAT = mean monthly air temperature (°F), and
z = depth in pavement layer (in.).

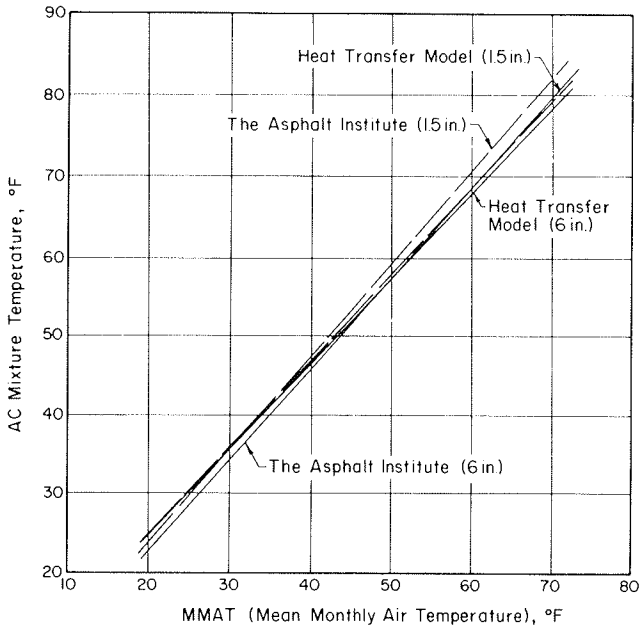

FIGURE 9 Comparison of the Asphalt Institute and heat-transfer model predictions.

Figure 9 shows comparisons between the Asphalt Institute procedure and the regression equations developed from the heat-transfer model data for the combined Rockford, Urbana, and Cairo data base. The agreement is excellent. It is encouraging to achieve such good concurrence between a theoretical heat flow model and a procedure derived from the statistical analysis of a comprehensive field-measured temperature data base.

Portland Cement Concrete (PCC) Pavement Curling

Temperature variations with depth through a PCC slab produce curling. The PCC slab can curl up, or down, or remain flat depending on the temperature gradient. There are large diurnal and seasonal variations in PCC slab gradients. The CMS heat-transfer model and Urbana, Illinois, climatic data were used to establish typical temperature-depth relations for a 9-in. PCC slab. Thermal properties of the PCC and subgrade soil are given in Table 4. Typical diurnal effects are shown in Figures 10–12 for April, July, and November.

TABLE 4 TEMPERATURE EFFECTS ON FWD DEFLECTION (9-in. PCC slab)

Time	8-Kip Deflection[a] (mils)	Air Temperature (°F)
7:45 a.m.	26.0	69
9:00 a.m.	17.5	76
10:30 a.m.	12.5	79
11:30 a.m.	9.0	83
1:00 p.m.	11.0	84
2:00 p.m.	8.0	87
3:00 p.m.	9.5	85
4:00 p.m.	10	82

[a]Edge loading at a transverse joint (dowel load transfer).

It is apparent that PCC temperature-depth relations are complex. A constant gradient (maximum temperature difference/slab depth) is obviously not the general case. In future University of Illinois studies, procedures will be developed to more accurately characterize temperature and depth relations and

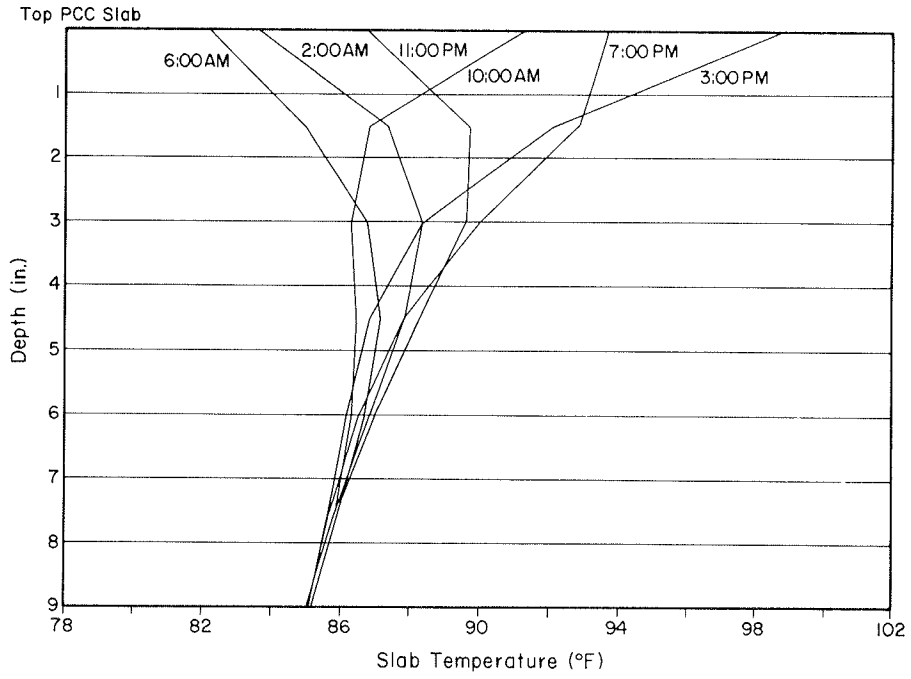

FIGURE 10 Temperature distribution in PCC slab (April, Urbana, Illinois).

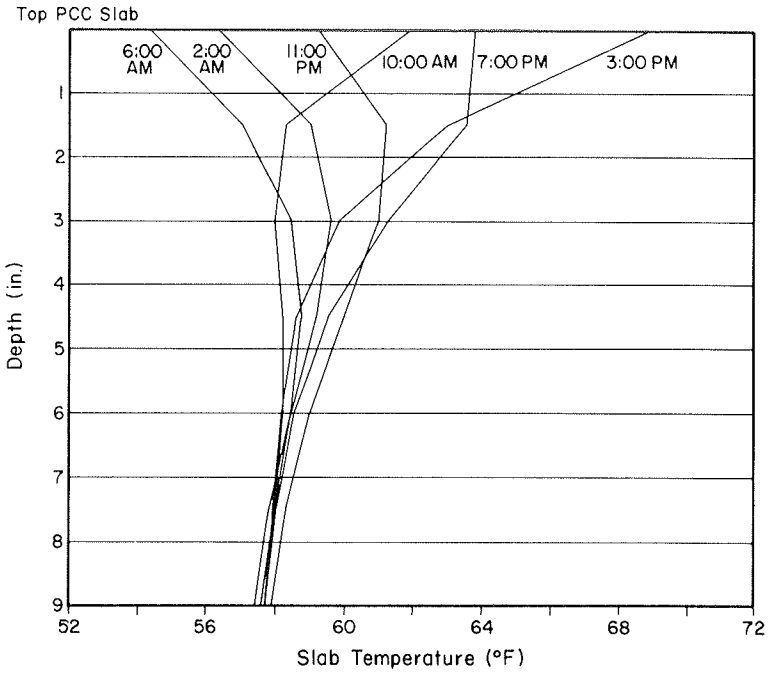

FIGURE 11 Temperature distribution in PCC slab (July, Urbana, Illinois).

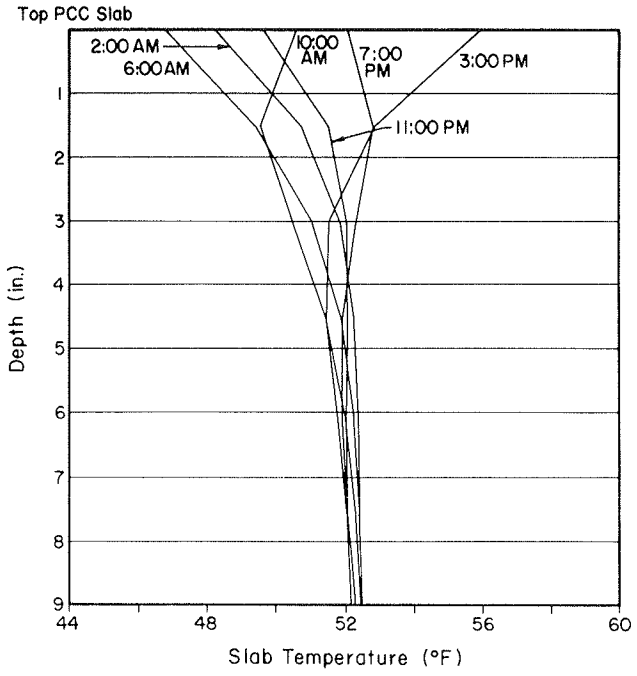

FIGURE 12 Temperature distribution in PCC slab (November, Urbana, Illinois).

PCC slab curling mechanics. Curling stresses should be included in the analysis and design of PCC pavements. The nondestructive testing deflection data in Table 4 demonstrate the significant effect of temperature on the structural response of pavement. The increased early morning deflections are due to the curled-up condition of the PCC slab and the accompanying loss of slab support.

SUMMARY

Pavement temperatures can be accurately quantified with the CMS computer model developed at the University of Illinois. Required CMS inputs for temperature modeling are *(a)* thermal properties of materials and soils, *(b)* air temperature data, *(c)* solar radiation data, and *(d)* wind velocity data.

In this paper the development and use of a comprehensive Illinois Climatic Data Base for Pavements are presented. Air temperature data are summarized on a weekly basis and solar radiation and wind speed data are presented in the form of a monthly state map.

Illustrative applications-oriented examples are presented for

- Strength–degree-day curing relations for pozzolanic stabilized base materials,
- Asphalt concrete moduli–pavement temperature effects, and
- Temperature gradients in portland cement concrete slabs.

The emphasis in the paper is on the concepts and techniques used to establish the Illinois Climatic Data Base for Pavements. The illustrative information demonstrates the versatility and usefulness of the Climatic Data Base and heat-transfer model procedures in pavement analysis and design.

The procedures and techniques described can be used to establish a climatic data base for other states and locations. The climatic data base–CMS model approach is recommended for quantifying temperature effects in flexible and rigid pavement analysis and design.

REFERENCES

1. M. R. Thompson, and B. J. Dempsey. *Final Report–Durability Testing of Stabilized Materials.* Civil Engineering Studies, Transportation Engineering Series 11. University of Illinois at Urbana-Champaign, June 1974.

2. M. R. Thompson and K. Cation. *Proposed Full-Depth Asphalt Concrete Thickness Design Procedure.* Civil Engineering Studies, Transportation Engineering Series 45. University of Illinois at Urbana-Champaign, July 1986.
3. B. J. Dempsey and M. R. Thompson. A Heat Transfer Model for Evaluating Frost Action and Temperature Related Effects in Multi-Layered Pavement Systems. In *Highway Research Record 342*, HRB, National Research Council, Washington, D.C., 1970, pp. 39–56.
4. B. J. Dempsey, W. A. Herlache, and A. J. Patel. Climatic-Materials-Structural-Pavement Analysis Program. In *Transportation Research Record 1095*, TRB, National Research Council, Washington, D.C., 1986, pp. 111–123.
5. R. F. Scott. Estimation of the Heat-Transfer Coefficient Between Air and the Ground Surface. *Transactions of the American Geophysical Union*, Vol. 38, No. 1, 1957.
6. R. F. Scott. *Heat Exchange at the Ground Surface.* U.S. Army Materiel Command, Cold Regions Research and Engineering Laboratory, Hanover, N.H. 1964.
7. R. F. Scott. Heat-Transfer at the Air-Ground Interface with Special Reference to Freezing and Thawing Problems Below Airfield Pavements. Thesis. Massachusetts Institute of Technology, Cambridge, 1955.
8. R. L. Berg. *Energy Balance on a Paved Surface.* U.S. Army Terrestrial Sciences Center, Hanover, N.H., 1968.
9. B. J. Dempsey, W. A. Herlache, and A. J. Patel. *Environmental Effects on Pavements—Theory Manual.* FHWA/RD084-115. FHWA, U.S. Department of Transportation, 1985, Vol. 3.
10. M. S. Kersten. *Thermal Properties of Soils.* Bulletin 28. Engineering Experiment Station, University of Minnesota, Minneapolis, 1949.
11. E. J. Barenberg and M. R. Thompson. *NCHRP Synthesis of Highway Practice 37: Lime-Fly Ash Stabilized Bases and Subbases.* TRB, National Research Council, Washington, D.C., 1976.
12. *Shell Pavement Design Manual.* Shell International Petroleum Company, Ltd., London, England, 1978.
13. *Research and Development of the Asphalt Institute's Thickness Design Manual (MS-1) Ninth Edition.* Research Report 82-2. The Asphalt Institute, College Park, Md., Aug. 1982.
14. M. W. Witczak. Design of Full Depth Asphalt Airfield Pavements. *Proc., Third International Conference on the Structural Design of Asphalt Pavements*, London, England, 1972.

Publication of this paper sponsored by Committee on Strength and Deformation Characteristics of Pavement Sections.

Temperature Response of Concrete Pavements

JAMSHID M. ARMAGHANI, TORBJORN J. LARSEN, AND LAWRENCE L. SMITH

Displacements of concrete pavement slabs are mainly associated with temperature. Slab curling and joint movements greatly influence the response of concrete pavements to traffic loads. Identifying the times and temperature conditions at which the pavement system offers the least resistance to traffic loads should be a prime concern to pavement engineers. Therefore research has been initiated to analyze pavement temperatures and evaluate the vertical and horizontal displacements in the pavement slabs. At the Bureau of Materials and Research of the Florida Department of Transportation, a specially designed test road was constructed to simulate actual design features of Florida highways. This test road was instrumented with linear variable differential transformers and thermocouples at various locations. A data acquisition and control unit was used to record and store simultaneously the pavement displacements and the temperatures at specified time intervals. Pavement temperatures collected over a period of 3 years were analyzed. Vertical displacements at slab corners, edges, and centers were evaluated. Horizontal slab movements at doweled and undoweled joints were also determined. This paper may provide some understanding of pavement response to temperature and further strengthen awareness of the effect of temperature on pavement system stiffness.

Temperature is an important factor influencing the functioning of concrete pavements. Variations in concrete temperature cause horizontal as well as vertical displacements in pavement slabs. Such displacements affect two sets of stiffness parameters, *(a)* the shear and moment resistance at joints, which determine the load transfer between adjoining slabs, and *(b)* the magnitude and direction of slab curling, which determine the degree of support offered by the subgrade. Consequently, the structural response of concrete pavements under traffic loads is highly dependent on temperature and its variation.

Temperature effects on concrete pavement behavior have been recognized since the mid-1920s. Westergaard *(1)* identified temperature curling as an important parameter affecting the structural behavior of concrete pavements. In 1940 Lang *(2)* studied the movement of concrete pavement slabs resulting from changes in temperature and moisture. He analyzed temperature data obtained from a 7-in. concrete slab over a period of 1 year. Friberg *(3)* presented a mathematical evaluation of horizontal slab movements, and the effect of the subgrade frictional resistance, on stress development in pavements. Harr and Leonards *(4)* conducted laboratory tests to measure temperature curling and compute subsequent stresses. They correlated the results from the laboratory tests with predicted response with an analytical model that they developed. Tayabji and Colley *(5)* reported that excessive slab movements caused by temperature variations may result in lockups of doweled joints. This could result in midslab cracking and spalling of the concrete surrounding the dowels.

It is the objective of this paper to more precisely describe the displacements of a concrete pavement slab associated with temperature variation and weather. Temperature data, accumulated between 1983 and June 1986 from a test road, are analyzed. This is followed by a description of pavement response to temperature, which is based on the analysis of displacement measurements that were obtained from test road slabs.

Bureau of Materials and Research, Florida Department of Transportation, P. O. Box 1029, Gainesville, Fla. 32602.

TEST ROAD

A concrete test road was constructed at the Bureau of Materials and Research of the Florida Department of Transportation. The layout of the test road, shown in Figure 1, incorporates six slabs with doweled and undoweled joints. Each slab is 20 ft long, 12 ft wide, and 9 in. thick. Since its construction in 1982, this test road has been used for a number of research activities designed to obtain basic understanding of concrete pavements.

Instrumentation

Air and pavement temperatures were measured using thermocouples. Figure 1 shows four locations in which arrays of thermocouples were imbedded in concrete at the time of construction. Arrays of two thermocouples were used in Slab 3, and in Slab 4 arrays of five thermocouples were installed. Figure 1 shows details of the arrangement of thermocouples in Slabs 3 and 4. Another thermocouple was used to monitor ambient temperature. This thermocouple was housed in a white-painted wooden box, with open bottom and numerous 1-in.-diameter holes on the sides. The box was installed on a 5-ft wood post and was 8 ft away from the nearest building.

Slab displacements were monitored using linear variable differential transformers (LVDTs). The LVDTs were installed in vertical and horizontal directions. The horizontal LVDTs were installed across doweled Joint 5 and undoweled Joint 4. A detailed diagram of a horizontal LVDT is shown in Figure 1. The brackets used to hold the LVDT were made out of a brown phenolic board that is highly weatherproof. The vertical LVDTs were installed at the center and edge of Slab 4. Two more vertical LVDTs were placed at both sides of Joint 4 at corners of Slabs 3 and 4. Figure 1 shows a schematic diagram of a vertical LVDT. As shown in this diagram, the LVDT is held at one end by a bracket fastened to the side of the slab. The

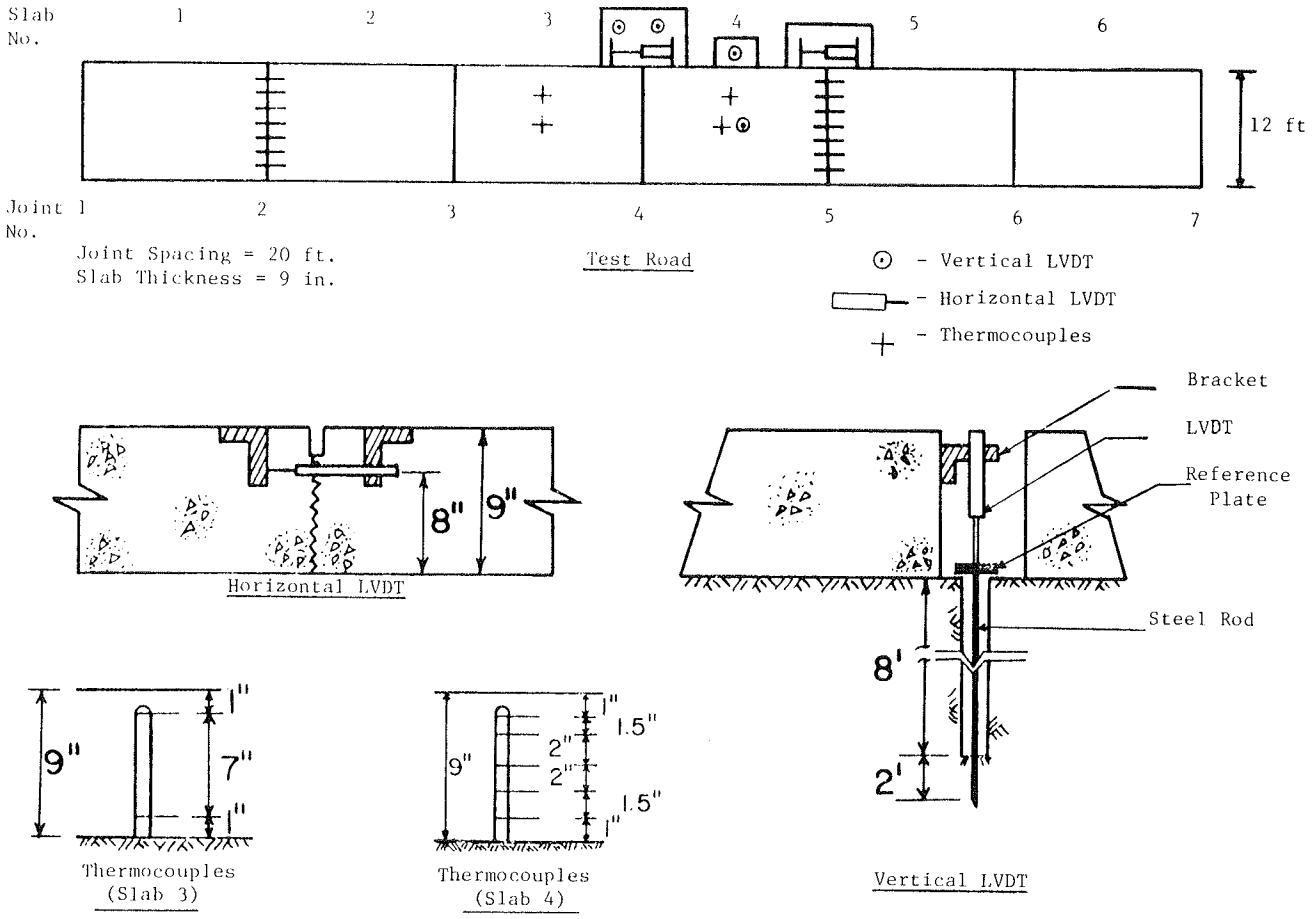

FIGURE 1 Layout of test road and details of instrumentation.

transformer core rests against a reference plate fastened to a 10-ft-long invar steel rod. This arrangement was necessary to isolate the reference plate from the surroundings and thus ensure precise measurement of slab displacements. The two corner LVDTs at Joint 4 were 4 in. apart, and the edge LVDT was installed midway between Joints 4 and 5.

Data Collection

Temperature measurements from the test road were recorded between 1983 and 1986. Pavement and air temperatures were normally recorded at 1-hr intervals. However in conjunction with other tests, temperatures were measured at 30- or even 15-min intervals. A programmable Fluke data logger was used to record simultaneously measurements from pavement and air thermocouples. Consecutive 24-hr cycles of temperature measurement were collected during the monitoring period. However, periods of interruption in data collection were experienced because of equipment maintenance.

The second part of the study, which involved the measurement of slab displacements, was conducted between January and June 1986. A data acquisition and control unit (HP 3497A) was programmed by an HP85B computer to record simultaneously the LVDT and thermocouple measurements at 30-min intervals. Horizontal slab displacements were monitored at the undoweled Joint 4 and the doweled Joint 5. Displacements in the vertical directions were also measured at the adjoining corners of Slabs 3 and 4 and at the center and edge of Slab 4. Data collection was continuous except during March, when the data recording system was unavailable. It should be mentioned that daily observations of weather conditions were documented to assist in the analysis of data.

ANALYSIS OF TEMPERATURE DATA

Information obtained from the temperature records included average pavement temperatures, temperature differentials, and characteristics of the different temperature gradients across the slab thickness. Average pavement temperatures were computed from temperature readings of the five thermocouples at the edge of Slab 4. Temperature differentials were computed by subtracting temperature readings at 8 in. below the slab surface from those at 1 in. below the surface. Negative temperature differential implied that surface temperature was lower than bottom temperature, and positive temperature differential indicated that the slab was warmer at the surface. Variation of temperature with time was determined for each of the five depths (1, 2.5, 4.5, 6.5, and 8 in.). Thorough examination of hourly temperatures at different slab depths revealed certain trends in temperature distribution across slab thickness.

Air and Pavement Temperatures

Figure 2 shows typical variation of air and pavement temperatures with respect to time during clear and sunny weather.

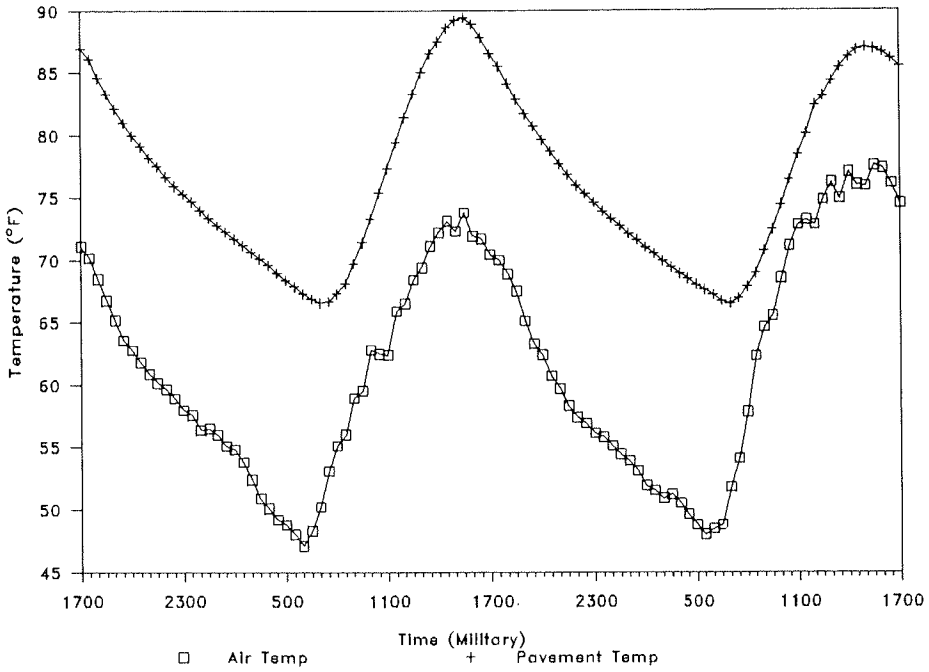

FIGURE 2 Temperature versus time.

Under such conditions, the temperature variation approximates a sine wave. However, it was observed that during cloudy and rainy weather temperature variation in the pavement did not follow any particular pattern. It is interesting to note that variation in pavement temperature follows a pattern that is similar to that of air temperature. The rate of variation in pavement temperature is higher during daytime than during nighttime. Solar radiation is likely responsible for the high rate of temperature variation during daytime hours.

Figure 2 also shows that pavement temperature is higher than air temperature. This observation was not limited to the data presented in Figure 2; a general trend was noted from the accumulated data. Under clear skies pavement temperatures were normally 15°F to 25°F higher than ambient temperatures. However, the difference in temperature drastically decreased during cloudy and rainy weather.

Maximum and minimum pavement temperatures occurred normally 1 to 2 hr after air temperatures reached their maxima and minima.

This trend is evident not only from the sample of data presented in Figure 2; it was observed in the majority of the samples that were randomly selected from the collected temperature data. Table 1 gives the results of the statistical analysis of temperature data obtained between 1983 and June 1986. A population of 230 sample days was randomly selected for the analysis. All months were represented in the analysis with equal numbers of samples. It is obvious from Table 1 that minimum temperatures occur most frequently between 5:00 a.m. and 7:00 a.m. for air and between 6:00 a.m. and 8:00 a.m. for pavement. On the other hand, maximum temperatures occur most frequently between 12:00 noon and 2:00 p.m. for air and between 1:00 p.m. and 3:00 p.m. for pavement.

Temperature Distribution

Figure 3 shows typical 24-hr variation in temperature at different slab depths. The temperature data were obtained on a clear day. As may be expected, the surface of the slab experiences the highest rate of temperature change. The rate of temperature change decreases with depth, reaching minimum at the bottom of the slab. It is evident from Figure 3 that slab temperatures during the night are coolest at the surface and warmest at the bottom. Soon after daybreak, the temperature at the slab surface starts to increase rapidly. After a short transition period, slab temperatures become warmest at the surface and coolest at the bottom.

Table 1 gives the most frequent times at which minimum and maximum temperatures occurred at the surface, center, and bottom regions of the slab. It can be observed that the different slab depths reach maximum and minimum temperatures at different times. Obviously, the temperature at the slab surface reaches maximum or minimum first, and the bottom temperature reaches similar levels last. The delay, as indicated by the data in Table 1, is between 2 and 4 hr.

The temperature differential between the surface and the bottom of the slab is responsible for the magnitude and direction of slab curling. Figure 4 shows typical variation of temperature differential with respect to time of day. It is evident that temperature differential is negative during night hours and positive during daytime hours. Figure 4 shows that maximum negative and positive temperature differentials occurred at 6:00 a.m. and 1:00 p.m., respectively. Table 1 gives similar times for a population of 230 days of temperature records.

The transition between negative and positive temperature differentials occurred twice during the 24-hr thermal cycle. It can be seen from Figure 4 that zero temperature differential occurred at approximately 9:00 a.m. and 7:00 p.m.

TABLE 1 MOST FREQUENT TIMES OF OCCURRENCE OF MAXIMUM AND MINIMUM TEMPERATURES

Description	Minimum		Maximum	
	Time (Military)	Percent Frequency	Time (Military)	Percent Frequency
Air Temperature	500 - 700	64	1200 - 1400	36
Average Pavement Temp.	600 - 800	81	1300 - 1500	68
Pavement Surface Temp.	600 - 800	72	1300 - 1500	71
Pavement Center Temp.	700 - 900	74	1500 - 1700	68
Pavement Bottom Temp.	800 - 1000	71	1700 - 1900	61
Negative Temp. Differential	---	---	500 - 700	54
Positive Temp. Differential	---	---	1200 - 1500	67

No. of Samples = 230 --- Not Applicable

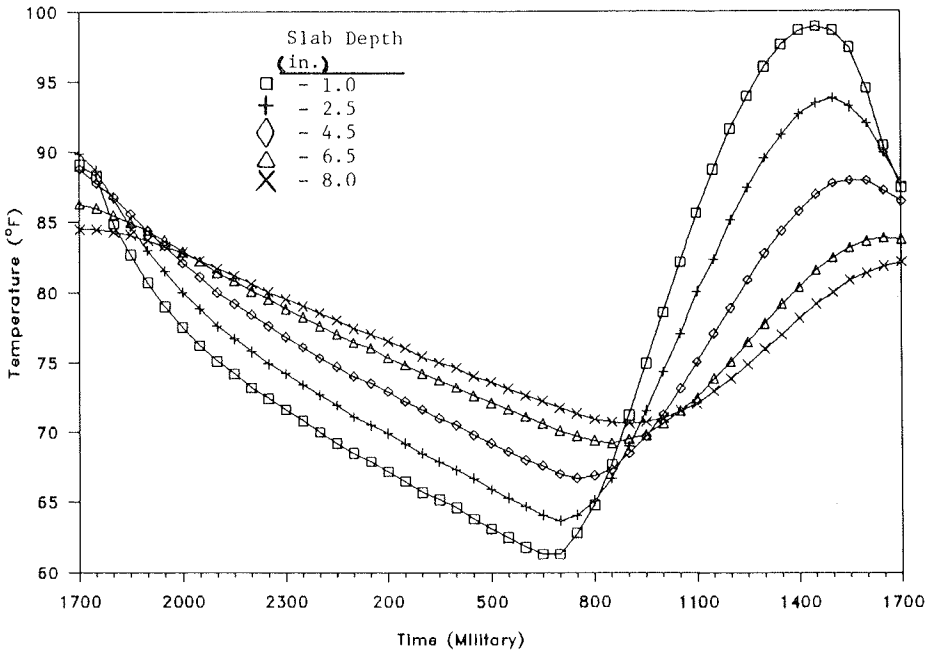

FIGURE 3 Temperature variation at different slab depths.

Figure 5 shows typical temperature gradients across the 9-in.-thick slab. The temperature gradients can be described as nonlinear. Results from another study (see paper by Richardson and Armaghani in this Record) showed that the temperature distributions are best modeled by parabolic equations. However, in many analyses of thermal stresses, temperature gradients have been assumed to be linear. This assumption has simplified the modeling of pavements without significantly affecting the accuracy of the computations. Therefore, for all practical purposes the temperature gradient can be approximated by a linear curve.

Effect of Weather Conditions on Pavement Temperature

Relating temperature data to weather conditions provided interesting information on the sensitivity of pavement temperature to changes in the weather. As might be expected, pavement temperatures fluctuated from season to season in a manner similar to fluctuations of ambient temperatures. However, temperature differential of the slab was not as much influenced by the magnitude of ambient temperature as it was by weather conditions. For example, the maximum temperature differentials were generally higher on clear days than on hazy or cloudy

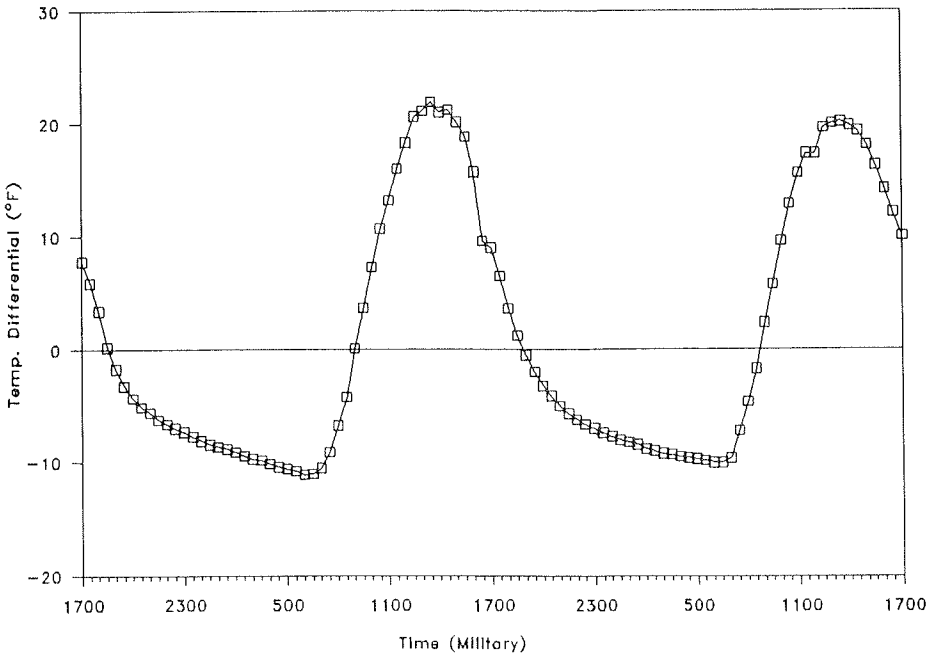

FIGURE 4 Temperature differential versus time.

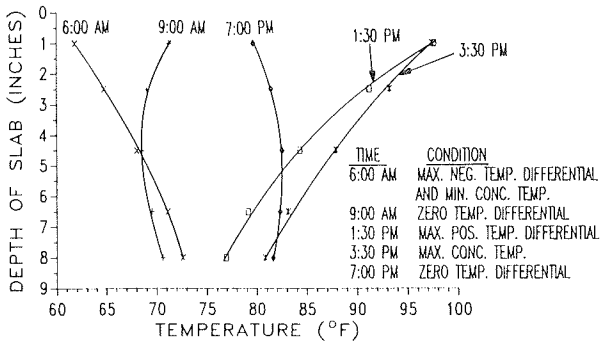

FIGURE 5 Typical temperature gradients for 9-in. slab.

days. Obviously, greater variations in air temperature are responsible for higher maximum temperature differentials.

An experiment was performed on the test road to study the effect of shade (normally associated with cloudy weather) on pavement temperature. Temperatures were measured from thermocouple arrays at the edge and the center of Slab 4 on 2 consecutive sunny days. During the first 24 hr, the thermocouple array in the center was covered with a white wooden box. At the end of this period the box was removed to provide equal exposure at both locations for the next 24 hr. Figure 6 shows the effect of shade on surface temperature at the center of the slab. It can be observed that during daytime the temperature of the shaded center is much lower than that of the edge. Such differences became insignificant during the night. However, when the shade was removed, temperatures at both locations were quite close; temperatures at the center were slightly higher during daytime.

A second test was conducted on the test road to determine the effect on pavement temperature of sudden exposure to moisture. The test was intended to model the temperature "shock" that results from an afternoon rain (a common weather situation in Florida during summer) on a hot pavement surface.

Figure 7 shows the air and pavement temperatures with respect to time. The linear temperature gradient, designated as A, represents the dry hot pavement at 3:00 p.m. Water at 76°F was applied to the surface of Slab 4 shortly after 3:00 p.m. An hour later, with surface flooding in progress, substantial changes in pavement temperature were observed, as illustrated by Condition B. Surface temperature dropped 8.5°F while the bottom of the slab had not yet felt the effect of surface quenching. As a consequence, the shape of the temperature gradient across the slab thickness shifted from linear to nonlinear. It has been demonstrated that the nonlinearity associated with rapid cooling of a pavement surface produces high tensile stresses, which could be critical if combined with stresses induced by traffic and slab curling (see paper by Richardson and Armaghani in this Record).

CONCRETE PAVEMENT RESPONSE TO TEMPERATURE

Under ideal conditions, a pavement slab responds to the temperature differential across its thickness in the manner shown in Figures 8*a*, 8*b*, and 8*c*. The ideal slab assumes a no-curl (flat) condition at zero temperature differential. At negative temperature differential the slab curls upward at the edges, with the corners exhibiting the largest curling while the center is in contact with the subgrade. In contrast, positive temperature differential causes upward curling at center and downward curling along the edges.

In reality, however, pavement slabs do not necessarily assume a no-curl position at zero temperature differential. In a separate study *(6)*, surface elevations along the undoweled Joint 4 of the test road were measured at various temperature differentials, as shown in Figure 9. It can be observed that the slab assumed the no-curl condition at +9°F temperature differential. The logical explanation for such inconsistency between the ideal and the observed pavement responses is the

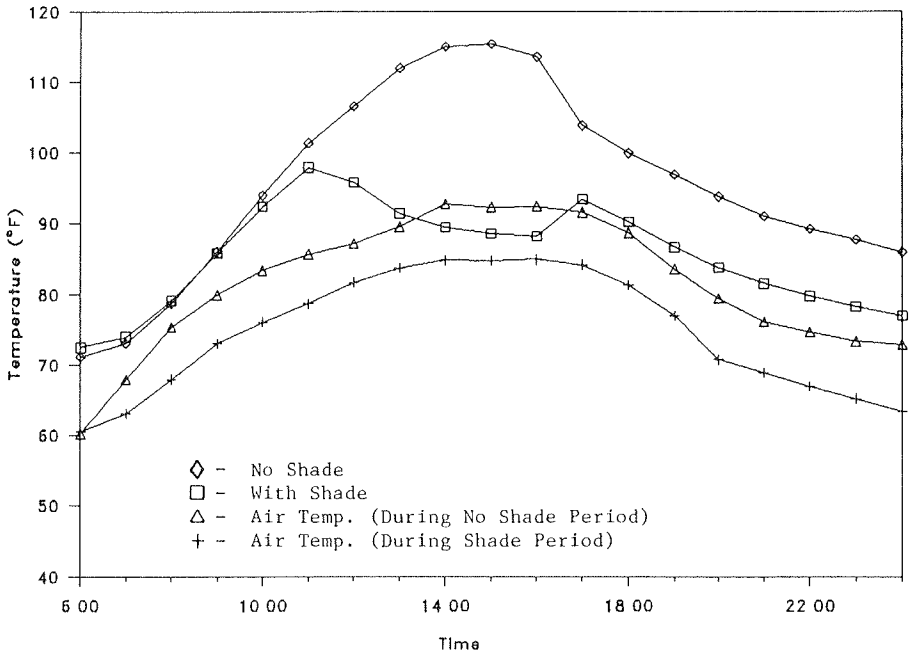

FIGURE 6 Effect of shade on concrete temperature.

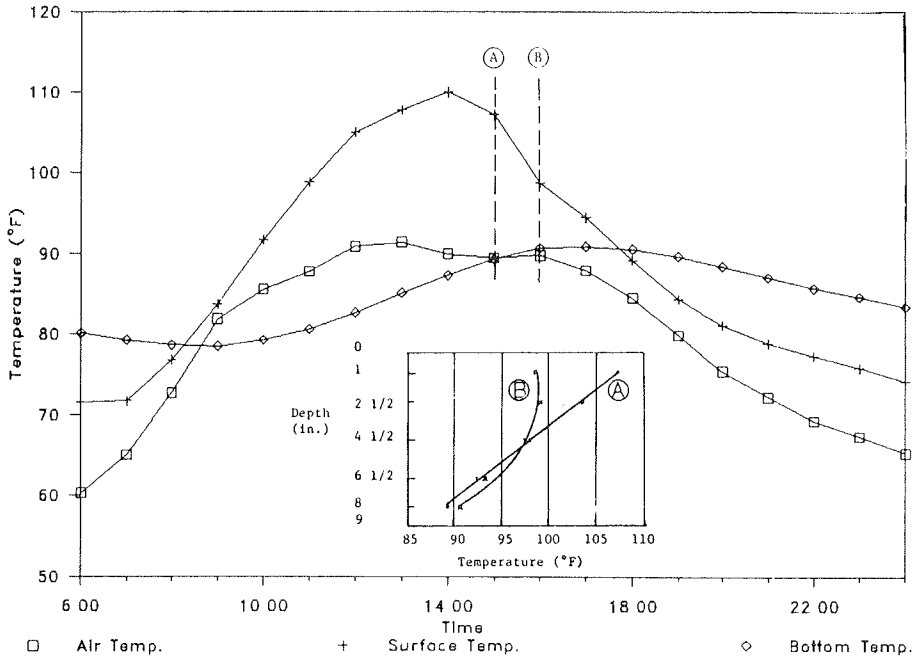

FIGURE 7 Effect of sudden exposure to moisture on concrete temperature.

possible influence on displacements of moisture or shrinkage differentials, or both, within the slab. Warping of slabs associated with moisture and shrinkage had also been observed by Harr and Leonards *(4)* and by Childs *(7)*. Figures 8*d* and 8*e* show upward warping due to moisture and shrinkage warping, respectively. It is therefore logical to assume that a +9°F temperature differential is required to offset the upward warping of the test road slabs associated with moisture or shrinkage, or both.

Analysis of Vertical Slab Displacements

Simultaneous recording of vertical displacements at the corner, edge, and center of a slab provided an excellent opportunity to compare the responses of different slab positions to variations in temperature. Figure 10 shows vertical slab displacements with respect to time. The four curves presented in this figure reflect surface elevations at the edge, center, and corner of Slab 4 and also at the corner of Slab 3 adjoining Slab 4. Slab displacements shown in Figure 10 correspond to temperature differentials shown in Figure 4.

It can be seen from close examination of Figures 10 and 4 that vertical slab displacements are highly sensitive to changes in temperature differential of the slab. Evidence of such sensitivity is the close association between rates of slab displacements, particularly at the corners, and the rate of change in temperature differential. Furthermore the maximum displacements

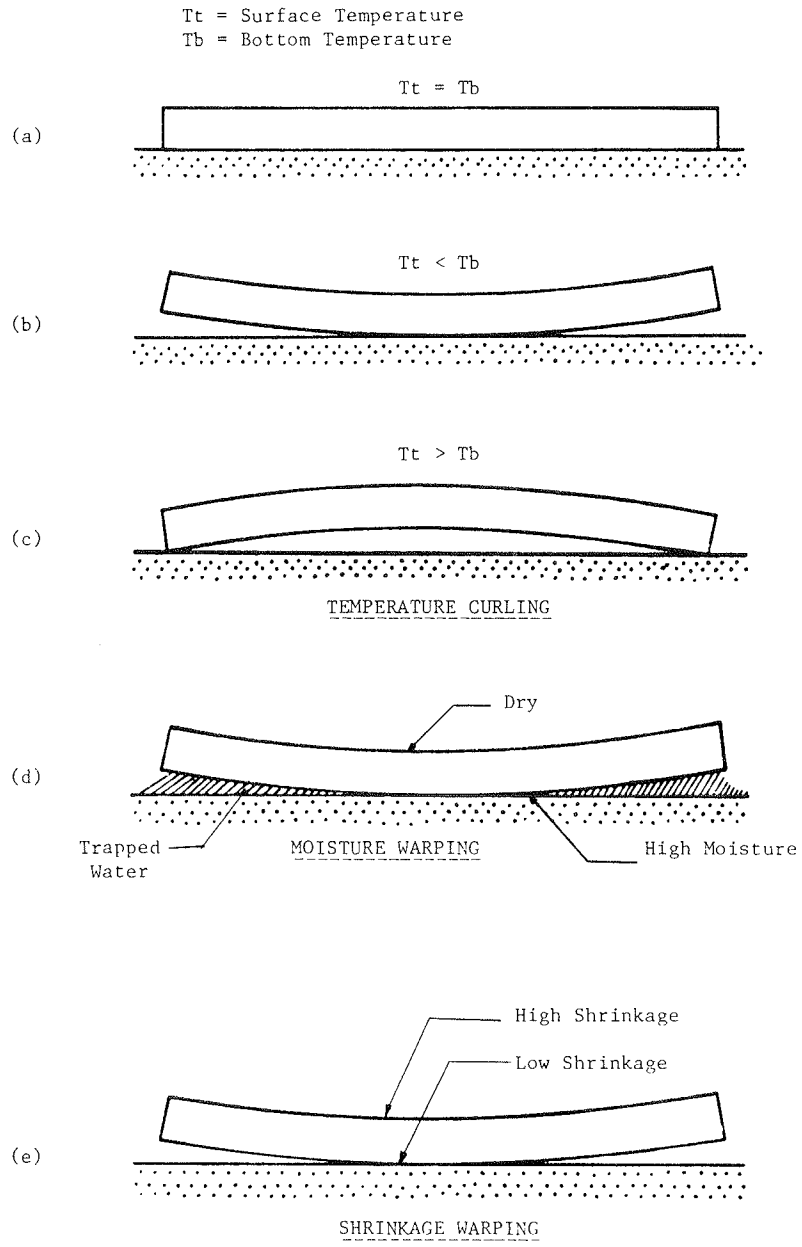

FIGURE 8 Curling and warping of pavement slabs.

at the different slab positions are almost concurrent with the maximum negative and positive temperature differentials.

The slab edge and corner displaced in a direction opposite to the displacement at the center. However, maximum displacements at the three positions were reached at about the same time. In reference to Figures 4 and 10, as the temperature differential changes from positive to increasingly negative, the edge and corner of the slab curl upward (indicated by an increase in negative displacement) while the center curls downward (indicated by an increase in positive displacement). The three slab positions reach maximum curling at approximately 6:00 a.m., which is about the time when temperature differential reaches maximum negative. Conversely, as the temperature differential gradually changes from negative to positive, the edge and corner of the slab curl downward while the center curls upward. The maximum displacements coincide at approximately 2:00 p.m., the time at which maximum positive temperature differential is also reached. It is interesting to note that the rate of vertical displacement is higher during the daytime. This can be attributed to a rapid increase in surface temperature of the pavement, which is associated mainly with intensifying solar radiation.

In addition to reaffirming that maximum slab curling occurs at the corner, Figure 10 shows another important characteristic of corner displacements at undoweled joints. Despite equal slab lengths, the adjoining corners of Slabs 3 and 4 exhibited variable displacements or uneven curling. Therefore it is logical to assume that the variability would be even higher if one of the adjoining slabs were shorter than the other, as in the case of randomly spaced pavement slabs. Such variability in displacements can result in possible restraint of joint movements, which in turn may induce stresses in the pavement.

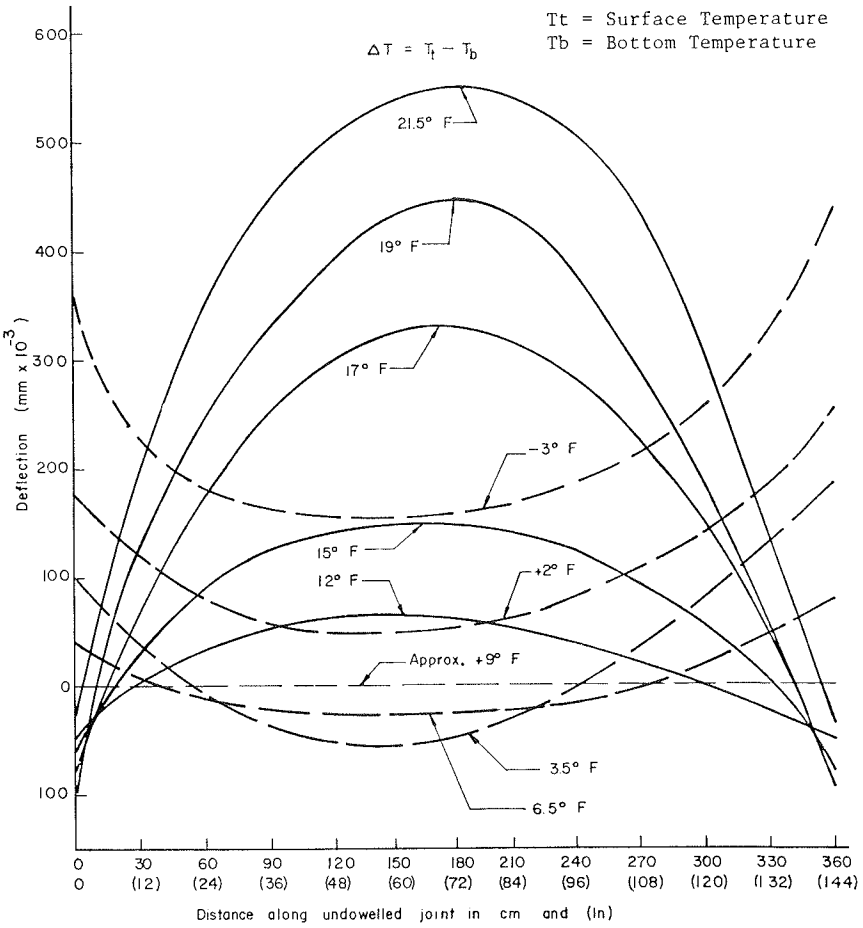

FIGURE 9 Deflection profiles along a joint due to change in the temperature differential.

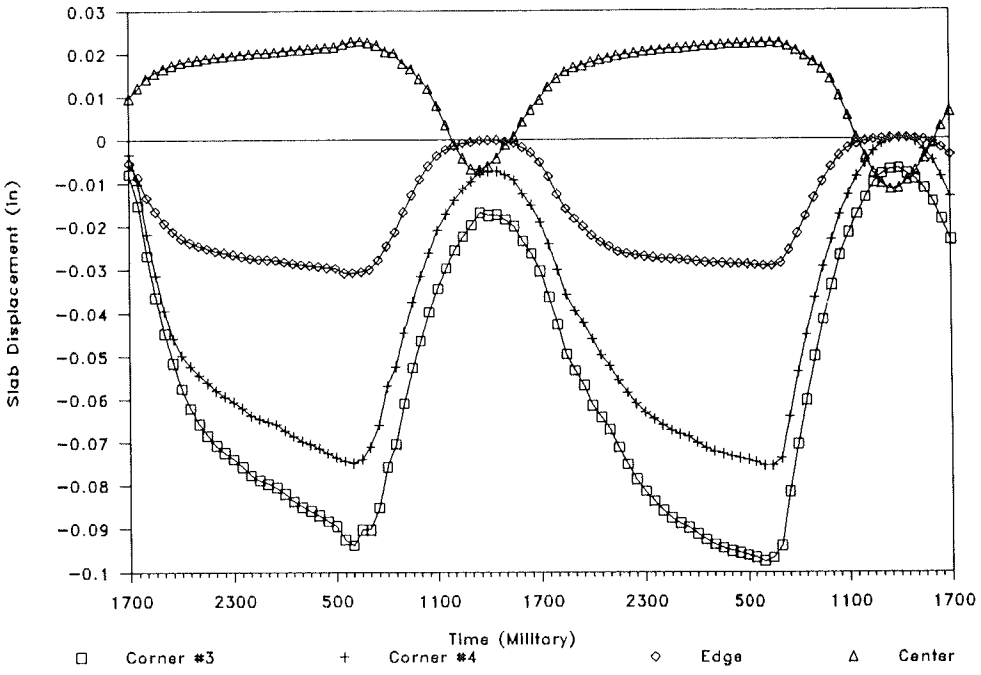

FIGURE 10 Vertical displacements of slab at center, edge, and corner (joint).

TABLE 2 MAXIMUM VERTICAL DISPLACEMENTS OF TEST ROAD SLABS

MONTH	TIME (MILITARY)		TEMPERATURE DIFFERENTIAL (°F)		AVERAGE CONCRETE TEMP. (°F)		MAXIMUM VERTICAL DISPLACEMENTS (inch)			
							CORNER		EDGE	CENTER
	FROM	TO	FROM	TO	FROM	TO	SLAB 3	SLAB 4	SLAB 4	SLAB 4
JAN.	700	1400	-7	+17	52	69	0.046	0.046	0.019	0.021
	1400	700	+19	-7	66	51	0.051	0.050	0.020	0.023
FEB.	600	1400	-9	+17	54	71	0.059	0.059	0.023	0.022
	1400	600	+17	-5	71	62	0.044	0.042	0.017	0.020
APRIL	600	1400	-11	+20	68	86	0.098	0.085	0.030	0.037
	1400	600	+21	-10.5	88	66	0.092	0.077	0.029	0.037
MAY	500	1300	-8	+25	77	99	0.089	0.068	0.028	0.045
	1400	500	+25	-7	103	86	0.084	0.066	0.026	0.040
JUNE	500	1400	-6.5	+23	89	107	0.081	0.065	0.026	0.036
	1400	500	+23	-6	107	89	0.080	0.066	0.027	0.035
					AVERAGE		0.072	.063	.025	.032

Table 2 gives the results of analysis of temperature and displacement data obtained from the test road between January and June 1986, excluding March. Listed in Table 2 are two maximum displacements observed for each of the 5 months. The first represents total displacement that occurred between early morning and afternoon. Directions of these slab displacements are downward at the edge and corner and upward at the center. The second maximum displacement represents the total displacement that occurred between afternoon and early morning of the following day. Directions of these slab displacements are upward at the edge and corner and downward at the center. The range of temperature differentials and average concrete temperature within which the maximum displacements occurred are also listed in Table 2.

The data in Table 2 indicate that higher displacements are associated with greater variations in daily temperature differentials. Almost all maximum monthly displacements occurred during dry, sunny days, characterized by wide variation of temperatures between day and night. Obviously, such weather conditions induced the necessary range of temperature differentials in the pavement slab to cause maximum vertical displacements.

The largest displacements occurred in April and May (Table 2). Such displacements were concurrent with the largest variations in temperature differential. The largest displacements at the corner, edge, and center were 0.098, 0.030, and 0.045 in., respectively. The average values of maximum displacements at the adjoining corners of Slabs 3 and 4 were 0.072 and 0.063 in., respectively. These values reflect the nonuniformity of displacements at the two adjoining corners. The differences were evident at larger displacements.

The influence of slab curling on pavement stiffness is clearly shown in Figure 11 *(6)*. At a high negative temperature differential the corner deflections are significantly high. This reflects a reduced stiffness in the pavement system, brought about by loss of subgrade support, which is associated with upward curling. As the temperature differential becomes less negative and gradually more positive, the slab corner will displace downward, increasing the area of subgrade support. Figure 11 shows that the corner deflections decrease as the temperature differential becomes gradually more positive. This

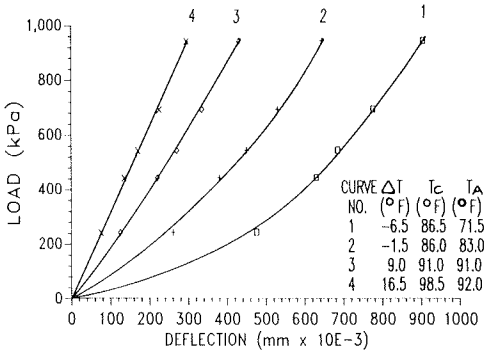

FIGURE 11 Typical load deflection relations at slab corner (ΔT = temperature differential, Tc = concrete temperature, and TA = air temperature).

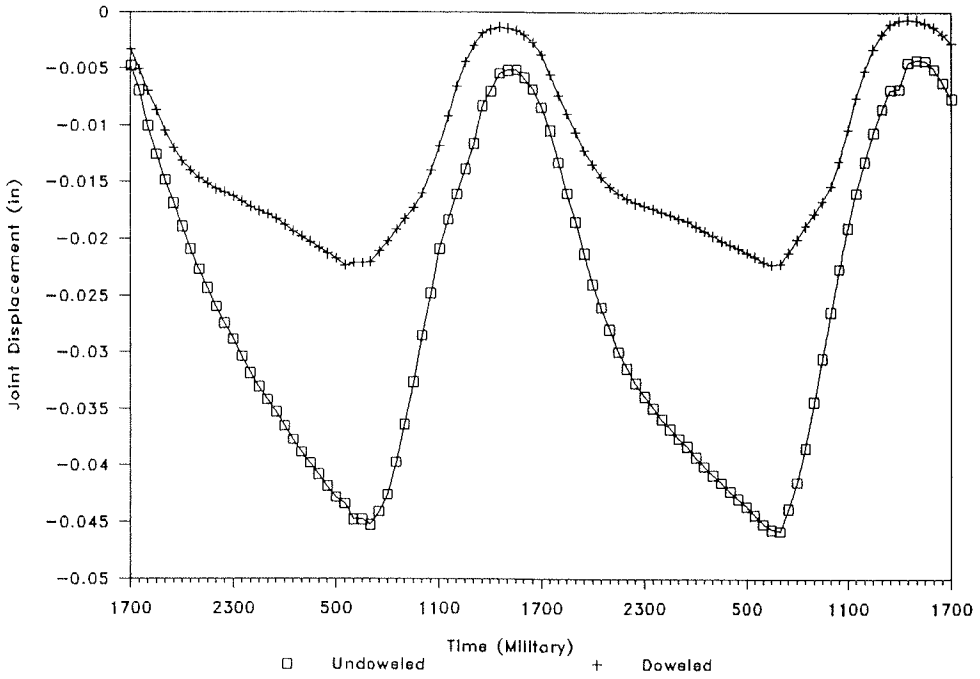

FIGURE 12 Horizontal joint displacement.

TABLE 3 MAXIMUM HORIZONTAL DISPLACEMENTS AT TEST ROAD JOINTS

MONTH	TIME (MILITARY)		TEMPERATURE DIFFERENTIAL (°F)		AVERAGE CONCRETE TEMP. (°F)		MAXIMUM HORIZONTAL DISPLACEMENTS (inch)	
	FROM	TO	FROM	TO	FROM	TO	UNDOWELED JOINT	DOWELED JOINT
JAN.	800	1400	-11	+12	39	55	.034	.010
	1400	800	+7	-11	59	39	.033	.009
FEB.	800	1400	-9	+12	49	62	.034	.018
	1500	800	+11	-7	73	58	.030	.012
APRIL	700	1500	-11	+21	67	88	.043	.023
	1500	700	+21	-10.5	88	65	.043	.021
MAY	600	1500	-7	+26	72	96	.041	.016
	1500	600	+26	-6	96	75	.037	.018
JUNE	600	1300	-6	+20	84	102	.035	.016
	1300	600	+22	-6	105	88	.033	.014
					AVERAGE		.036	.016

implies that, as a result of improved stiffness, a pavement system offers greater resistance to applied traffic loads.

Analysis of Horizontal Slab Displacements

Figure 12 shows typical slab displacements at undoweled and doweled joints. Pavement temperatures recorded during the same period were shown in Figure 2. It is obvious that displacements at both joints are sensitive to fluctuations in pavement temperatures. Pavement slabs expand and contract in response to increase and decrease of pavement temperatures, as clearly demonstrated by Figures 12 and 2. During the night, as pavement temperature decreases, the joint opening will increase correspondingly. Maximum opening occurs at approximately 7:00 a.m., which is concurrent with minimum pavement temperature. Shortly after daybreak, the joint opening will begin to close as the pavement temperature starts to increase and the opening will reach minimum width at approximately 2:00 p.m. This timing coincides with maximum pavement temperature.

It should be noted that slab curling can also contribute to joint opening and closing. The rotation associated with curling of adjoining slabs can cause further opening and closing of joints depending on the direction of rotation. However, because of the difficulty in assessing the contribution of slab curling, joint movements are normally attributed to expansion-contraction by changes in pavement temperature.

An important observation can be made from Figure 12. The doweled joint allowed only about 50 percent of the slab displacements allowed by the undoweled joint. This observation is true not only for the sample data presented in Figure 12. Table 3 gives the results of analysis of data recorded throughout the 6-month study. The largest joint displacements were recorded in April. The displacement at the doweled joint was 0.023 in. compared with 0.043 in. at the undoweled joint, a difference of about 46 percent. Looking at the averages of monthly maximum displacements, the difference is even greater, about 55 percent. This is a strong indication of the resistance offered to slab displacements by doweled joints. Such movement restraints can contribute to stress development in the pavement. These stresses may be critical if they occur in conjunction with stresses that are induced by traffic loads and temperature.

CONCLUSIONS

Temperature records obtained from a concrete test road in Florida were analyzed. Slab displacements associated with temperature variation were also measured and analyzed. On the basis of findings from this study, the following conclusions are drawn:

1. Pavement slabs reach their minimum daily temperatures between 6:00 a.m. and 8:00 a.m., and their maximum temperatures occur between 12:00 noon and 2:00 p.m.
2. Maximum and minimum pavement temperatures generally occur about 1 hr after ambient temperature reaches similar levels.
3. The maximum negative and positive temperature differentials in pavement slabs occur, on average, at 6:00 a.m. and 2:00 p.m., respectively. Such timing almost coincides with minimum and maximum pavement temperatures.
4. The largest vertical displacements recorded at the corner, edge, and center of the slab were 0.098, 0.030, and 0.045 in., respectively. Maximum daily displacements were concurrent with maximum temperature differentials in the slab.
5. Vertical displacements exhibited by the two sides of an undoweled joint were nonuniform. On average, one side of the joint displaced about 13 percent more than the other side.
6. The largest horizontal displacements recorded at undoweled and doweled joints were 0.043 and 0.023 in., respectively. Maximum joint opening and closing were reached at approximately 7:00 a.m. and 3:00 p.m., respectively.
7. The average horizontal displacement at the doweled joint was only 45 percent of the displacement at the undoweled joint. This suggests that doweled joints offer resistance to slab movements, a condition that can induce stresses in the pavement.
8. Weather conditions significantly influenced temperature response of pavements. Clear, sunny weather characterized by wide variations of ambient temperature produced larger displacements in pavement slabs.
9. The temperature distribution in the pavement slab changed drastically in response to sudden exposure to moisture and shade at the pavement surface.

ACKNOWLEDGMENT

The authors gratefully acknowledge the contributions of Gabriel Alungbe and Jeff Couch in the data analysis. Thanks are also extended to Chuck Davis, Darlene Padgett, and Tammy Sheese for their help.

REFERENCES

1. H. M. Westergaard. Analysis of Stresses in Concrete Pavements Due to Variations of Temperature. *HRB Proc.*, Vol. 6, 1926, pp. 201–217.
2. F. C. Lang. Temperature and Moisture Variations in Concrete Pavements. *HRB Proc.*, Vol. 21, 1941, pp. 260–272.
3. B. F. Friberg. Frictional Resistance Under Concrete Pavements and Restraint Stresses in Long Reinforced Slabs. *HRB Proc.*, Vol. 33, 1954, pp. 167–184.
4. M. E. Harr and G. A. Leonards. Warping Stresses and Deflections in Concrete Pavements. *HRB Proc.*, Vol. 38, 1959, pp. 286–320.
5. S. D. Tayabji and B. E. Colley. Improved Rigid Pavement Joints. In *Transportation Research Record 930,* TRB, National Research Council, Washington, D.C., 1983, pp. 69–78.
6. J. M. Armaghani, J. M. Lybas, M. Tia, and B. E. Ruth. Concrete Pavement Joint Stiffness Evaluation. In *Transportation Research Record 1099,* TRB, National Research Council, Washington, D.C., 1986, pp. 22–37.
7. L. D. Childs. A Study of Slab Action in Concrete Pavement Under Static Loads. *HRB Proc.*, Vol. 27, 1947, pp. 64–84.

Publication of this paper sponsored by Committee on Strength and Deformation Characteristics of Pavement Sections.

An Examination of Environmental Versus Load Effects on Pavements

W. R. HUDSON AND PATRICK R. FLANAGAN

This paper is a summary of the results of a study undertaken to examine environmental versus load effects on pavements. Pairs of pavement sections were examined at 14 locations in five states. At each location, one section had received normal traffic and the other had never been opened. Visual condition surveys were performed on each section, and pavement condition was compared. It is concluded that traffic loadings are a much more significant cause of pavement distress than are environmental problems.

Much of the U.S. highway infrastructure has fulfilled its useful life and needs replacement or rehabilitation. High inflation rates and increased competition for tax dollars caused maintenance to be deferred on a large portion of the highway system. The Congress and state legislatures are faced with finding a funding source for maintenance, rehabilitation, and reconstruction.

To fairly allocate highway maintenance costs, it is essential to know the relative amounts of damage that result from various causes. The best-known causes of pavement damage include environment, poor materials, and traffic loads. It is often assumed that there is some base environmental- and materials-related damage to be charged equally to all users. The remaining costs are then allocated to system users according to the damage caused by each class of user.

The problem with determining the amount of damage due to each cause separately is that there are interactions between causes *(1, 2)*. For example, without precipitation rigid pavements would not pump. By the same token without loads crossing joints and cracks in the pavement during the rain there would be no pumping. Therefore pumping is caused by a combination of environment and traffic. The relationship between traffic loads and pavement damage was quantified during the AASHO Road Test, which was a comprehensive, large-scale experiment designed to determine the effects of various vehicle loads on pavement performance and on deterioration rates *(3)*.

The road test findings, published in 1962 *(4)*, show that the damaging effects of heavy axle loads are extremely large compared with damage caused by light axle loads. In spite of the evidence produced by the AASHO Road Test, there are many claims that trucks cause little or no more damage to pavements than do automobiles. These claims accompany political pressure to raise legal axle load limits without proportional increases in user fees and taxes.

W. R. Hudson, Department of Civil Engineering, The University of Texas at Austin, Austin, Tex. 78712. P. R. Flanagan, Austin Research Engineers, Inc., 20 Victor Square, Scotts Valley, Calif. 95066.

BACKGROUND

Pavement damage generally results from three factors: environmental effects, materials problems, and loads. The most important environmental effects are moisture and temperature effects. Moisture in the pavement produces several problems including surface oxidation, ice lens formation (swell), base failure, slope instability, volume changes, and stresses *(5)*. Temperature differentials cause shrinkage and expansion, and these induce stresses in pavement.

Materials or poor construction quality control, or both, can also result in accelerated pavement damage. An obvious materials problem is poor aggregate in rigid pavements. Certain aggregates can cause deterioration cracking, known as D-cracking. This distress is evidenced by hairline parallel cracks at slab corners and edges. As the cracks grow, pieces of slab work loose. Ultimately, the slab falls apart. Poor construction quality can also result in problems such as misaligned dowel bars, concrete voids under the reinforcement, and concrete mixes that are too rich or too lean. These in turn lead to premature pavement damage.

As indicated in previous reports, the primary cause of pavement damage is traffic loading generated by heavy trucks *(6)*. Some sources point to parkways (car-only roadways) such as the Baltimore-Washington Parkway and the Merrit Parkway in Connecticut as evidence that parkways wear out just as fast as highways that carry truck traffic. Studies by Hudson and Seeds *(6, 7)* looked at performance of these and other parkways to determine if they were performing properly. These studies concluded that damage to the Baltimore-Washington Parkway was primarily due to a poor choice of aggregates and not to automobile use. Damage on the Merrit Parkway was due primarily to studded snow tires, which have since been banned. These studies also concluded that properly designed parkways can be relatively thinner than Interstate highways and still meet and often exceed design lifetimes, in terms of both cumulative traffic loadings and years of expected service life.

OBJECTIVE

This study was done as a follow-on to several reports by Hudson and Hudson and Seeds that have examined the relationship between traffic, especially heavy truck traffic, and pavement damage *(5–8)*. The objective was to illustrate the relative damage due to environmental forces and materials problems compared with that caused by loads. The approach was to examine several pairs of pavement sections with similar

characteristics that have been subjected to different traffic levels. Several pairs of sections in different environments were compared to examine the load-environment interaction.

The purpose of this research effort was to examine the current condition of pavements that were constructed to carry normal traffic but that have not been trafficked on a regular basis since construction. Pavements examined included primary and Interstate highway sections that were built for traffic but received little or no traffic due to legal or other delays.

The normally constructed but untrafficked pavements were compared in each case with similar pavements that received regular highway traffic. In each case, the highway agency involved was contacted to obtain detailed design, construction, and traffic information on the sections observed. Condition surveys concentrated on distress that results from environment and load.

SCOPE

The project scope was to compare pairs of pavement sections, nearly identical in character with the exception of traffic. Ideally, pairs of sections would have identical materials, construction, age, and environmental history. To draw valid conclusions, the sections were to be part of the same pavement, with the untrafficked section having had no traffic. Observed differences in distress levels could then be related to observed differences in traffic and environment.

Because of the importance of environmental effects, sections were sought in several environmental regions that varied with respect to freezing and thawing and moisture. For this study, the six AASHTO environmental regions were adopted:

I Wet, no freeze
II Wet, freeze-thaw cycling
III Wet, hard-freeze, spring thaw
IV Dry, no freeze
V Dry, freeze-thaw cycling
VI Dry, hard-freeze, spring thaw

These regions are shown in Figure 1. The regions range from Region II (wet, freeze-thaw cycling) as the most environmentally destructive to Region IV (dry, no freeze) as the least destructive.

The search was concentrated in Texas for Region I, Maryland for Region II, Minnesota for Region III, California for Region IV, and Arizona for Region V.

CONDUCT OF RESEARCH

Initial contact was made with personnel from state transportation agencies in an attempt to locate study sections for comparison. Sought were stub ends, spurs, lanes, and ramps of primary or Interstate highways that were constructed but never opened to traffic. These sections were then visited and surveyed for visual condition.

Several standard terms were selected to simplify description of pavement units. A "section" is a portion of pavement that has either been trafficked or untrafficked. "Location" corresponds to a pair of sections, one trafficked, one untrafficked. In addition, as a result of the number of pavement sections, the

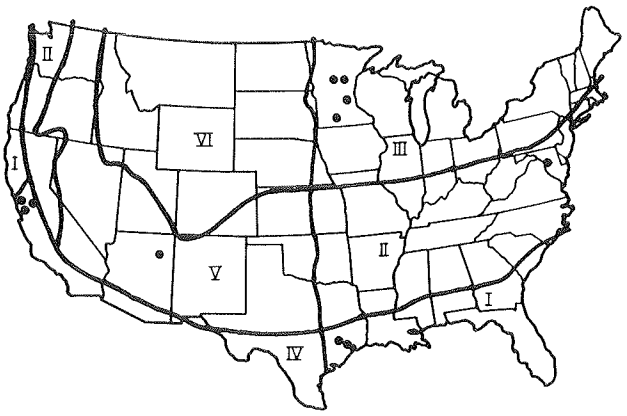

REGION	CHARACTERISTICS
I	Wet, No Freeze
II	Wet, Freeze-Thaw Cycling
III	Wet, Hard-Freeze, Spring Thaw
IV	Dry, No Freeze
V	Dry, Freeze-Thaw Cycling
VI	Dry, Hard Freeze, Spring Thaw

FIGURE 1 Test locations and environmental regions.

following identification system was adopted. Each location is identified by the two-letter code of the state in which it is situated, followed by a number assigned to that location. For example, the Minnesota locations are identified as MN1 through MN7. Sections are further identified by T for "trafficked" and U for "untrafficked." The untrafficked section at the seventh Minnesota location then is MN7U.

Example Location

Data from the Milaca, Minnesota, location (MN7) are presented as an example of the procedure used. MN7 is located approximately 1 mi south of Milaca (Figure 2) where US-169 changes from a four-lane divided highway to a two-lane undivided highway. MN7T is south of the point where the northbound traffic moves off the undivided AC pavement. MN7U is a stub end approximately 50 ft long (Figure 3).

Construction

MN7 is an asphalt concrete pavement built in 1972 with the following pavement structure:

- 1-in. AC hot mix,
- 1½-in. bituminous base, and
- 6-in. aggregate base.

Traffic

Traffic, including 7 percent trucks, is as follows:

Year	*ADT*
1984	2,425
1982	2,150
1980	2,025
1978	2,038
1976	1,843

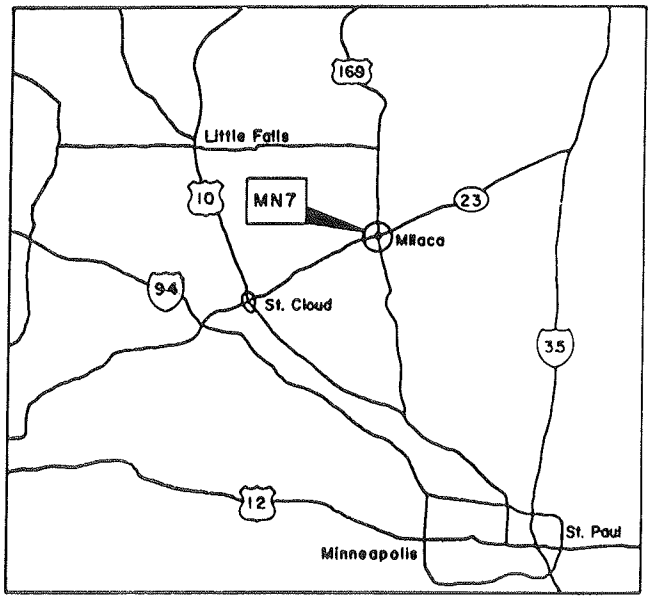

FIGURE 2 Milaca, Minnesota, location.

Environment

MN7 is located in Environmental Region III (wet, freeze).

Distress

MN7T is cracked into 10- to 15-ft blocks with all cracks spalled 1/2 to 1 in. The wheelpaths are slightly alligator cracked and have ruts 1/8 to 1/4 in. deep. The area between the wheelpaths is slightly raveled. The cracks on MN7U are not spalled and are 25 to 30 percent as dense as those on MN7T.

Observations

There is a clear difference in cracking severity for this section. The cause of the cracking and severity of the distress between MN7T and MN7U demonstrates that, although this distress is environmentally caused, it is accentuated by traffic.

Results

As the study progressed, 14 suitable pairs of pavements were located. A complete data set was collected for 11 of these and is given in Table 1. Although some data (traffic and construction) were unobtainable for three sections (located in Arizona and California), visual condition survey data on these sections are given in Table 2.

Two trends are apparent in the data:

- For each pair of sections, the diversity, extent, and distress are greater for trafficked sections than for untrafficked sections.
- The effect of environment is not constant across different environmental regions.

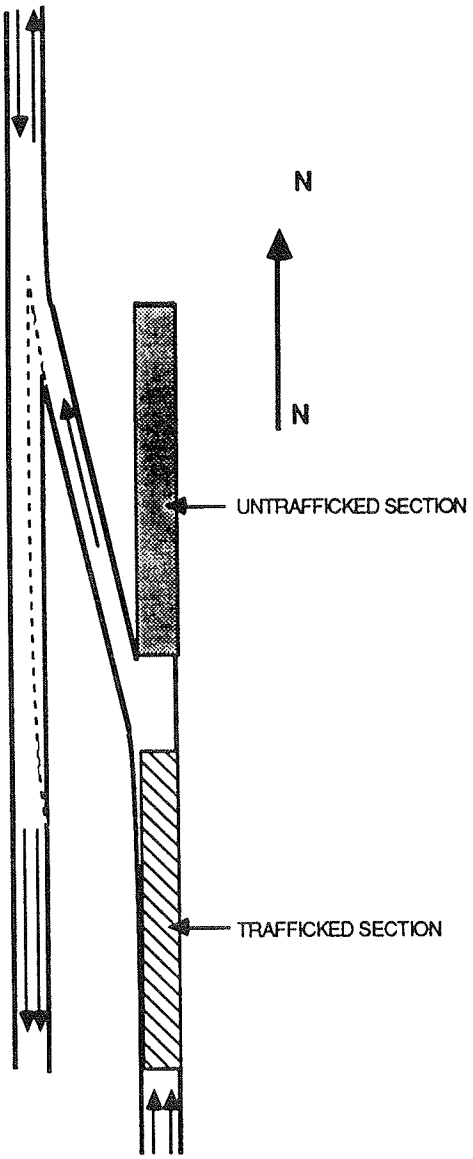

FIGURE 3 Detail of Milaca location.

Effect of Traffic

For every pair of sections examined there was significantly more distress with respect to type, extent, and severity on the trafficked than on the untrafficked section.

Effect of Environment

Environmental forces caused distress in the untrafficked sections. In all but a few of these sections there was distress, although it was universally less than distress on the comparable trafficked section.

DISCUSSION OF FINDINGS

The information collected here is from a series of case studies that were examined to compare pavement damage. In each case, one pavement section was subjected to environmental forces only while a companion section was subjected to the combined effects of traffic loads and environmental forces.

TABLE 1 COMPLETE INFORMATION ON LOCATIONS

STATE	ROUTE	CITY	ENVIRONMENTAL REGION	T-TRAFFICKED U-UNTRAFFICKED	PAVEMENT STRUCTURE: PAVEMENT TYPE	PAVEMENT STRUCTURE: SURFACE THICK. INCHES	AGE (YEARS)	TRAFFIC: ADT	TRAFFIC: % TRUCKS	RIGID: FAULTING	RIGID: D CRACKING: SLIGHT	RIGID: D CRACKING: MODER.	RIGID: PATCH & POTHOLES	RIGID: PUNCHOUTS	RIGID: TRANS CRACKS: < 1/4"	RIGID: TRANS CRACKS: 1/4"-1/2"	RIGID: SCALING/ABRASION	RIGID: SEALANT DAMAGE	RIGID: CORNER CRACKS	RIGID: SPALLING: < 1/2"	RIGID: SPALLING: > 1/2"	RIGID: POLISHED AGGREG	FLEXIBLE: CRACKING: SLIGHT	FLEXIBLE: CRACKING: MODER	FLEXIBLE: BLEEDING	FLEXIBLE: RUTTING	FLEXIBLE: RAVELLING	FLEXIBLE: FATIGUE CRACKING
MD	I-95	WASHINGTON, DC	II	T	CRCP	8/9	15	30K	17		X		X	X	N		X			X								
				U	CRCP	8/9	15	0	0									X										
TX	US 290	CYPRESS	I	T	JCP	10	20	18K	10			X	X		X			X		X		X						
				U	JCP	10	20	0	0						X													
	SH 146	SEABROOK	I	T	JCP	10	15	16 6K	6		X				X		X	X										
				U	JCP	10	15	0	0								X											
MN	I-94	ST PAUL (WESTBOUND)	III	T	JCP	10	14	47 4K	6	X		X	X			X	X	X			X							
				U	JCP	10	14	0	0						X						X							
		ST PAUL (EASTBOUND)	III	T	JCP	10	14	47 4K	6				X		X		X				X							
				U	JCP	10	14	0	0											X								
	I-35 W	MINNEAPOLIS	III	T	JCP	10	10	37 4K	5 6				X															
				U	JCP	10	10	0	0									X										
	US 280	MINNEAPOLIS	III	T	JCP	9	14	15K	8 8	X			X					X	X		X							
				U	JCP	9	14	0	0						X			X		X								
	SH 60	ST JAMES	III	T	JCP	9	8	2 4K	16									X	X	X								
				U	JCP	9	8	0	0											X								
	US 10	RANDALL	III	T	AC	3	7	2K	10												X			X			X	
				U	AC	3	7	0	0														X					
	US 169	MILACA	III	T	AC	3	14	2 4K	7												X			X		X	X	X
				U	AC	3	14	0	0											X								
CA	SR 17	SUMMIT	IV	T	AC	5	15	51K	6 2				X											X		X	X	X
				U	AC	5	15	0	0																			

N - NORMAL TRANSVERSE CRACKING FOR CRCP

TABLE 2 LOCATIONS WITH INCOMPLETE INFORMATION

STATE	ROUTE	CITY	ENVIRONMENTAL REGION	T-TRAFFICKED U-UNTRAFFICKED	PAVEMENT STRUCTURE	RIGID												FLEXIBLE					
					PAVEMENT TYPE	FAULTING	D CRACKING		PATCH & POTHOLES	PUNCHOUTS	TRANS CRACKS		SCALING	SEALANT DAMAGE	CORNER CRACKS	SPALLING		POLISHED AGGREG.	CRACKING		BLEEDING	RUTTING	RAVELLING	FATIGUE CRACKING
							SLIGHT	MODER.			< 1/4"	1/4" TO 1/2"				< 1/2"	> 1/2"		SLIGHT	MODER.				
CA	I 280	SAN JOSE	IV	T	JCP						X					X								
				U	JCP											X								
	I 380	SAN FRANCISCO	IV	T	JCP	X					X													
				U	JCP																			
AZ	I-40	HOLBROOK	V	T	AC																X	X	X	X
				U	AC																			

The case study locations were situated in four of the severest environmental regions used to classify areas of the United States (Figure 1). Although these 14 case studies do not represent all possible combinations of traffic, pavement strength, and environmental conditions, they do represent a good cross section of pavements in the United States. The significant factor is that in every case the section subjected to the combination of traffic and environment suffered greater damage than did the section subjected to environment alone. In most cases, the difference was rather dramatically greater when traffic was added.

As previously pointed out, the observed difference was probably not due to traffic alone. In some cases it is due to the interaction between traffic and environment. For example, the environment can induce a temperature crack that is aggravated and intensified by traffic repeatedly passing over it. In some of the cases, the same type of distress was observed on both sections, but the severity of the distress was much greater on the trafficked than on the untrafficked section. In these cases, the distress was of the type that is usually environmentally induced and then load enhanced. In the case of thermal cracking, for example, not only was the spalling of the cracks more severe under traffic but the density of the cracks in the section was also more severe.

At some of the observed sections, there was considerable distress of a given type in the trafficked section but no such distress in the untrafficked section. In such cases, it is probable that traffic was the initiating cause of the damage, because it occurred only in the trafficked sections. It is probable that the environment then enhanced or increased the effect of the load-induced damage.

Examination of the data shows differences between levels of severity of distress in the regions where freezing was a factor. In both freeze-thaw-cycling and hard-freeze regions, the difference in the levels of severity of distress was greater than in the no-freeze region. In other words, in both freeze-related regions where environmental distress is expected to be greater, the difference in distress between trafficked and untrafficked sections is greater than in the milder region. This suggests again that the interaction of load with the environment has a severe effect. Location MN7 at Milaca, Minnesota, clearly illustrates this interaction. Similar results are observable for differences in distress between wet and dry areas, as evidenced by location TX1 at Cypress, Texas.

An example of the phenomenon with respect to wet and dry areas is the previously cited pavement pumping problem. Clearly pumping and related damage is induced by loads in the presence of water, but such interaction is also more prevalent in wet areas than in dry areas. Thus the effect of loads is not only more severe than the effect of environment but the effect of load is compounded more severely in harsh environments than in mild environments.

SUMMARY

The objective of this study was to examine the relative amount of damage caused by environmental forces versus that caused by loads. Fourteen similar pairs of pavement sections were examined. Each pair consisted of a pavement section that had received traffic and a similar one that had not. To strengthen possible conclusions from the data, the sections selected were generally of identical construction and age. Untrafficked pavements were sections that had never been opened to traffic for various reasons. The trafficked sections consisted of adjacent pavement subjected to normal traffic. Sections were examined in Arizona, California, Maryland, Minnesota, and Texas to give wide coverage of environmental variables.

For all 14 case study pairs the damage on trafficked sections is more severe than the damage on untrafficked sections. In addition, the total damage with traffic loading was generally greater in harsh environments than in mild environments. Therefore, although quantitative conclusions cannot be drawn, these data support the conclusion that the damaging effect of traffic is generally more severe than the effect of environment alone and that the damaging effect of traffic is proportionally greater in harsh environments than it is in mild environments.

There remains the important need to collect more adequate data on pavement performance to quantify relationships and develop mathematical models. These models will, in turn, define the relative effects of load and environment and their interaction on pavement damage and ultimately pavement performance. Although the Strategic Highway Research Program proposes to undertake such a study, the results will be 5 to 10

years or longer in coming. Until such results are available, it is essential that the findings of small studies such as this one be used to help assess realistic relationships for defining the effects of damage and using these relationships in the difficult task of allocating pavement costs.

REFERENCES

1. W. R. Hudson and V. L. Anderson. *An Assessment of Load and Environmental Effects on Pavement Deterioration.* Report RR1/3. Association of American Railroads, Washington, D.C., Dec. 1981.
2. R. Haas and W. R. Hudson. *Pavement Management Systems.* McGraw Hill, New York, 1978.
3. *Special Report 61E: The AASHO Road Test, Report 5: Pavement Research.* HRB, National Research Council, Washington, D.C., 1962.
4. *Special Report 73: The AASHO Road Test, Proceedings of a Conference Held May 16–18, 1962, St. Louis, Missouri.* HRB, National Research Council, Washington, D.C., 1962.
5. W. R. Hudson. *An Examination of Use and Non-Use Related Causes of Pavement Deterioration.* Report RR1/2. University of Texas at Austin and Austin Research Engineers, Inc., 1984.
6. W. R. Hudson and S. B. Seeds. *Overview of Factors Associated with Pavement Damage.* Final Report RR-8/1. Association of American Railroads, Washington, D.C., March 1985.
7. W. R. Hudson and S. B. Seeds. *An Examination of Pavement Deterioration in the Presence of Automobile Traffic, Phase I.* Report RR-7/1. Association of American Railroads, Washington, D.C., March 1983.
8. W. R. Hudson and S. B. Seeds. *An Examination of Pavement Deterioration in the Presence of Automobile Traffic, Phase II.* Report RR-7/1. Association of American Railroads, Washington, D.C., July 1984.

Publication of this paper sponsored by Committee on Strength and Deformation Characteristics of Pavement Sections.

Moisture in Portland Cement Concrete

DONALD J. JANSSEN

Moisture gradients in concrete pavements cause differential shrinkage between the top and the bottom of the pavement. This leads to curling stresses in which the top of the pavement is in tension while the bottom is in compression. The magnitude of these stresses is determined by the moisture distribution, the volumetric aggregate content of the concrete, and the elastic modulus of the concrete. Pavement moisture contents were determined by field moisture measurements, laboratory measurements, and computer simulation. These indicated that substantial drying occurred only at the top surface, to a depth of less than 2 in. The rest of the pavement remained at 80 percent saturation or higher. A typical pavement moisture distribution was determined, and using an aggregate content of 74 percent and an elastic modulus of 3.6×10^6 psi, a stress distribution was calculated. The tensile strength of the concrete at the surface was exceeded, and cracks could be expected to form to a depth of 3/4 in. Because the tension in the concrete was concentrated near the surface instead of decreasing linearly with depth, the actual moment in the pavement caused by the moisture gradient was only 40 percent of the moment capacity of the unreinforced concrete.

Portland cement concrete shrinks as it dries, and, if this shrinkage is restrained in any way, tensile stresses will develop in the concrete. If there is a moisture gradient in the concrete, the concrete will have a tendency to curl. The weight of the concrete tends to resist the curling in installations such as pavements, and this leads to curling stresses. This has been recognized in pavements for many years. Normally moisture gradient curling stresses in pavements are ignored because of the difficulty in estimating their magnitude and because it is believed that they are cancelled out by the effect of temperature gradient–induced warping *(1)*. It is the purpose of this paper to estimate the magnitude and locations of moisture gradient–induced curling stresses.

BACKGROUND

Drying shrinkage in concrete is complex and has been investigated in detail by others *(2–6)*. Essentially shrinkage occurs when water is removed from the hardened cement paste. Figure 1 is adapted from Mindess and Young *(2)* and shows drying shrinkage for a typical cement paste as a function of degree of saturation. Saturated moisture content for this paste is 28 percent, defined by drying to constant weight at 115°C. Aggregate in concrete restrains this shrinkage, and the amount of restraint depends on the volumetric aggregate content of the concrete. This is shown in Figure 2, taken from Powers *(4)*. As the aggregate content increases, the amount of shrinkage in the concrete decreases. For a typical pavement concrete with approximately 74 percent of the volume filled with aggregate *(7)*, the total concrete shrinkage would be approximately 10 percent of the paste shrinkage for the same amount of drying.

If the concrete is restrained from moving as it shrinks, the stresses that develop can be calculated by elasticity. The elastic modulus of normal weight air-entrained concrete can be calculated *(8)* by

$$E_c = 57{,}000 \sqrt{f'_c} \quad (1)$$

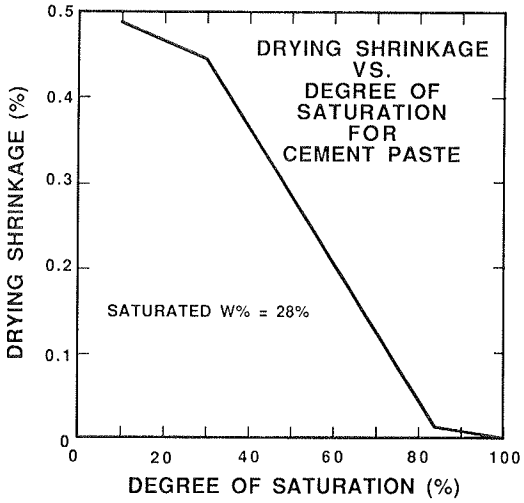

FIGURE 1 Drying shrinkage for a typical cement paste, after Mindess and Young *(2)*.

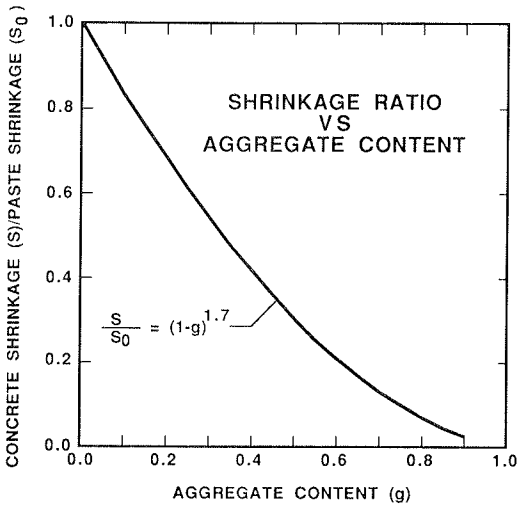

FIGURE 2 Relative shrinkage as a function of aggregate content *(4)*.

Department of Civil Engineering, University of Washington, Seattle, Wash. 98195.

where E_c is the elastic modulus of the concrete (psi) and f_c' is the 28-day compressive strength of the concrete (psi). For concrete with a compressive strength (f_c') of 4,000 psi, the elastic modulus (E_c) would be approximately 3.6×10^6 psi.

Elastic stresses could be calculated by

$$\sigma_E = E_c \times e\%/100 \quad (2)$$

where

σ_E = elastic stress (psi),
E_c = elastic modulus (psi), and
$e\%$ = percent strain.

For a percent strain in the concrete of 0.01, with 4,000 psi concrete the elastic stress would be 360 psi.

PROCEDURES AND RESULTS

To determine reasonable estimates of the degree of saturation at various depths in a concrete pavement, three methods were used. The methods are briefly described; detailed descriptions are given in Janssen *(7)* and Janssen et al. *(9)*.

Field Testing

Field moisture contents were determined by installing psychrometers in three pavement sections. Psychrometers measure relative humidity, which is converted to degree of saturation by means of laboratory calibrations. A description of the procedures can be found in Janssen *(7)*. The psychrometers were installed in a ramp for I-72, west of Champaign, Illinois, and in two locations in a ramp on I-57, north of Champaign. The I-72 installation was at depths of 2 and 4½ in., and the I-57 installations were at 2 and 5½ in. and at 2, 5½, and 7 in. Each installation was in triplicate at each depth.

Readings were taken for the I-72 location on March 22, 1984, and from July 10 through November 13, 1984. Following the March 22 readings, a snowplow destroyed the electrical leads and considerable work was required to repair them before readings could resume. The first I-57 location was monitored from June 8 through July 10, 1984, and readings were taken at the second I-57 location from June 7 through June 27, when this location was overlaid. Saturated moisture content for the I-57 locations was determined to be 7.6 percent *(7)*.

Results of the field moisture content determinations are given in Tables 1–3. Each value shown is the average of the readings taken for that location and depth. It should be noted that readings were not always possible because of equipment problems. Missing data are indicated in the tables by dashes. The mean, high, and low values for each depth and location are shown in Figures 3–5. These figures indicate that there was little change in degree of saturation for the depths shown.

Laboratory Testing

Laboratory moisture determinations were made after conditioning three laboratory-cast cylinders by slow freeze-thaw cycling. It is believed the freeze-thaw action is a major driving

TABLE 1 DEGREE OF SATURATION, I-72 LOCATION

	Degree of Saturation (%)	
Date	2-in. Depth	4½-in. Depth
3-22	85	82
7-10	92	94
7-11	88	92
7-18	83	90
7-25	79	95
7-30	78	–
7-31	90	86
8-3	87	88
8-14	87	87
8-21	79	82
8-22	83	83
8-28	79	83
9-4	79	88
9-6	78	78
9-11	90	87
9-13	92	–
9-18	83	–
9-19	85	94
9-20	83	–
9-25	88	86
9-27	90	–
10-2	79	–
10-4	81	–
10-8	82	85
10-10	87	86
10-24	79	94
11-2	78	77
11-12	85	94
11-13	91	–

TABLE 2 DEGREE OF SATURATION, I-57 LOCATION A

	Degree of Saturation (%)	
Date	2-in. Depth	5½-in. Depth
6-8	95	94
6-11	–	77
6-13	82	–
6-19	87	–
6-21	88	87
6-22	85	94
6-25	–	91
7-3	–	83
7-5	–	87
7-6	83	87
7-10	87	–

TABLE 3 DEGREE OF SATURATION, I-57 LOCATION B

	Degree of Saturation (%)		
Date	2-in. Depth	5½-in. Depth	7-in. Depth
6-7	87	–	–
6-8	95	95	95
6-11	–	85	92
6-13	82	–	–
6-19	85	–	–
6-21	87	94	94
6-22	90	90	95
6-25	–	92	96
6-27	85	94	–

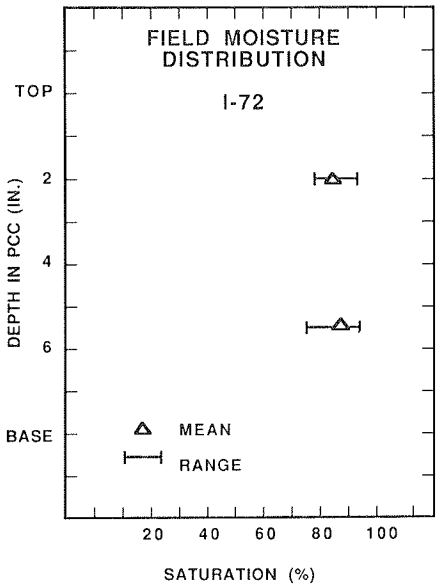

FIGURE 3 Degree of saturation (mean, high, and low) I-72.

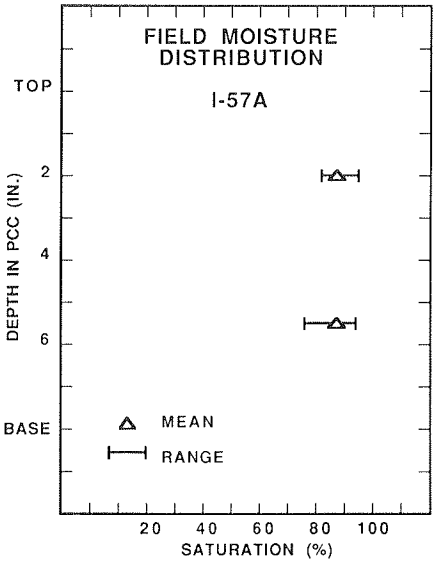

FIGURE 4 Degree of saturation (mean, high, and low) I-57A.

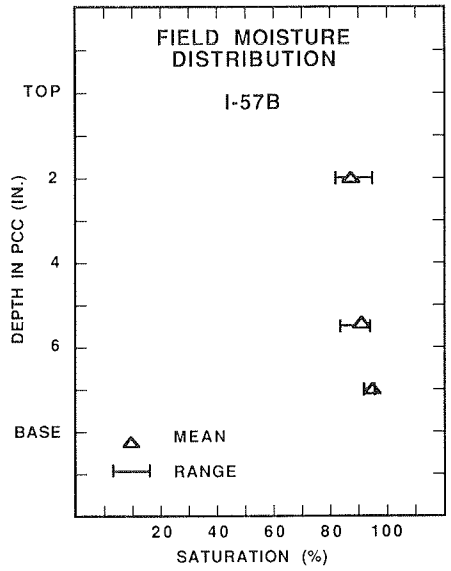

FIGURE 5 Degree of saturation (mean, high, and low) I-57B.

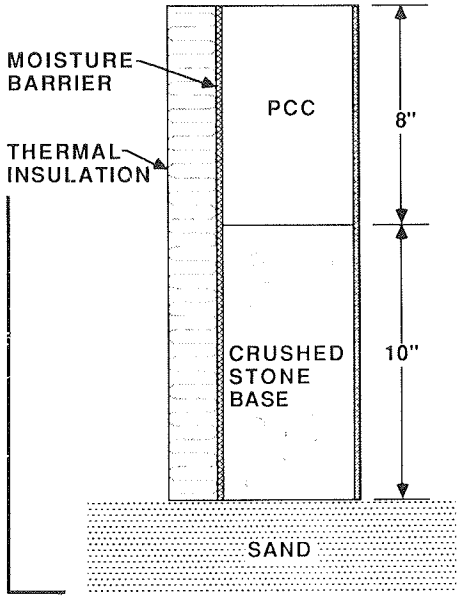

FIGURE 6 Laboratory sample.

force for moisture movement in concrete pavements *(7)*. Concrete samples, 4 in. in diameter by 8 in. long, were placed vertically on a 10-in. dense crushed-stone base. Horizontal moisture and thermal movements were prevented by use of moisture barriers and thermal insulation. The top surface of the concrete was open to evaporation, and the bottom of the crushed-stone base was in contact with free water (Figure 6). The samples were subjected to 200 freeze-thaw cycles over a period of 5 months. This is the equivalent to about 4.3 years of field exposure for central Illinois. Details of the freeze-thaw work can be found elsewhere *(7, 9, 10)*. The saturated moisture content for the samples was 7.8 percent. The initial degree of saturation before freeze-thaw conditioning was 73 percent.

After this conditioning, the concrete cylinders were broken into approximate quarters and dried at 115°C to determine moisture contents. Degrees of saturation for the three samples are shown in Figure 7. As did the field moisture measurements, the laboratory samples show little variation in moisture from top to bottom. It should be noted that the samples were broken into approximately 2-in. pieces for the moisture content determinations, and any shallow surface drying would not show in these data.

Computer Modeling

Moisture movement was modeled in the concrete by means of a finite-difference computer program developed by Boast *(11)*. This program, although developed for moisture movement in soil, is applicable to any porous solid for which the appropriate inputs are known *(7)*. The system modeled consisted of an 8-in. concrete layer in contact with a free water source on the bottom

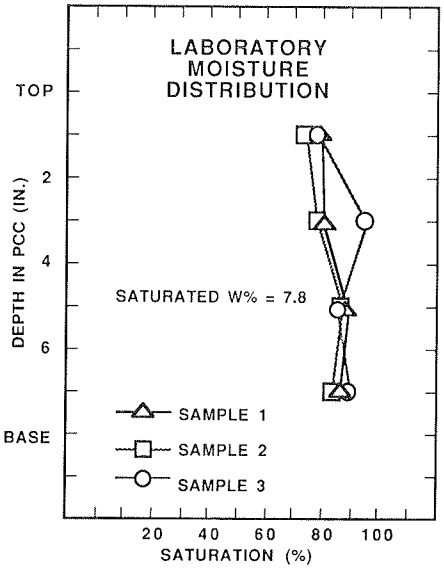

FIGURE 7 Laboratory moisture distribution.

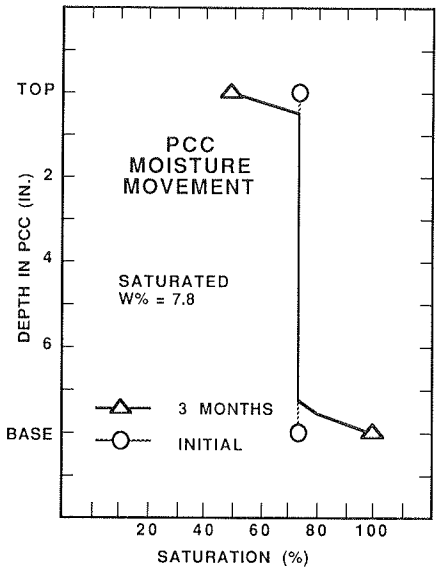

FIGURE 8 Simulated moisture profile, initial 73 percent saturation.

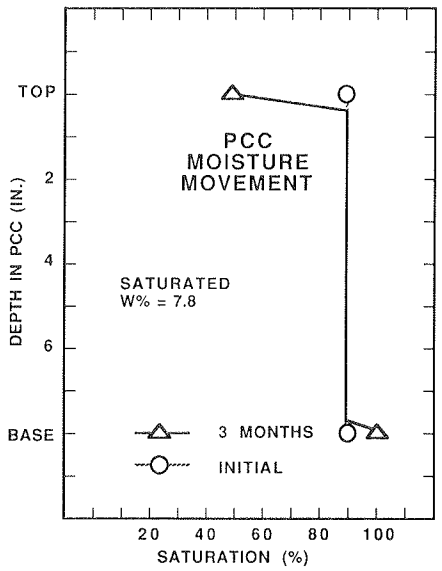

FIGURE 9 Simulated moisture profile, initial 90 percent saturation.

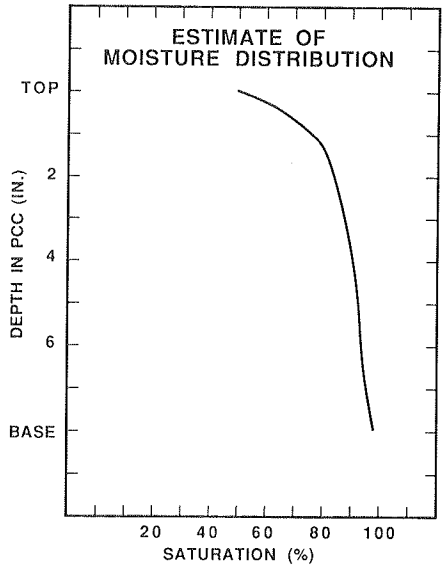

FIGURE 10 Estimate of moisture profile.

and 50 percent relative humidity on the top. Two initial conditions were tested: an initial degree of saturation of 73 percent, which corresponded to the concrete laboratory samples before freeze-thaw conditioning, and an initial degree of saturation of 90 percent, which corresponds to typical values found in the field investigation. The modeling was simulated for a period of 3 months, and the results are shown in Figures 8 and 9. It appears that the surface drying does not extend very far into the concrete, which probably explains why surface drying was not measured at the 2-in. depth in the field and was not pronounced in the top 2 in. in the laboratory samples.

APPLICATION

Using the laboratory and field measurements along with the computer modeling as a guide, Figure 10 was prepared as an estimate of degree of saturation versus depth for an 8-in. concrete pavement in a moderate climate subject to freeze-thaw cycling. The surface is only at 50 percent saturation, but the moisture content increases rapidly with depth to close to saturation at the base. This agrees with the measured laboratory and field moisture. The shallow drying at the surface is in agreement with the computer modeling. The reason that the drying does not extend very far into the pavement is the very low permeability of concrete *(7)*.

Percentage of saturation is converted into shrinkage using Figures 1 and 2 and assuming that all of the moisture loss in this range of saturation occurs in the paste. Converting shrinkage strain into stress for 4,000-psi concrete using Equation 2 yields the stress distribution shown in Figure 11. This stress distribution has been balanced for zero resultant force (tension on top of slab causes compression on the bottom) and

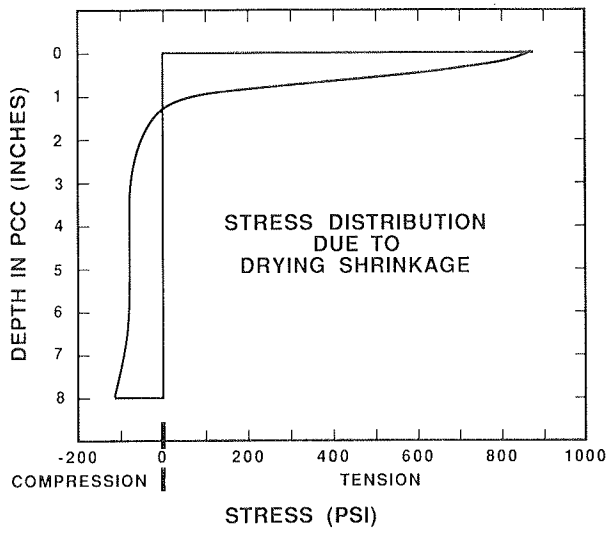

FIGURE 11 Moisture gradient stress distribution.

ignores any outside forces. The effect of reinforcing steel in the concrete is also ignored, though concrete shrinkage would cause compression in the steel. This would have minimal effect on the concrete stress distribution. The resultant moment due to the moisture gradient in the concrete is approximately 2,500 in.-lb per inch of slab width. The failure moment for 4,000-psi concrete, 8 in. thick, in pure flexure is about 6,200 in.-lb per inch width *(8)*. This assumes that the stress in the concrete up to failure is elastic and the stress distribution is linear with the neutral axis at the center. But the stress distribution shown in Figure 11 is far from linear. If the tensile strength of concrete is approximately equal to 10 percent of the compressive strength, Figure 11 indicates that the tensile strength is exceeded down to a depth of approximately 3/4 in. for this 4,000-psi concrete. This means that shallow hairline cracks can be expected to form in concrete slabs that exhibit moisture distributions similar to those shown in Figure 10. These hairline shrinkage cracks are probably what can be seen on concrete pavements as water evaporates after a rain.

CONCLUSIONS

This research has led to the following conclusions, which apply to the effects of moisture gradients in concrete pavements:

1. Significant drying in a concrete pavement can be expected only to a rather shallow depth;
2. The resulting moisture gradient can be expected to cause curling stresses in a pavement with the top of the pavement in tension and the bottom in compression;
3. Though the magnitude of the resulting moment would not cause failure in the concrete, the stress distribution is such that the tensile strength of the concrete would be exceeded to a depth of approximately 3/4 in.; and
4. This shallow cracking could be significant in situations in which concrete permeability is important, such as protective cover over steel reinforcement.

To evaluate the existence and extent of shallow cracking, cores that include a hairline crack should be taken. Hairline cracks are located by wetting the concrete surface and then allowing the water to evaporate. If present, cracks will appear as the surface dries. The cores can then be inspected in the laboratory by liquid penetrant inspection (ASTM E 165) to determine depth of cracking.

ACKNOWLEDGMENTS

This paper was prepared from a study conducted by the Department of Civil Engineering, in the Engineering Experiment Station, University of Illinois at Urbana-Champaign, in cooperation with the Illinois and U.S. Departments of Transportation. Special thanks are given to the Illinois Department of Transportation personnel for their assistance with this investigation and to Arti Patel and James DuBose for their assistance with the laboratory, computer, and field work. Thanks also to Duane Wright for producing the graphics used in this paper.

REFERENCES

1. C. H. Oglesby and R. G. Hicks. *Highway Engineering,* 4th ed. John Wiley and Sons, New York, 1982.
2. S. Mindess and J. F. Young. *Concrete.* Prentice-Hall, Inc., Englewood Cliffs, N.J., 1981.
3. A. M. Neville. *Properties of Concrete.* Pitman Publishing, London, England, 1975.
4. T. C. Powers. Causes and Control of Volume Change. *Journal,* Portland Cement Association, Research and Development Laboratories, Vol. 1, No. 1, Jan. 1959, pp. 29–39.
5. C. A. Menzel. Strength and Volume Change of Steam Cured Portland Cement Mortar and Concrete. *Proc., American Concrete Institute,* Vol. 31, 1935, pp. 125–148.
6. G. Pickett. Effect of Aggregate on Shrinkage and a Hypothesis Concerning Shrinkage. *Proc., American Concrete Institute,* Vol. 52, 1956, pp. 581–590.
7. D. J. Janssen. The Effect of Asphalt Concrete Overlays on the Progression of Durability Cracking in Portland Cement Concrete. Ph.D. dissertation. University of Illinois, Urbana, 1985.
8. P. K. Mehta. *Concrete—Structure, Properties, and Materials.* Prentice-Hall, Inc., Englewood Cliffs, N.J., 1986.
9. D. J. Janssen, B. J. Dempsey, J. B. DuBose, and A. J. Patel. *Predicting the Progression of D-Cracking.* Transportation Engineering Series 44, Illinois Cooperative Highway and Transportation Series 211, Final Report. Department of Civil Engineering, University of Illinois, Urbana-Champaign, Feb. 1986.
10. D. J. Janssen and B. J. Dempsey. The Effect of AC Overlays on D-Cracking in PCC Pavements. In *Transportation Research Record 1062,* TRB, National Research Council, Washington, D.C., 1986, pp. 70–75.
11. C. W. Boast. Soil Water Simulation Computer Program for Teaching Purposes. *Journal of Agronic Education,* Vol. 4, 1975, pp. 98–105.

Publication of this paper sponsored by Committee on Strength and Deformation Characteristics of Pavement Sections.

Effect of Rainfall on the Performance of Continuously Reinforced Concrete Pavements in Texas

C. SARAF, CHIA-PEI CHOU, AND B. FRANK MCCULLOUGH

The effect of rainfall on the performance of continuously reinforced concrete (CRC) pavements in Texas was studied by analyzing the condition survey data on CRC pavements throughout the state. A study of the annual rainfall data within the state of Texas indicated that it varies from 10 to 52 in. Rigid pavement condition survey data have been collected for 10 years, beginning in 1974. For the purpose of this study, the data were grouped into districts, and the average performance of pavements in each district was estimated for each survey year (surveys were conducted in 1974, 1978, 1980, 1982, and 1984). The average performance of CRC pavements was determined by adding the number of patches and punchouts in the pavement and estimating the number of failures per mile. The average rate of failures per mile (*RFPM*) per year was estimated for a period of 10 years for each district and a simple relationship was determined: log (*RFPM*) = − 4.05 + 2.35 log (*P*) where *P* is the average annual precipitation in the district. The results of this study indicated that the effect of average annual rainfall on the performance of CRC pavements in Texas is significant. Therefore the existing rigid pavement design procedures in Texas require review and possible modifications to accommodate the effect of this important variable on the performance of CRC pavements. A study of some individual pavement sections was also performed. This study indicated that the initial performance of pavements located in different rainfall areas is practically the same. However, when the pavement starts developing failures (punchouts and patches), the *RFPM* is affected by the average rainfall of the area. Pavements located in 10-in. rainfall areas generally showed an almost zero rate of failure development, whereas pavements located in 52-in. rainfall areas developed failures at a rate of about one failure per mile per year.

The structural performance of continuously reinforced concrete (CRC) pavements is generally influenced by several factors, among which construction materials, traffic loads, and environment are most important. Past research in pavements has yielded methods that can be used to estimate the effects of construction materials and traffic loads on the performance of rigid pavements *(1)*. However, the research on the effects of environmental factors on the performance of rigid pavements is not adequate. The effects of environmental factors, such as temperature, rainfall, and freeze-thaw cycles, on the performance of rigid pavements are only partly known. In general, existing design methods will consider the worst environmental conditions to arrive at a suitable design. For example, the current test procedures generally recommend that the modulus of subgrade reaction for rigid pavement design be determined under the most unfavorable saturated subgrade conditions *(2)*. This will yield only one thickness of pavement if the soil type, traffic, and other design parameters are the same. If these pavements are built in two different rainfall zones, their performance will be different. The pavement built in a low-rainfall zone will perform better than the pavement built in a high-rainfall zone. Therefore, to estimate the difference in their performance, it is essential that the effect of environmental factors such as rainfall on the performance of pavements be considered. The new AASHTO Design Guide *(3)* recommends the testing of materials for actual site conditions not the worst conditions, as was the case in the past.

The effect of other environmental factors can be similarly determined and incorporated appropriately in the design procedures.

The objective of the study summarized in this paper was to investigate the possibility of developing a model that could provide an estimate of the effect of rainfall on the performance of CRC pavements. The pavements in Texas were selected for this study because there is a rigid pavement condition survey data base for the state of Texas that contains a pavement condition history of CRC and other types of rigid pavements throughout the state for the past 10 years. Also, the geographic locations of the pavements cover a wide range of rainfall areas, from 10 to 52 in. per year.

For the purpose of this study, the effect of rainfall on pavement performance was determined in the following manner:

1. A relationship was developed between rainfall and the performance parameter of pavements located in the areas of known rainfall and
2. A relationship was developed between the subgrade soil characteristics and the performance of pavements located in areas where rainfall may affect the characteristics of subgrade soil and subsequently the performance of pavements built on these subgrades.

The details of this study are described in the following paragraphs.

PAVEMENT SECTIONS

Figure 1 shows the boundaries of districts within the state of Texas where the pavement sections used in this study are

Center for Transportation Research, The University of Texas at Austin, Austin, Tex. 78705-2650.

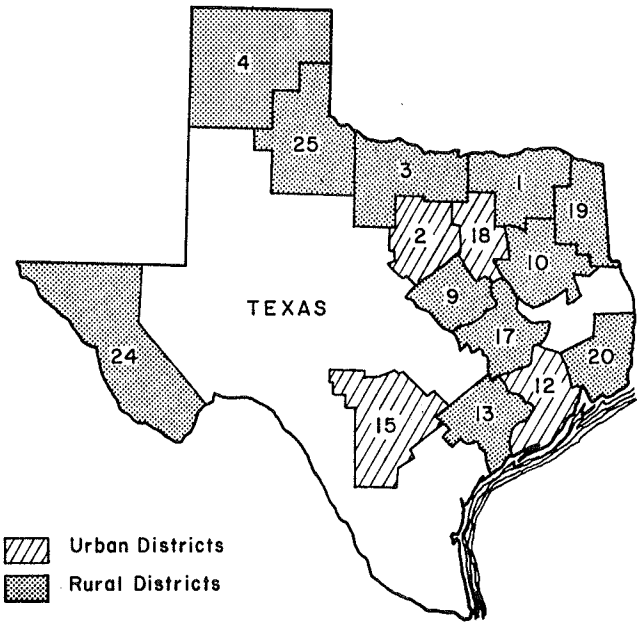

FIGURE 1 Location of districts within the state of Texas that were included in rigid pavement condition surveys.

TABLE 1 SUMMARY OF CRCP CONDITION SURVEY DATA AND ANNUAL RAINFALL FOR VARIOUS DISTRICTS IN THE STATE OF TEXAS (1979–1984 data)

District Number	Total Length of Unoverlaid Sections, Miles	Annual Rainfall (Inches)	Rate of Failures Per Mile/Year (FPM)
1	48	43	.69
3	95	29	.14
4	105	18	.07
9	47	34	.30
10	167	42	.71
13	166	38	.68
17	225	40	.49
19	112	46	.73
20	57	52	.80
24	122	10	.02
25	62	22	.20
Total	1,206		

located. The average annual rainfall in these districts varies from 10 to 52 in., as indicated by the data in Table 1. The total mileage of unoverlaid pavement sections in each district is also listed in Table 1.

All pavement sections were designed using the standard procedures in existence at the time of their construction. A design period of 20 years was used for all pavements.

About 90 percent of the CRC pavements in Texas were built with 8-in.-thick slabs and 0.52 percent longitudinal steel. The remaining 10 percent are 9, 10, and 13 in. thick with 0.52 percent steel. Practically all sections are on the Interstate highway system. According to the surveys conducted in 1980, the traffic on these sections ranges from 1.2 to 7.8 million equivalent single axle loads (ESALs) per year.

The following four types of subbases were used underneath the CRC pavement slabs:

1. Cement treated (37 percent of sections),
2. Asphalt treated (29 percent of sections),
3. Lime treated (25 percent of sections), and
4. Flexible (9 percent of sections).

Subgrade soils contain sandy and clayey materials in different proportions. Some clays found in Texas are highly swelling clays. However, the swelling characteristics of each clay are not the same as those reported by Machado *(4)*.

PAVEMENT CONDITION SURVEY DATA

Pavement condition survey data have been gathered for the past 10 years for the pavement sections included in this study. These surveys were conducted for the first time in 1974. Subsequent surveys were conducted in 1978, 1980, 1982, and 1984. Only continuously reinforced concrete pavements (CRCPs) were included in this study.

The condition survey data included the following distress manifestations of the pavements *(5)*:

1. Transverse cracks with severe spalling.
2. Minor and severe punchouts, and
3. Asphalt and cement concrete patches.

The definitions of these types of distress and the procedures used to record them are described in the condition survey manual *(6)*.

The portions of the pavements that were overlaid during the study period were excluded from this study. However, the sections that were subjected to routine maintenance were retained without any special consideration.

RAINFALL DATA

The average annual rainfall data for each district included in this study were obtained from records compiled by the Texas Department of Water Resources. These records have been collected since 1951 and the averages were obtained for a period of 30 years (1951–1980). Table 1 gives these data.

EFFECT OF RAINFALL ON CRC PAVEMENT PERFORMANCE

The rigid pavement condition survey data collected during the past 10 years (1974–1984) have been stored in a data base, which is maintained by the staff of the Center for Transportation Research (CTR) at The University of Texas at Austin. The data base contains the condition history of CRC and other types of rigid pavements recorded at every 0.2 mi of the pavement section except in 1984, when the data were recorded at every 0.4 mi of the section.

Condition survey data for the years 1974 and 1984 were selected for this study. Those pavement sections that were overlaid during this period were not included in the study. The condition survey data for each district were summarized by combining the patches and punchouts in the following manner:

Total number of failures per mile *(NFPM)* = Sum of total number of patches and punchouts in the unoverlaid part of the pavement/total length of the overlaid part of the pavement (1)

The average rate of *NFPM* per year *(RFPM)* was calculated by the following relationship:

$$\text{Average } RFPM = \frac{\text{Total } NFPM \text{ in } 1984 - \text{Total } NFPM \text{ in } 1974}{10} \quad (2)$$

The estimated values of *RFPM* for each district are given in Table 1.

A regression analysis of the data in Table 1 was performed to determine the relationship between the average rate of *RFPM* and the average annual precipitation *(P)* of the district. The following equation was obtained:

$$\log (RFPM) = -4.05 + 2.35 \log (P)$$
$$(R^2 = 0.94;\ S = 0.129) \quad (3)$$

This is a simple one-variable regression analysis. The value of $R^2 \approx 1.0$ indicates that there is a strong correlation between *RFPM* and *P*. *RFPM* increases with an increase in *P* as shown in Figure 2.

Three districts with typical low, medium, and high rainfall were selected to study the development of failures in the CRC pavements located in these areas. Figure 3 shows a plot between *NFPM* and the age of pavements. It is evident that the *NFPM* in high-rainfall regions (46 in./year) increases at a greater rate than in medium- (38 in./year) or low- (18 in./year) rainfall regions, as was indicated by Equation 3. Also, the *NFPM* in these districts remains low for several years irrespective of rainfall. However, when the pavements start developing some initial damage, the *NFPM* in high-rainfall areas increases at a greater rate than in lower-rainfall areas. In an area with 18 in. of rainfall per year (District 4), only about one failure per mile was observed after about 15 years, whereas District 19, with 46 in. of rainfall per year, developed about seven failures per mile during the same time, as shown in Figure 3.

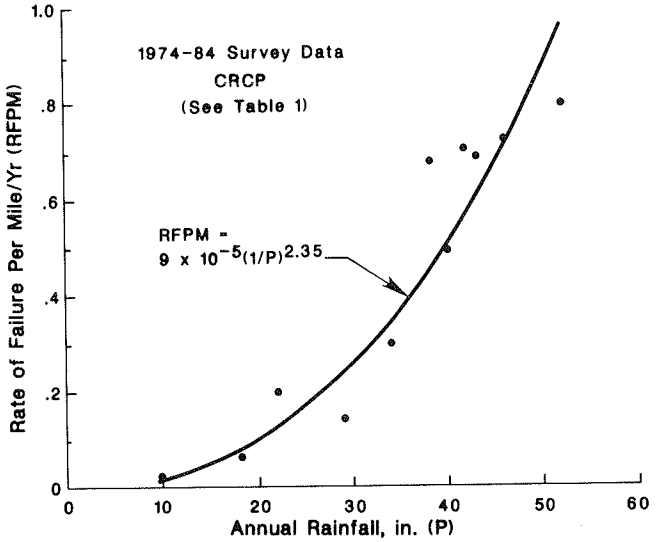

FIGURE 2 Effect of rainfall on the rate of failure per mile per year.

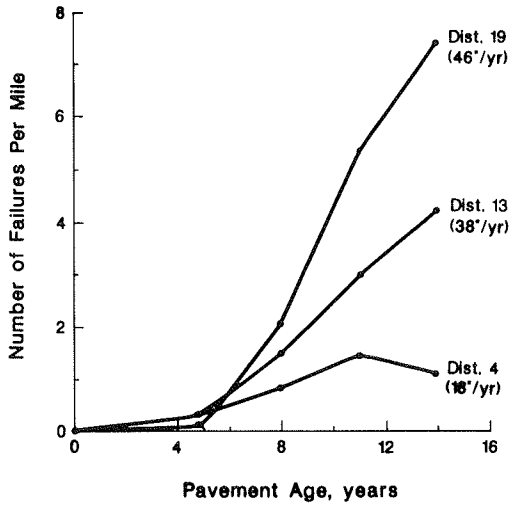

FIGURE 3 Performance history of CRCP located in different rainfall areas.

EFFECT OF SUBGRADE SOIL ON PERFORMANCE OF CRCP

It is generally assumed that if the modulus of subgrade reaction of soils at two different sites is the same, the pavement thickness will also be the same if all other conditions are the same. This assumption would be valid for sites where subgrade soils remain unaffected by rainfall during the service life of the pavement. However, the assumption will not be true if the soils at these sites differ in clay content and their swelling characteristics. This was revealed by an analysis of data collected from District 19, where the annual rainfall is 46 in. Two sections with different clays were selected for analysis. The performance of these two sections is plotted in Figure 4. This

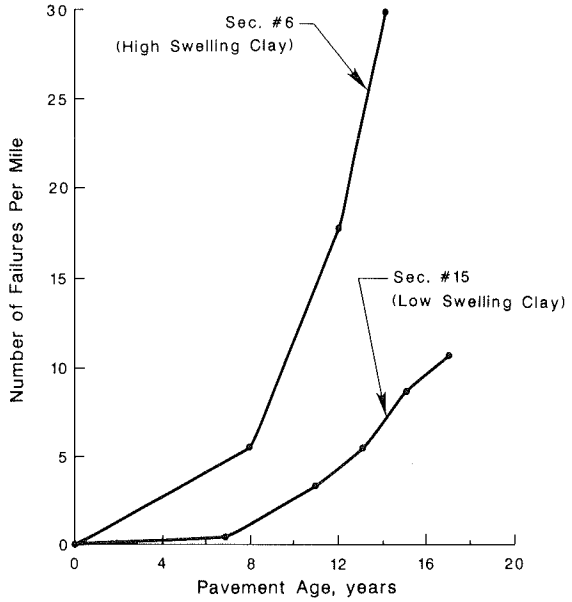

FIGURE 4 Performance history of pavements in District 19.

figure clearly shows that Section 15, built on subgrade containing low swelling clay, did not develop as many failures per mile as Section 6, which was built on soil with montmorillonitic clay mud (high swelling). Because rainfall and other conditions are approximately the same, it appears that the swelling clayey material is responsible for the higher *NFPM* in Section 6.

The effect of subgrade soil on the performance of CRCP was further studied by analyzing data from several other districts. Figures 5 and 6 show the effect of rainfall on the performance of CRCP in two different subgrade soil conditions. Pavements built on subgrade soil containing 100 percent clay were selected for Figure 5. These pavements are located in two different districts, which have rainfall of 43 and 18 in. per year, respectively. It is evident from this figure that the pavement built in the high-rainfall (43 in./year) area developed more failures per mile than the pavement built in the low-rainfall (18 in./year) area. On the other hand, if the clay content of subgrade soil is almost zero, then the effect of rainfall on pavement performance is almost negligible, as shown in Figure 6.

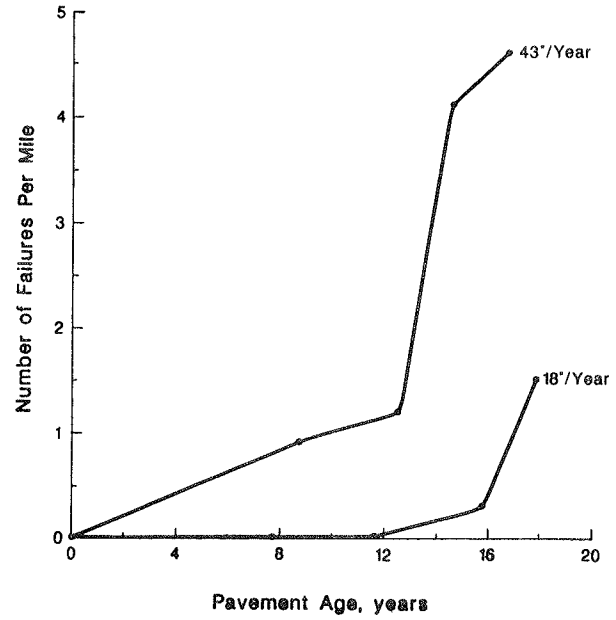

FIGURE 5 Effect of rainfall on pavement performance (subgrade = 100 percent clay).

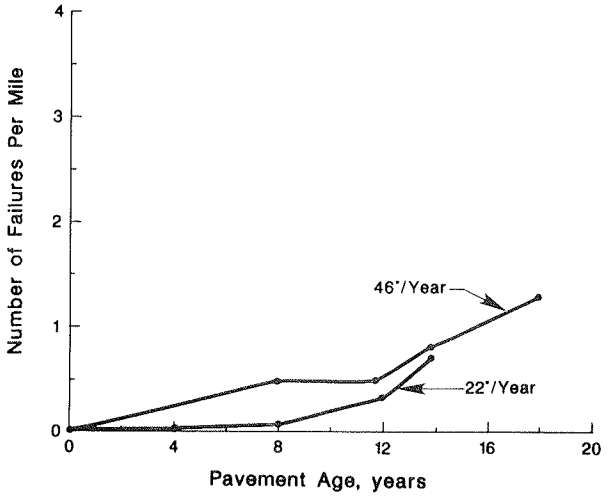

FIGURE 6 Effect of rainfall on pavement performance (subgrade = 0 percent clay).

SUMMARY OF RESULTS

The results of the study can be summarized as follows:

1. An analysis of condition survey data for the past 10 years indicated that the average annual rainfall in an area affects the performance of pavements significantly. Areas of high rainfall developed failures at a faster rate than areas of low rainfall (see Figures 2 and 3).
2. The effect of rainfall on the performance of pavement built in areas of different rainfall intensities is almost negligible for the first few years, until the pavements start developing failures. After the pavements develop failures, the effect of rainfall on pavement performance is significant (see Figure 3).
3. The swelling characteristics of clay in the subgrade soil affect the performance of pavements. A high swelling clay in subgrade soil causes more failures in pavements than a low swelling clay in the subgrade, when the pavements are located in areas of like rainfall (see Figure 4).
4. The effect of rainfall in areas where subgrades have high clay content is more intense than in areas where subgrades contain no clay (see Figures 5 and 6).

CONCLUSIONS AND RECOMMENDATIONS

The analysis of limited data reported in this paper indicates that swelling characteristics of subgrade clays and rainfall at the pavement site affect pavement performance during its service life. Current design procedures are based on material properties determined at the worst possible condition. In practice, these conditions may not always exist. Therefore the performance of these pavements is likely to be different if the soils at the site perform differently than assumed in the design. In view of this, it would be desirable to review current design procedures and incorporate necessary modifications to accommodate the effect of the two factors mentioned in this paper—rainfall and subgrade soil type. The new AASHTO design manual *(3)* recommends testing materials for actual site conditions.

ACKNOWLEDGMENT

The authors are pleased to acknowledge the combined support of the Center for Transportation Research at The University of Texas at Austin and the Texas State Department of Highways and Public Transportation, in cooperation with the Federal Highway Administration, U.S. Department of Transportation. Special acknowledgment is made to the staff of the Center for Transportation Research of The University of Texas at Austin for their assistance in preparing the drafts and figures of this paper.

REFERENCES

1. *Interim Guide for Design of Pavement Structures.* AASHTO, Washington, D.C., Chapter III, revised 1981.
2. E. J. Yoder and M. W. Witzack. *Principles of Pavement Design,* 2nd ed. John Wiley & Sons, Inc., New York, 1975.
3. *Guide for Design of Pavement Structures.* AASHTO, Washington, D.C., 1986.
4. J. P. Machado. *Continuously Reinforced Concrete Pavement: Prediction of Distress Quantities.* M.S. thesis. The University of Texas at Austin, 1977.
5. C. L. Saraf, B. F. McCullough, and W. R. Hudson. *Condition Surveys and Pavement Evaluation of Existing and Overlaid Rigid Pavements.* Research Report 388-5F. Center for Transportation Research, The University of Texas at Austin, Nov. 1985.
6. C. Saraf, V. Torres-Verdin, and B. F. McCullough. *Manual for Condition Survey of Continuously Reinforced Concrete Pavements and Jointed Concrete Pavements.* Research Report 388-3. Center for Transportation Research, The University of Texas at Austin, May 1985.

Publication of this paper sponsored by Committee on Strength and Deformation Characteristics of Pavement Sections.

Effect of Moisture on the Structural Performance of a Crushed-Limestone Road Base

N. H. THOM AND S. F. BROWN

A series of repeated load triaxial tests on a crushed-rock aggregate is described, including variations in grading and degree of compaction as well as moisture content. The effects of these variables are discussed and it is found that elastic stiffness tends to decrease slightly with increased moisture content for broadly graded materials. The influence of density is negligible, and that of grading minor, which results in some stiffness reduction as the fines content increases. The accumulation of permanent strain under multicyclic loading is found to be strongly dependent on density; denser material performs better. Grading has a minor effect. Increased moisture content results in substantially increased straining. The value of suction, which could exist in a granular material, is then explored indirectly by means of unconfined compression tests, and its effect on drainage is noted. Permeability measurements are given and their possible effect on drainage considered. Finally, computations are presented that illustrate the influence of partial and full saturation of a base layer of a pavement structure.

The need to avoid excessive water accumulating in a granular road base material has been experientially proved many times in post mortem analyses of failures. Generations of practical engineers have insisted that drainage is of first importance in road design though it is often not effective in the long term. There is uncertainty about how much water is permissible and how this relates to variables such as grading, density, and loading frequency.

To provide some information on these points, a series of triaxial tests was performed on a particular crushed-rock material (dolomitic limestone) at different gradings and densities. The tests were aimed at exploring both elastic behavior, which controls the load-spreading ability of the granular layer, and development of permanent deformation under repeated loading. Further tests were performed to measure permeability, determine approximate suction values, and establish compaction characteristics.

REPEATED LOAD TRIAXIAL APPARATUS

All tests were performed on specimens 75 mm in diameter and 150 mm in height. The triaxial loading arrangement involved air pressure to generate confining stress. Deviator stress was applied by a servo-hydraulic actuator operating on feedback from a load cell. A signal generator, giving sinusoidal output at frequencies up to 10 kHz, provided the repeated loading facility. Three hertz was the maximum frequency used because of the constraints of the servo-hydraulic system.

Deformations were measured between studs embedded in the sides of the specimen using the technique developed by Boyce and Brown *(1)*. These were arranged in diametrically opposite pairs at approximately the 1/4 and 3/4 height points. A pair of linear variable differential transformers (LVDTs) gave the axial deformation of either side of the specimen. Strain-gauged epoxy hoops gave the radial deformation at two levels. Facilities to introduce or extract water from the specimen were provided through the loading platens. The whole arrangement is shown diagrammatically in Figure 1.

MATERIAL AND SPECIMEN PREPARATION

The material chosen was dolomitic limestone, commonly used in road construction in England. The gradings investigated are shown in Figure 2 and range from nearly uniform to very broadly graded, but all had a maximum particle size of 10 mm, dictated by the test specimen diameter.

All specimens were made by tamping the material into a mold of the appropriate size. The membrane, with studs attached, was held against the wall of the mold by vacuum. Compaction was generally carried out in 5 layers, although, where extremely heavy tamping was required, this was increased to 10 layers.

TEST PROGRAM

Initially, a full series of tests was carried out on the material in a dry state. Three specimens were made at each grading, each at a different level of compaction. Various stress paths were used to determine elastic behavior, and repeated loading on a single stress path (the same for all specimens) was applied to study permanent deformation. Finally, each specimen was brought "close" to failure in order to determine the failure stress state. On completion of this test sequence, water was passed through the specimen to measure permeability and then allowed to drain, which gave an "equilibrium" moisture content.

Compaction curves were obtained on all but the two most uniform gradings. To be of direct relevance to the triaxial testing, compaction was carried out in the same mold, and with a number of blows per layer in the middle of the range used in specimen preparation. Clearly, a higher level of compaction

Department of Civil Engineering, University of Nottingham, University Park, Nottingham, United Kingdom.

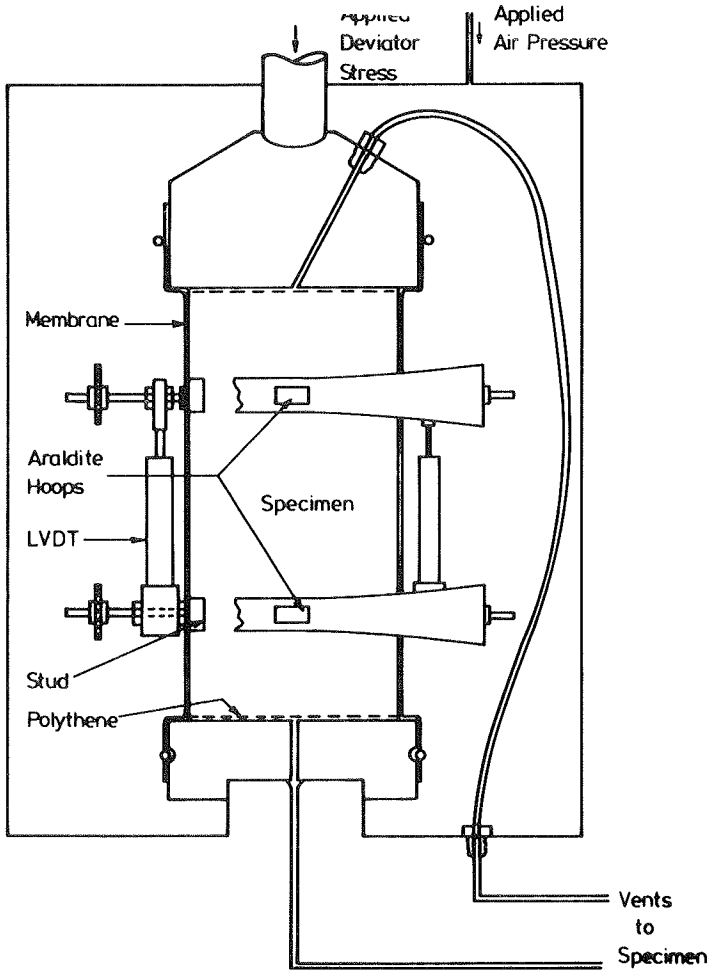

FIGURE 1 Triaxial specimen arrangement.

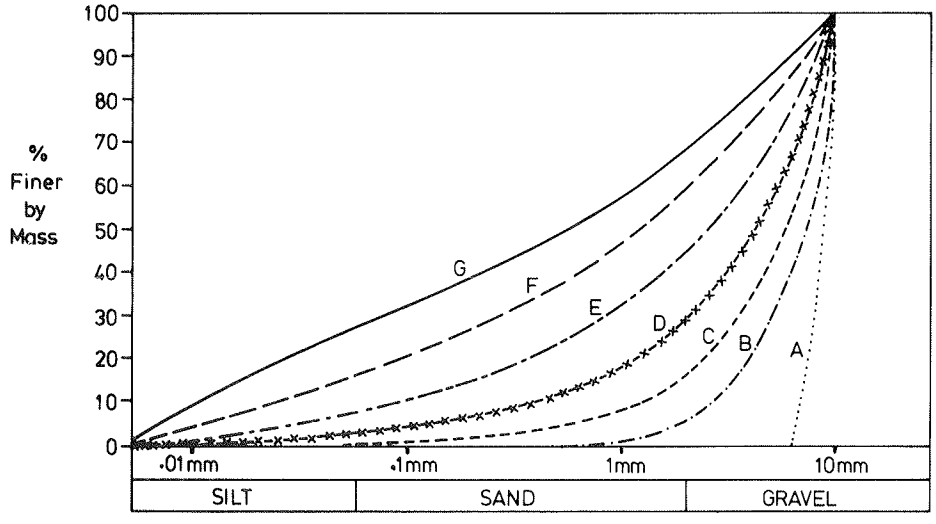

FIGURE 2 Particle size distribution chart.

would reduce the optimum moisture content and probably also the pessimum on the compaction curve. The results obtained are shown in Figure 3.

A series of drained repeated load triaxial tests was performed on material from Gradings D, E, and F (Figure 2). At least two specimens were made for each grading. Moisture content was varied during testing and results for both elastic behavior and permanent deformation were obtained for each moisture level. The stress paths used are shown in Figure 4. Moisture content was determined by monitoring the weight of the whole apparatus together with the specimen.

Finally, a series of unconfined compression tests was performed on dry specimens of all gradings and wet specimens of Gradings D, E, and F, at similar densities, and at moisture

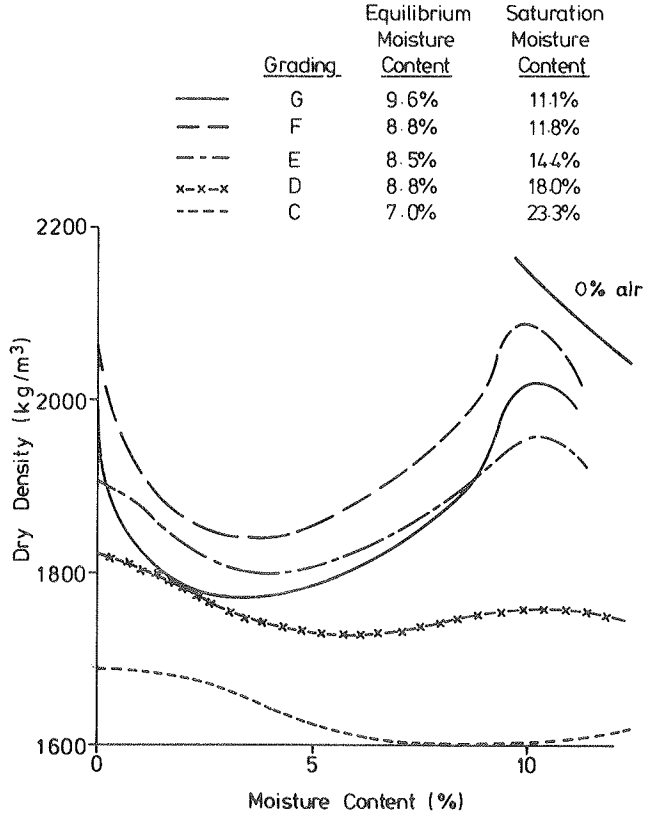

FIGURE 3 Compaction curves.

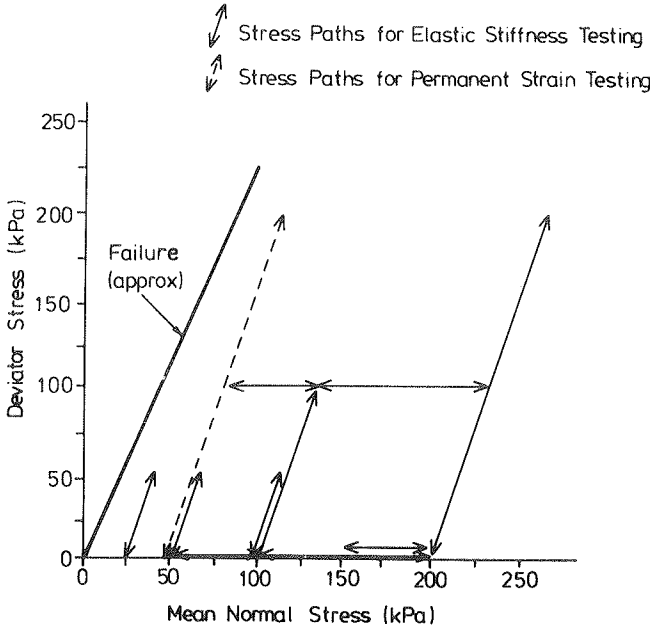

FIGURE 4 Stress paths used.

contents likely to correspond to the maximum suction value. The difference between the wet and the dry results gives a strong indication of the value of suction.

COMPACTION CHARACTERISTICS

The results of compaction tests on materials at Gradings C to G are shown in Figure 3. The general shape is a familiar one, with a pessimum at a relatively low moisture content and an optimum at a higher one. The shape is lost on the more uniform materials because of their inability to retain large quantities of moisture and because the effects are much smaller.

Other important moisture contents are also shown in Figure 3, those at saturation and equilibrium. Equilibrium is defined here as the moisture content that remains when a saturated specimen has been allowed to drain under gravity until no further moisture emerges. Suction can be expected to exist at moisture contents below equilibrium. It is considered that the maximum suction will, approximately, coincide with the pessimum on the compaction curve because suction is likely to impede compaction by increasing interparticle forces.

ELASTIC CHARACTERISTICS

It is not the purpose of this paper to discuss in any detail the real nonlinear behavior of a granular material, which has been done previously *(2)*. The purpose of this paper is to compare behavior at different gradings, moisture contents, densities, and frequencies. Elastic stiffness will, therefore, be expressed here simply as the value of resilient modulus (repeated deviator stress divided by resilient axial strain) averaged over the five stress paths used involving cyclic deviation stress (Figure 4). These stress levels would be at the upper end of the expected range for a road base layer.

Figure 5 is a plot of elastic stiffness from drained tests on three specimens at Grading E, chosen because it approximates to a one-third scale British Type 1 subbase material *(3)*. Specimens 1 and 2 were compacted dry, and Specimen 3 at or near optimum moisture content. Dry densities were 2000, 1995, and 2006 kg/m^3, respectively. Specimen 2 had water added before

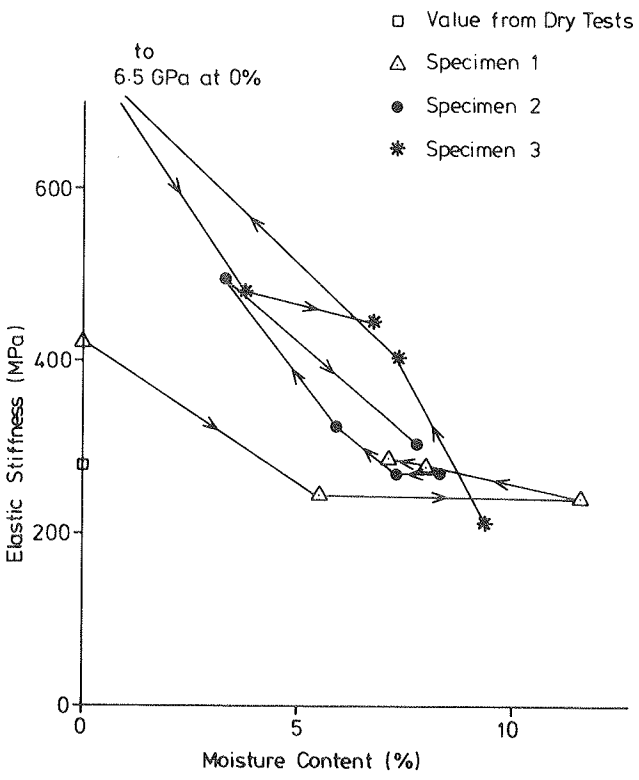

FIGURE 5 Elastic stiffness variation, Grading E.

any testing was done. The progression of wetting and drying may be seen by the direction of the arrows in Figure 5. For comparison, the elastic stiffness obtained during the series of dry tests (299 MPa) is also shown.

The amount of variability among specimens is quite considerable, but a trend of decreasing stiffness with increasing moisture content is clearly apparent.

It can also be seen that stiffness increases to a far greater value after drying than before initial wetting. This may be attributed to cementation between the limestone particles.

The decrease in stiffness with increased moisture content agrees with results from Smith and Nair *(4)*, who attributed it to pore pressure increases. However, for the tests described here, which were drained, frequency of sinusoidal load pulsing was varied over a range of 0.1 to 3 Hz with no discernible differences in stiffness. This indicates that, at the degrees of saturation used (up to 85 percent), no pore pressures developed, which confirms earlier work by Brown *(5)*.

The different effects of moisture on different gradings are shown in Figure 6 for Gradings D, E, and F. The elastic stiffnesses from initial dry testing are also included for all gradings. All specimens were compacted dry using identical compactive efforts. The same trends in behavior can be seen for the three gradings, but variations are evidently quite slight for Grading D. It is logical to expect that the effect of moisture increases with the amount of fine material present and that material at the more open gradings (A, B, and C) will show little stiffness variation in the partly saturated state.

Results for the dry state over the whole range of gradings indicate no substantial variation but a general trend of decreasing stiffness with increasing fines content. Not shown here are the stiffnesses obtained on dry materials at levels of compaction different from that used for the wet material.

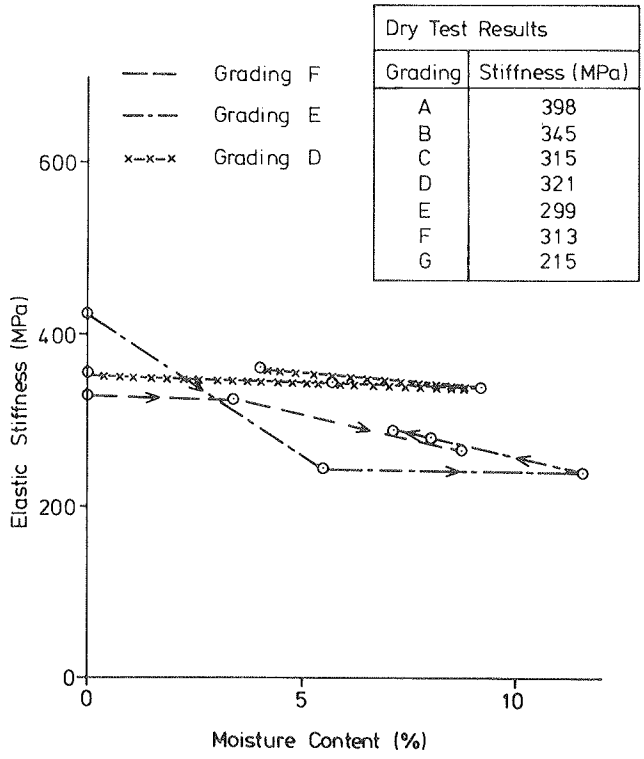

Dry Test Results	
Grading	Stiffness (MPa)
A	398
B	345
C	315
D	321
E	299
F	313
G	215

FIGURE 6 Elastic stiffness for different gradings.

Interestingly, elastic stiffness was found to vary only slightly (± 10 to 15 percent) over a large range of compactive efforts. This was true of all seven gradings.

As indicated previously, over the range of moisture contents covered, no noticeable pore pressures were developed. The moisture effect may, therefore, be some form of lubrication. However, if the material is close to saturation, pore pressures will clearly develop and the effective stresses decrease, as was recognized by Smith and Nair *(4)*. Research has shown [e.g., Pappin *(6)*], and the present work confirms it, that the effective stress principle is still broadly applicable. The knowledge that is required, therefore, in order to predict pore pressures, involves permeability (discussed later), loading time, and drainage path length as well as degree of saturation. It is an almost incalculable problem, but a worst possible case can be obtained by assuming completely undrained saturated conditions and this is included in the computations in a section of this paper.

PERMANENT DEFORMATION BEHAVIOR

The method of presenting permanent strain results is in a plot of strain rate (permanent shear strain per cycle) against shear strain, and the measure of permanent shear strain used is the difference between the axial and radial strains at the end of a loading cycle. Experience has shown that a decrease of strain rate is the usual result, which gives a straight line if a logarithmic scale is used for strain rate. Figure 7 shows the results of three specimens at Gradings D, E, and F, which had moisture added during testing. The stress path used was a cell pressure of 50 kPa and a deviator stress cycling between zero and 200 kPa (Figure 4).

The major feature of Figure 7 is the considerable increase in strain rate resulting from the addition of water. The effect of moisture addition is slightly greater when the fines content is higher but is still quite significant for Grading D. It appears that a relatively small moisture content is required to trigger the strain rate increase and that addition of further water has little effect. The exception is Grading F the strain rate of which increased in two stages. Loading frequency had a minor effect; higher frequency gave a slightly lower strain rate.

The implication of the dramatic increase in strain rate on wetting is clearly that the rutting potential of the granular layer will increase by a significant factor. This has been noted in tests using the Heavy Vehicle Simulator in South Africa *(7)*. Because no recognizable pore pressures are involved, it appears that the water merely acts as a lubricant on the particles.

It is of interest to summarize here the pattern of permanent deformation results from dry material over all of the gradings and covering a large range of compactive efforts. The different gradings produced similar results at high compactive efforts, but, at lower levels, the more open gradings performed better. For any one grading, density variation (due to different compactive efforts) had a dramatic effect; denser specimens performed far better. This was particularly true for the more broadly graded materials.

This gives rise to a dilemma. Because the highest densities are achieved at optimum moisture content and density is so important for permanent deformation resistance, it is logical to use material at that moisture content. However, once the material is placed, the water is a problem that can lead to increased

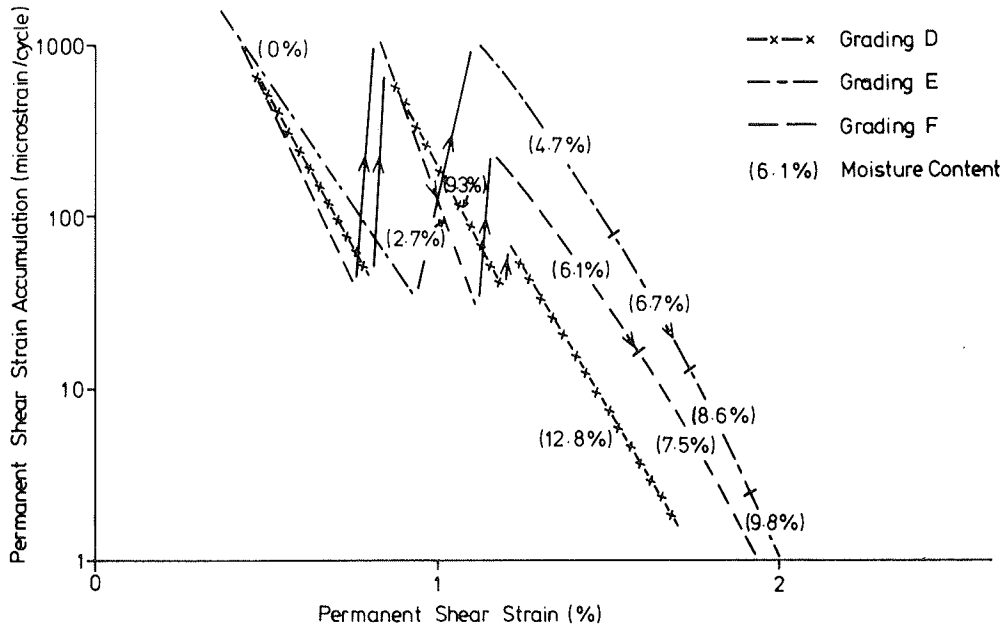

FIGURE 7 Accumulation of permanent strain.

permanent deformation and, if saturation occurs, the problems could multiply.

SUCTION CHARACTERISTICS

Suction measurement is notoriously difficult, particularly for granular materials the values of which are low. For this reason it was decided not to measure suction directly but to deduce it using the effective stress principle.

It was noticed that compacted dry graded aggregates tend to display an unconfined compression strength that is typically 20 to 30 kPa and a failure envelope at low confining stress, as shown in Figure 8, for material at Grading D. Unconfined means zero cell pressure and the membrane hanging loosely around the specimen. Thus, if any suction were operating, the unconfined strength would increase because, as well as aggregate interlock, the suction would act in the same way as confining stress. The suction value is therefore given by the difference between wet and dry strengths divided by the slope of the failure line. The only requirement is to achieve a wet specimen at the same dry density that is used in dry testing. This was done, at pessimum moisture contents, for materials at Gradings D to G and the deduced suction values are plotted in Figure 9. Different densities would undoubtedly affect these values.

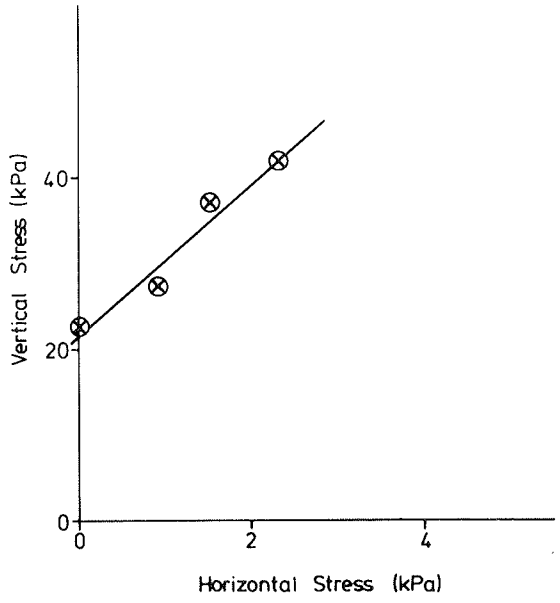

FIGURE 8 Failure envelope at low stresses.

As may be seen, the numbers are relatively small and would probably not have any great effect on the elastic performance of a road base, but they are quite significant for drainage. For example, 3.1 kPa for Grading F represents a head of 300 mm of water. Thus a drain less than 300 mm below the bottom of the subbase layer would be relatively ineffective for such a material. A drain level with the bottom of the subbase would hardly allow better than equilibrium conditions to prevail.

PERMEABILITY

The coefficient of permeability is also a difficult parameter to measure consistently, but it has obvious application to drainage problems. It could also have significance in determining pore pressure development if the base material ever approached saturation. Permeability values are shown in Figure 10 for the gradings investigated. They were obtained using ordinary tap water through a small specimen with a scaled-down aggregate grading. The values may therefore be lower than expected on site, but relative permeabilities are probably correct.

As an example of the effect of low permeability, a 5-m-wide, 200-mm-thick layer of material at Grading F, with a coefficient of about 2×10^{-6} m/sec, draining along the length of one side under a head of 200 mm could pass about 100 mL of water per hour per meter length of road. Over the same meter

length, moderate rain may give rise to 20,000 mL of water per hour. Thus it may readily be seen how easily such a layer could become saturated if the surface were not adequately sealed.

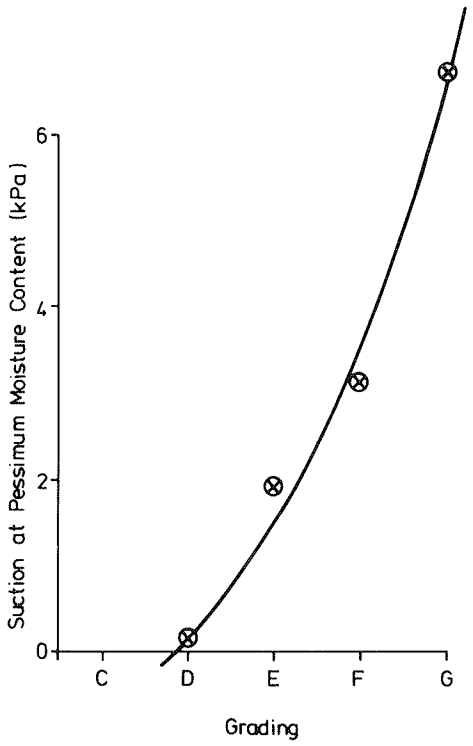

FIGURE 9 Deduced maximum suction values.

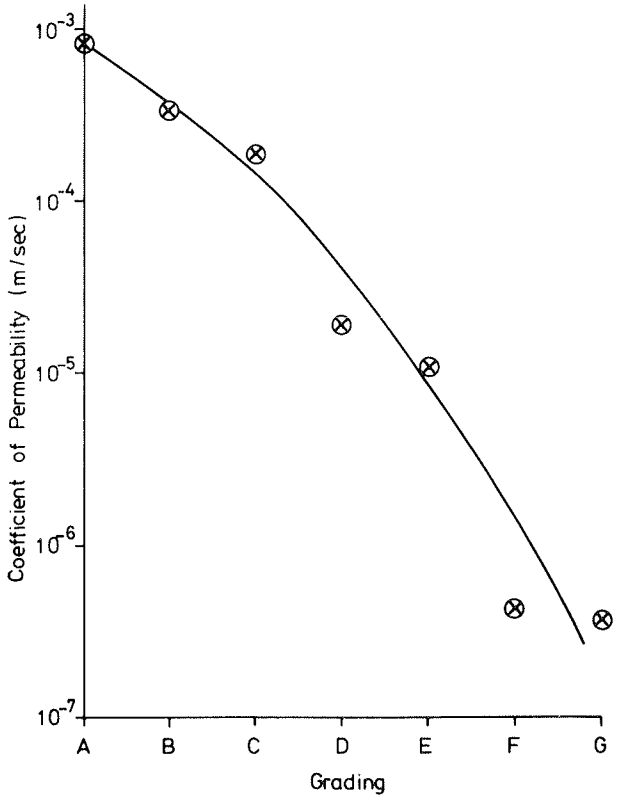

FIGURE 10 Coefficient of permeability for all gradings.

PAVEMENT ANALYSIS

The changes in elastic stiffness that occur because of changes in moisture content have been described. In this section the results of pavement analysis using these data are given. A standard pavement, incorporating material at Grading E in the dry state, was selected for analysis. The parameters were then adjusted to allow for material at optimum moisture content (about 10.5 percent). Finally, the pavement was analyzed using the parameters for optimum moisture content but assuming full saturation and no drainage. The pavement details and analysis results are given in Tables 1 and 2.

TABLE 1 PAVEMENT DETAILS USED IN ANALYSIS

Layer	Thickness (mm)	Stiffness (MPa)	Density (kg/m^3)
Asphalt	50	5000	2500
Base	200	150 (dry) 120 (wet)	2200
Subgrade	3000	100	2000
Bedrock	-	∞	-

Two programs for pavement analysis were used. BISTRO *(8)* deals with linear elastic layered systems and allows analysis of the first two situations. GRANMAT is a new program that incorporates nonlinear behavior in the subbase and is still under development at Nottingham. It allows the saturated undrained situation to be modeled.

The significant quantities emerging are tensile strain at the bottom of the asphalt layer (controls cracking) and vertical strain at the top of the subgrade (indicates rutting potential). Surface deflections under the load are also included.

It can be seen from both BISTRO and GRANMAT that the effect of using optimum moisture content parameters rather than dry ones is small. The difference between the two programs is probably due to the difficulty in selecting the appropriate single value of elastic stiffness of a granular layer for use in BISTRO. However, the saturated undrained results from GRANMAT demonstrate the immense weakening that is theoretically possible if a pavement becomes saturated. Both strains have increased enormously, giving a manyfold decrease in expected pavement life; the order of magnitude may be found using a design method such as that described by Brown et al. *(9)*.

CONCLUSIONS

The presence of moisture in an aggregate "lubricates" the particles and increases both elastic and, particularly, permanent deformation. This takes place with no apparent pore pressures being generated. The permanent deformation accumulation rate can increase tenfold on wetting.

Subsequent drying out of a limestone aggregate can allow cementation and greatly increased stiffness.

TABLE 2 RESULTS OF PAVEMENT ANALYSIS

Run	Asphalt Tensile Strain (microstrain)	Subgrade Strain (microstrain)	Surface Deflection (microns)
BISTRO (dry)	332	832	530
BISTRO (wet)	372	842	579
GRANMAT (dry)	510	945	1037
GRANMAT (wet)	615	720	1082
GRANMAT (sat.)	1320	4515	2459

Loading frequency has a negligible effect on strains at degrees of saturation up to 85 percent.

Suction values have been deduced that would affect drainage properties of an aggregate layer but have little effect on stress-strain relationships.

The magnitudes of permeability that were measured underline the danger of excessive fines in a road base; they lead to poor drainage and subsequent saturation.

Analysis of a typical pavement structure has indicated that moderate levels of moisture have only a minor effect on overall elastic behavior but that saturation of a poorly drained base layer has a drastic effect.

ACKNOWLEDGMENTS

This study is part of a project on road foundation design sponsored by the Science and Engineering Research Council in the United Kingdom. The facilities at the Civil Engineering Department of Nottingham University under Professor P. S. Pell were made available and used for all testing.

REFERENCES

1. J. R. Boyce and S. F. Brown. Measurement of Elastic Strain in Granular Material. *Géotechnique*, Vol. 26, No. 4, 1976, pp. 637–640.
2. S. F. Brown and J. W. Pappin. Modeling of Granular Materials in Pavements. In *Transportation Research Record 1022*, TRB, National Research Council, Washington, D.C., 1985, pp. 45–51.
3. *Specification for Roads and Bridges*. Department of Transport, United Kingdom, 1976.
4. W. S. Smith and K. Nair. *Development of Procedures for Characterization of Untreated Granular Basecourse and Asphalt Treated Basecourse Materials*. Report FHWA-RD-74-61. FHWA, U.S. Department of Transportation, 1973.
5. S. F. Brown. Repeated Load Testing of a Granular Material. *Journal of the Geotechnical Engineering Division*, ASCE, Vol. 100, No. GT7, 1974, pp. 825–841.
6. J. W. Pappin. *Characteristics of a Granular Material for Pavement Analysis*. Ph.D. dissertation. University of Nottingham, United Kingdom, 1979.
7. J. H. Maree, C. R. Freeme, N. J. Van Zyl, and P. F. Savage. The Permanent Deformation of Pavements with Untreated Crushed Stone Bases as Measured in Heavy Vehicle Simulator Tests. *Proc., 11th Conference of the Australian Road Research Board*, Part 2, 1982, pp. 16–28.
8. M. G. F. Peutz, H. P. M. Van Kempen, and A. Jones. Layered Systems Under Normal Surface Loads. In *Highway Research Record 228*, National Research Council, Washington, D.C., 1968, pp. 34–45.
9. S. F. Brown, J. M. Brunton, and A. F. Stock. The Analytical Design of Bituminous Pavements. *Proceedings of the Institution of Civil Engineers*, Part 2, Vol. 79, 1985, pp. 1–31.

Publication of this paper sponsored by Committee on Strength and Deformation Characteristics of Pavement Sections.

Water-Induced Distress in Flexible Pavement in a Wet Tropical Climate

T. F. FWA

A wet tropical climate characterized by abundance of rainfall and cool nights followed by hot days offers a favorable environment for the development of water-associated distress in flexible pavement. Surface deteriorations such as stripping and raveling have been widely reported and studied in the literature. Other forms of water-induced distress, which are caused by water trapped within the structural system of a flexible pavement, are described in this paper. The occurrence of such distress is difficult to predict, and the subsequent repair is usually quite costly and elaborate. A number of cases of water-induced distress in flexible pavement in Singapore and Malaysia are presented and discussed. The need for drainage analysis in pavement design and the importance of drainage consideration in pavement construction and maintenance are highlighted. On the basis of relevant experience in the region, some preventive measures are recommended for guarding against water-induced problems in flexible pavement.

The abundance of rainfall during the monsoon months each year in a tropical country poses special problems for highway pavement engineers. One of the most common sights immediately after a heavy rainstorm is the accumulation of dislodged aggregates at a road junction or along a bend. Also visible on the pavement surface are signs of stripping, which occurs at an accelerated rate during the rainy season. These forms of surface deterioration can be easily detected by a layman or the ordinary traveling public. Correction by surface treatment or overlay is usually used to restore the riding quality of the affected surface. These treatments are also necessary to prevent the surface deteriorations from developing into potholes and other serious structural defects. These water-related problems have been widely reported and studied in literature *(1, 2)*. Although no way has been found to completely prevent their occurrence, major repair of pavement is generally not required if the deteriorated surface is treated with timely corrective maintenance measures.

Another form of water-induced flexible pavement distress, the occurrence of which is difficult to predict and the subsequent repair of which is usually quite costly and elaborate, is described in this paper. This distress may manifest itself through one of the following phenomena: *(a)* localized wet softened areas of pavement materials that could lead to formation of potholes or depressions in the pavement surface, *(b)* localized upward heaving of the pavement surface, *(c)* separation and disintegration of various pavement layers or successive lifts of a given pavement layer, or *(d)* unevenness or undulation of the pavement surface.

Department of Civil Engineering, National University of Singapore, Kent Ridge, Singapore 0511.

This distress should be differentiated from that which results from failure or movement of the subgrade foundation. It is directly related to accumulation of water within a pavement structure. Typically, water is trapped in a relatively porous layer sandwiched between two impervious layers after a long, heavy rainfall. This is followed by an increase of water pressure that is responsible for the manifestations of damage described in the preceding paragraph. A few typical occurrences in Singapore and Malaysia are presented in this paper to illustrate the different ways in which water could enter a pavement structure and the different circumstances under which a buildup of water pressure could take place. Recommendations about ways and means of preventing the occurrence of such distress are made.

WATER INFLOW UNDER HYDRAULIC HEAD

Potholes were found to form rapidly on the surface of a four-lane undivided roadway in the month of December 1985, approximately 1 month after the monsoon rain season began. Field investigation determined that, at about 3:00 p.m. on a sunny day, isolated spots on the pavement surface began to swell upward. The center of each swelled area rose about 20 to 40 mm above the original pavement surface. Each affected spot was roughly circular in shape and measured about 250 mm in diameter.

The total affected area covered a distance of about 4 km. On a hot afternoon the worst affected area would have more than 10 swelling spots within a distance of 200 m. These heaved-up surfaces could be easily depressed and flattened when stepped on by a human being, but they slowly returned to the swelled condition in about 20 min after the load was removed. The swelling began to subside at night when the temperature dropped and disappeared completely by the following morning.

The construction history of the roadway revealed the pavement structure shown in Figure 1. There was a 230-mm-thick base course of crushed stone. A 90-mm dense asphalt concrete layer was constructed above it, followed by an open-graded 25-mm asphalt wearing course. After about 5 years in service, a 50-mm overlay of dense asphalt concrete was laid in July 1984. Records showed that the overlay construction was carried out during a dry period. Figure 2 shows the profile of a typical core sample of the pavement structure.

Several 600- by 600-mm pits were excavated to the base course for inspection. Typically, the uppermost overlay and the bottom 90-mm asphalt concrete layers were dense and intact. The intermediate 25-mm old wearing course was damp, soft,

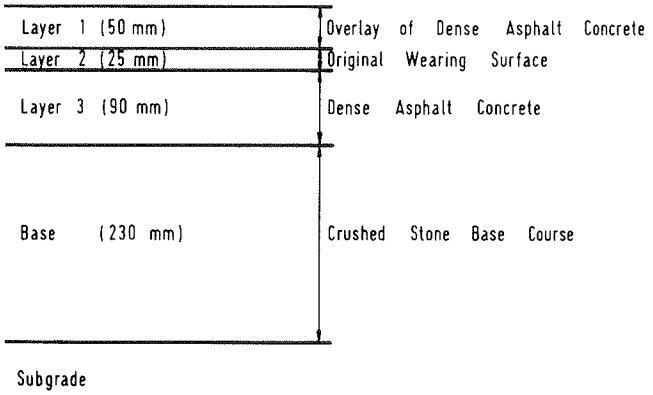

FIGURE 1 Profile of pavement structure.

and disintegrated as shown in Figure 3. Aggregates and bituminous binders of this second layer could be easily separated and extracted by bare hands. The water table was approximately 900 mm below the pavement surface. There was no sign of accumulated water within the base course, which was found to be dry and free draining. On the walls of each of these pits, as shown in Figure 4, water could be seen seeping out from the interface plane between the second and third layers. Pits were also excavated at the locations of swelling spots where only the top overlay layer was removed. There was no effective bond at the interface between this and the disintegrated layer below it. In about 15 to 20 min, approximately 40 mm of water would be collected in these pits from seepage from the underlying porous layer. A laboratory falling-head permeability test on cored samples indicated that the top and the bottom layers were practically impermeable, whereas the intermediate layer had horizontal permeabilities ranging from 2×10^{-5} to 5×10^{-2}

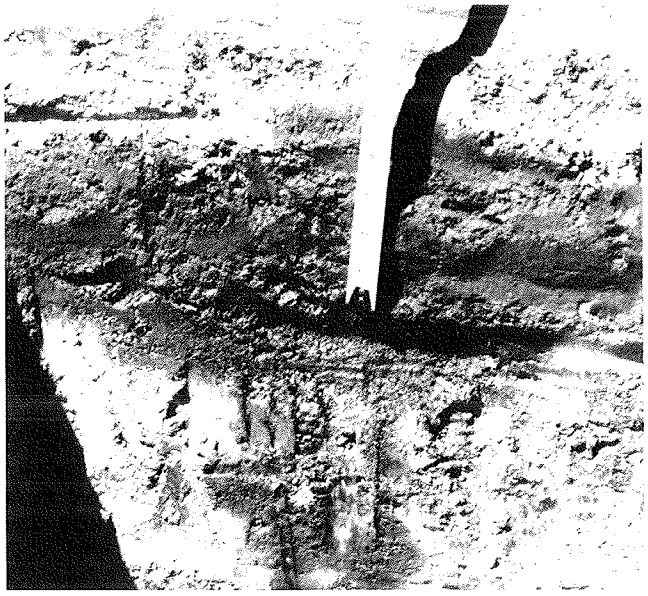

FIGURE 3 Soft damp material sandwiched between dense asphalt concrete layers.

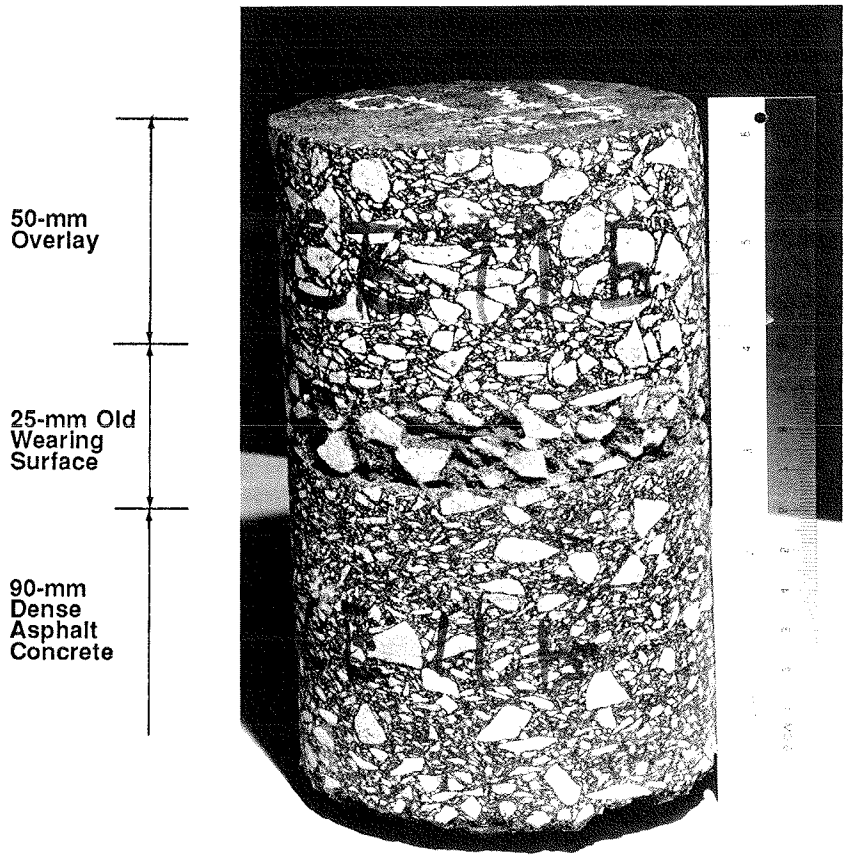

FIGURE 2 Core sample showing new overlay constructed on weathered old wearing surface.

FIGURE 4 Water seeping out from sandwiched damp layer.

cm/sec. It was believed that varying degrees of weathering and erosion by water of the old wearing surface were responsible for the large range of permeability values.

The borders of the roadway were laterite soils with poor permeability in the order of 1×10^{-5} cm/sec. During a heavy downpour, these borders were usually flooded. Field observation indicated that this floodwater took up to 8 hr to drain off. Meteorological data revealed that, in early December 1984, a 2-day and another 3-day rainstorm were recorded with 190 mm and 235 mm of rainfall, respectively.

During a site survey it was found that the flood on the borders of the roadway could achieve a sufficiently high hydraulic head (up to 125 mm) long enough for the floodwater to enter the sandwiched porous pavement layer from the edge joints of the road. For instance, under a sustained hydraulic gradient for a period of, say, 50 hr, and assuming a permeability of 5×10^{-2} cm/sec, water could travel a distance of 9.0 m in the porous pavement layer. After the subsidence of the flood, reverse flow of water was difficult because of the gentle cross-slope gradient and the unevenness of the pavement layer.

The possibility of water infiltration from the pavement surface was also examined. Field permeability tests conducted over a period of 2 days on the pavement surface indicated that infiltration through a crack-free bituminous mix was practically insignificant. Because the overlay surface was less than 5 months old and relatively free of cracks, it was unlikely that surface infiltration through cracks would cause such a widespread distribution of pressured trapped water as was found in the present case.

It is interesting to note the timing of surface swelling. The highest daytime temperature in Singapore and Malaysia, usually occurring at about 2:00 p.m., is around 32°C. The pavement surface temperature measured on a hot afternoon varies from 60°C to 70°C. The buildup of pressure that caused pavement surface swelling could possibly have resulted from *(a)* thermal changes that increased the pressure in the air and water trapped in the porous pavement layer and *(b)* lateral thermal expansion of aggregates and binders that reduced void spaces in the sandwiched pavement layer, which was confined in the vertical direction by two dense asphalt concrete layers and constrained laterally by concrete side curbs.

This water-induced problem required prompt correction because pavement deterioration in the form of potholes and surface disintegration was occurring at an accelerated pace under moving traffic. Surface treatments or additional overlay could not eliminate the problem. The only logical solution was to remove the sandwiched water-logged layer together with the top overlay surface for the entire length of the pavement. Measures were also taken to improve the drainage conditions of the area to avoid standing rain water on the borders of the roadway.

SURFACE INFILTRATION THROUGH JOINTS

A divided primary road, with two lanes in each direction, had badly deteriorated surface due to stripping and rutting. A 35-mm overlay of dense bituminous mix was applied in April 1984. Problems began to surface in September 1984 on the northbound pavement. Light brown stains in a straight-line pattern were observed on the pavement. Up to 2 weeks after a heavy rainfall, small patches of water were seen forming approximately in a straight line on the pavement surface during the warmer part of the day. Stains were left behind when these patches of water evaporated, as shown in Figure 5. Although no cracks were visible on the surface along the straight line on which stain marks were left, the line was later identified as the longitudinal joint between two neighboring overlay applications. Crack sealing was performed on locations where stain marks appeared.

Approximately 1 month after crack sealing, small patches of water and stains reappeared on stretches along the longitudinal joint. In addition, a series of longitudinal cracks with lengths varying from 200 to 450 mm was found on the wheelpaths adjacent to the longitudinal joint. Removal of the overlay layer revealed that the interface bond was ineffective at these wheelpath locations, and there were signs of accumulated water on the original deteriorated surface. It was estimated that stripping of the old surface had caused loss of binder to a depth of 20 mm. Failure to patch and seal or to mill off these stripped materials during the overlay operation had unknowingly incorporated a water-collecting layer within the pavement structure.

It was believed that after initial infiltration through the longitudinal construction joint, water worked its way along the plane of interface and collected in the stripped and rutted areas of the old surface. The disruption of interfacial bond and spreading of trapped water were aided by the pressure buildup due to rising temperature during hot afternoons as well as compression caused by traffic loadings. The initial sealing of longitudinal joints might have forced the trapped water to move sideways during a pressure buildup.

Because of budgetary constraints and possible inconvenience to the traveling public, repairs were carried out at night and only a few patches of areas that showed signs of distress were repaired at a time. At each location, as much as 60 mm of material was milled off to ensure that the deteriorated surface of the old wearing course was removed.

FIGURE 5 Patches of water emerged from pavement in hot afternoon and left stains behind when evaporated.

SURFACE INFILTRATION THROUGH CRACKS

Cracks in a pavement surface provide excellent storage space for surface water. A random survey, which was conducted on a secondary road after a 2-hr rainfall with a precipitation of 46 mm, indicated that many cracks, especially those wider than 0.5 mm, were still damp 24 hr after the rain had stopped. If these cracks are not repaired or sealed off, water that enters the cracks each time it rains tends to erode the interior of the pavement. Figure 6 shows a crack that could admit so much rain water that water was seen flowing out from the crack for several hours during the warmer part of the day after a heavy rainfall.

Given the presence of cracks and imperfect joints, it is possible that a pavement may become more permeable than the underlying base or subbase materials, thereby leading to a holding up of free water within the pavement structure during and after a heavy rainfall. Pressure buildup due to wheel load impacts or thermal changes could lead to erosion and disintegration of the pavement materials. Figure 7 shows a curb joint from which outflow of water and fines continued for more than 8 hr after a rainstorm had stopped.

CLOGGING OF SUBDRAINS

A secondary two-lane road located along the bank of an open unlined channel had the problem of water seeping out onto its

FIGURE 6 Water flowing out from crack after rain had stopped.

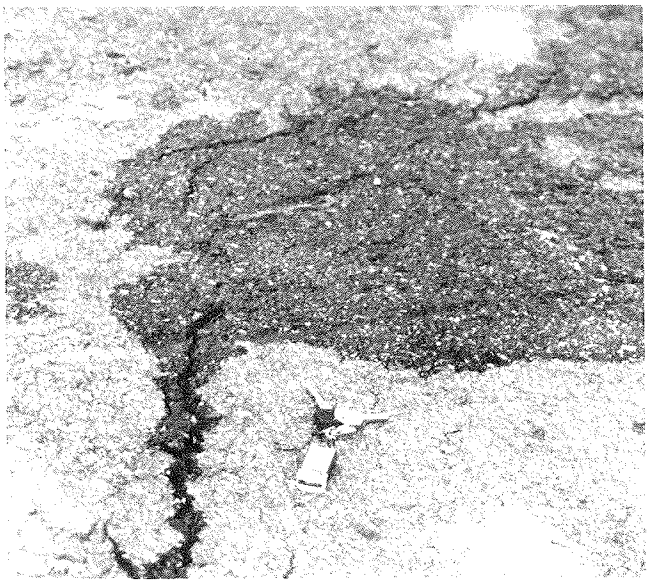

FIGURE 7 Outflow of water and fines from curb joint.

pavement surface during hot afternoons for several days after a rainfall. This problem began to appear about 2½ years after the road was constructed. At each affected spot, the upward flow of water could not be detected by the naked eye; only a damp area of irregular shape could be seen on the surface. Core samples extracted during the warmer part of the day were moist. Core samples extracted in the early morning contained fine water droplets in the bituminous mixture as a result of condensation. The total thickness of the bituminous layers was 105 mm.

Large fluctuations of groundwater table could be observed in the vicinity of the roadway. The normal water table was 760 mm below the pavement surface but rose easily to a few millimeters from the surface on a rainy day. In Singapore and Malaysia, the average number of days with rain is of the order of 155 each year *(3, 4)*. As a result of the frequent rise and fall of the water table, drainage passages tended to get clogged and

water became trapped within the pavement system. Moisture could move upward by capillary action or be forced upward by thermal pressure on a hot day.

The first sign of pavement distress, as shown in Figure 8, was cracks in the surface at each wet location. A slight heaving of the surface material could sometimes be observed. This was followed by breaking up of the surface layer and disintegration of the bituminous mixture. Shallow patching, which does not correct the subdrainage condition, would not offer a solution to the problem. Because reconstruction of the relatively new pavement was costly and the request for additional funding was difficult to justify, a "repair as it occurs" policy was adopted. Deep patching that involved replacement of drainage layers had to be carried out rather frequently.

FIGURE 8 Water-induced cracks in pavement before formation of pothole.

DRAINAGE PROBLEMS DUE TO BACKFILL OF UTILITY TRENCH

On city streets and residential roads in Singapore and Malaysia, cutting of trenches in existing pavements for utility installation or repair is quite a common occurrence. In addition, the frequent problem of differential backfill settlements that contribute to unevenness and poor ride quality, poor-quality backfills that interrupt subsurface drainage, and joints that admit water may cause accumulations of water in pavement systems and lead to structural failure of pavements.

Both transverse and longitudinal utility cuts can be found, and they have become a feature with which urban road engineers have to live. Although utility cuts may occupy a small proportion of the pavement area, they are usually deep enough to cut through the entire pavement structure. Proper backfilling of these cuts is important to the overall soundness of the pavement system. The boundary joints of a utility cut are potential planes of weakness structurally as well as from a drainage point of view. Joints that are not watertight admit into the pavement structure additional water, which is not planned for in the original design. The life of a pavement can be

FIGURE 9 Water bleeding from utility trench joint; photo taken 9 hr after rain had stopped.

FIGURE 10 Stain marks on the pavement shown in Figure 9 caused by fines transported by outflowing water.

significantly shortened if some of this additional water becomes trapped within the pavement.

In terms of drainage, longitudinal utility cuts are especially important because they cover a long stretch of pavement, and they cut across the lateral drainage path of the pavement. Figure 9 shows a poorly backfilled utility trench that effectively cut off the lateral subsurface drainage of the pavement. The road was originally constructed to have one-way lateral subsurface drainage across the width of the pavement. The backfill, which was not as permeable as the original pavement construction, acted as a barrier that held up water that was supposed to be discharged by the drainage layer of the pavement. Upward flow of water, as can be seen in Figures 9 and 10, continued for more than 16 hr after a heavy rainfall had stopped. Fines left on the pavement surface provided indications of the damaging effects on pavement sublayers.

Another common form of water-induced distress is pavement damage within a utility patch itself. The inability of utility cut backfill to drain off water that enters through the boundaries of utility trenches is a common cause of the problem that leads to pothole formation and disintegration of a utility trench patch.

PAVEMENTS IN CUT SECTIONS

Drainage design for pavements in cut sections is particularly important because surface runoff as well as subsurface seepage from both sides of the cut tend to converge toward the road section. Intercepting drains are usually constructed to prevent flooding of pavement by surface runoff. Cutting off of inward flow of subsurface seepage is a more difficult problem. It requires a careful study of the features of the site and ground conditions before an effective subsurface cutoff drain can be designed.

The amount of subsurface seepage can be quite substantial. Without performing a drainage calculation, there is a tendency for most designers to underestimate the amount of subsurface inflow after a heavy rainfall. Figures 11 and 12 show the surfaces of two secondary pavements in cut that were not provided with sufficient subsurface seepage cutoff. On both pavements, flows of water were found oozing slowly from the surface at several points after a rainfall. The upward flow of water would continue for 10 to 20 hr, depending on the intensity of precipitation, after the end of a storm.

Cracks would gradually develop around the point of outflow under the action of traffic. Further deterioration eventually would lead to the formation of potholes. During a spell of heavy rainy weather in December 1985, potholes occurred in such numbers in a matter of a few days that maintenance crews simply did not have the time to patch them properly. Figure 13 shows one of the repair patches where outflow of subsurface water still occurred long after a rain had stopped.

FIGURE 11 Water oozing from Point A after rainstorm.

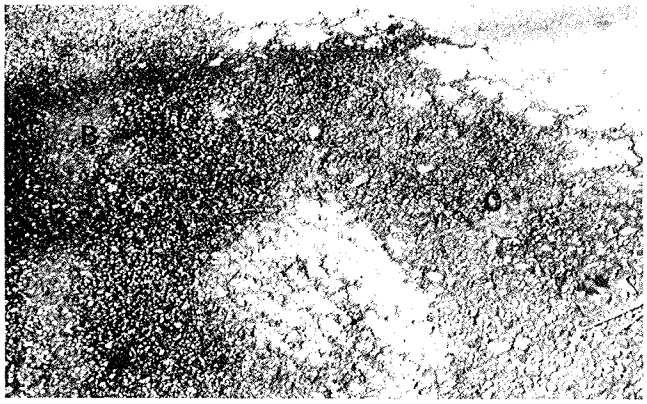

FIGURE 12 Water oozing from Points B and C after heavy rain.

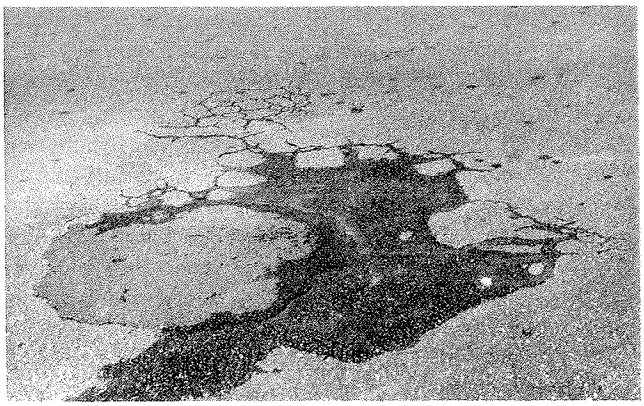

FIGURE 13 Water flowing from a poorly repaired patch.

FEATURES OF THE DISTRESS PROBLEM

Cases of pavement damage initiated or accelerated by the prolonged presence of water within pavement structures are presented and analyzed. Most of the cases presented contained telltale signs such as swelling of the wearing surface, appearance of moisture on the pavement surface, and upward bleeding of water from within the pavement system. It is clear, however, that there probably exist many other instances in which water-induced pavement damage took place without showing any telltale signs. Some important features of the distress problems follow.

- Porous layers or voids within a pavement structure serve as a storage space for water. Such storage space may be created when a porous layer is sandwiched between two relatively impervious layers, or when internal drainage paths of a pavement are interrupted by subsequent construction, or when voids are formed within pavement materials by progressive erosive action of water entering through surface cracks or joints.
- Rainfall is the source of water supply. Rainwater enters a pavement structure either by surface infiltration gravity flow through cracks or joints or by lateral or upward flow under a hydraulic head. The water may become trapped in storage spaces within the pavement structure or held up for a prolonged period because draining by gravity to pavement edges is usually slow because of the gentle gradient of pavement cross slopes.
- Pavement distress is accelerated by pressure buildup in the trapped water caused by thermal changes and vehicular loadings. The pulsating water pressure created by moving traffic appears to be a primary destructive mechanism leading to pavement damage.
- The resultant pavement damage usually takes the form of surface cracking, potholes, and disintegration of bituminous materials. It is important to note that these kinds of damage are water induced; they may not be initiated or preceded by failure in the subgrade or subbase layers.

Detection and repair of pavements affected by water-induced problems present a challenge to pavement engineers and maintenance staff. Water intrusion into a pavement structure is difficult to detect. By the time telltale signs are visible, it is too late for any preventive maintenance work because water has

already entered the pavement structure. It is practically impossible in most cases to remove the trapped water by any nondestructive means. Repair of affected pavements is also not straightforward. No standard repair procedure can be formulated because each case is likely to be different. An effective corrective repair can be achieved only when the exact causes and mechanism of the distress in question are determined.

Certain preventive maintenance activities may be useful in reducing the likelihood of water intrusion into pavements. Cracks and joints in pavement surfaces should be sealed watertight. Drainage facilities such as gutters, ditches, and pipes must be inspected and maintained regularly. Underdrains can be installed along edges of those pavements with poor surface drainage. Standing water in ditches and storm drains is a sign of potential water-induced problems. Areas of pavement surface that stay damp for a long period of time after the rest of the pavement surface dries after a rainfall deserve additional attention. A poorly compacted longitudinal joint will also appear damp long after the adjacent pavement surface dries.

CLIMATIC FACTOR

The occurrence of water-induced distress depends on two factors, the climate and the pavement. Good pavement design, construction, and maintenance practices cut down the number of cases of pavements with entrapped water. Areas of wet climate with frequent rainfall tend to be affected more by water-induced problems than are dry climatic regions, although the possibility of water-induced problems occurring in an arid climate after heavy rainstorms, which might occur only a few times each year, must not be ruled out. As long as a pavement is capable of trapping water within it, water-induced problems may arise whenever rainwater is available.

The threat of water-induced problems is ever present for the pavements in Singapore and Malaysia because of the abundance of rainfall. The region generally has rainfall throughout the year but tends to be particularly wet during the monsoon season from November to January. The average annual rainfall is around 2,000 mm (79 in.), and the average number of days with rain each year is about 155. The pavements in the region are also exposed to extensive sunshine each year. The annual average number of hours per day under bright sunshine is more than 5. Table 1 gives the yearly temperature range and rainfall data of Singapore for the past few years.

The general climatic pattern all year round is that of relatively hot days followed by cool nights. On a typical day, the maximum temperature is around 30°C and the minimum is 24°C *(3)*. The temperature variations on most road pavements are much larger than the changes in air temperature, ranging from around 25°C in the early morning to as high as 75°C on a hot afternoon. Three important characteristics of the wet tropical climate of Singapore and Malaysia can therefore be identified: *(a)* frequent rainfall with high precipitation throughout the year, *(b)* alternating rain and sunshine leading to a large number of wetting and drying cycles, and *(c)* repetitive daily cycles of cooling and heating due to temperature changes.

These three conditions present to pavement engineers a difficult task in keeping pavement surfaces watertight and resistant to stripping or disintegration of surface materials. Surface runoff and infiltration water, coupled with favorable temperature changes, wetting and drying, and traffic loading effects, are constantly causing deterioration of pavement materials and creating void spaces within pavement structures.

Pavement crown, cross section, and structural thickness usually receive the greatest attention from designers in Singapore and Malaysia. In the light of the highly favorable environment for the development of water-induced problems, it is thought that inadequate attention has been paid to the climatic factor in design to guard against water-induced problems. More emphasis should be placed on drainage considerations during pavement design as well as during construction and maintenance of pavements. On the basis of experience observing the performance of pavements in this region, some measures are recommended in the following section for the prevention of water-induced problems in flexible pavements.

RECOMMENDATIONS FOR PREVENTIVE MEASURES

Pavement design and construction practices in Singapore and Malaysia generally provide for side-drains to remove surface water and to lower the groundwater table. Cut-off drainage systems such as French drains are usually installed along edges of pavements constructed on cut sections. Unfortunately, rarely do pavement designers and constructors carry out detailed studies to guard against possible storing or holding up of rainwater within a pavement structure after a heavy rainstorm. Permeability requirements of base, subbase, and subdrain materials are not strictly specified and controlled.

Figure 14 shows one of the crushed-stone gradation limits commonly adopted in Singapore and Malaysia. Laboratory falling-head permeability tests were conducted using four different sets of samples with Gradations A, B, C, and D as shown

TABLE 1 RAINFALL AND TEMPERATURE CHARACTERISTICS OF SINGAPORE *(5)*

	Average Daily Temperature (°C)		Rainfall			
Year	High	Low	Total (mm)	Daily Maximum (mm)	Rainy Days	Daily Mean Hours of Sunshine
1979	31.0	23.9	2168	91	168	5.7
1980	31.0	23.9	2326	134	176	5.7
1981	31.3	24.2	1463	72	145	5.8
1982	31.4	24.6	1582	109	130	5.7
1983	31.7	24.9	1994	182	145	5.6

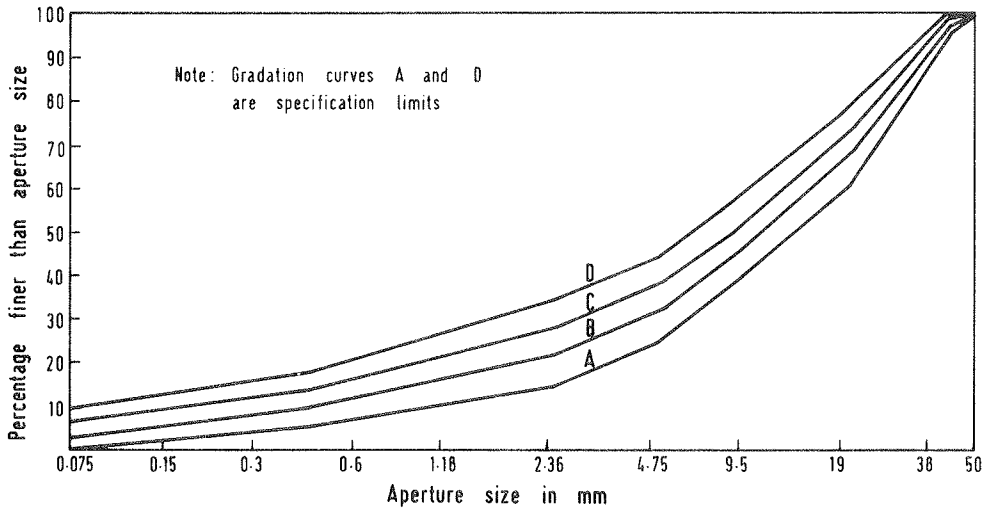

FIGURE 14 Aggregate gradations for base course materials.

in Figure 14. The results of these tests are given in Table 2. It is noted that materials that fall within the specified gradation limits could have permeability values varying from 1.57×10^{-1} cm/sec to 2.42×10^{-3} cm/sec. It appears that the gradation specification alone is insufficient from the point of view of pavement drainage.

TABLE 2 PERMEABILITY VALUES OF BASE MATERIALS

Gradation (see Figure 14)	Permeability cm/sec	ft/sec
A	1.57×10^{-1}	5.15×10^{-3}
B	1.73×10^{-2}	5.68×10^{-4}
C	1.01×10^{-3}	3.31×10^{-4}
D	2.42×10^{-3}	7.94×10^{-5}

NOTE: Permeability for each gradation obtained as average of six laboratory falling-head tests.

Specification of permeability requirements for base and subbase in a comprehensive pavement design represents only one preventive measure against water-induced pavement distress. In light of observations and investigations made on the pavements in Singapore and Malaysia, the following measures appear appropriate for controlling the occurrence of water-induced problems in construction of new bituminous pavements:

- Base and subbase materials should be sufficiently permeable to drain off surface water infiltration or other inflow of rainwater.
- Each pavement layer must be more permeable than the layer immediately above so that draining off of infiltrated water will not be impeded and no water will be held up in the upper layer.
- Good geometrics should be provided for pavement and adjacent features to aid drainage. Roadside drainage systems must be constructed and maintained such that flooding will not occur on the borders of the pavement. In areas where the surrounding land is flat and where standing water cannot be discharged quickly, the level and the cross section of the road must be such that lateral flow of water into the adjacent pavement structure will not take place.
- Along a cut section, French drains or other subdrainage systems may be used to discharge surface runoff and to lower the groundwater table.
- Full-width paving is desirable because it eliminates longitudinal joints that are potential points of moisture infiltration. Where such joints cannot be avoided, they should be properly constructed and sealed, if necessary, to remain watertight.
- On secondary roads and some primary roads where shoulders are not provided, the use of curbs as edge restraints is recommended. Sufficient drainage facility should be provided so that water will not accumulate at the curb line.
- When a thick bituminous layer is compacted in lifts, it is important to monitor the construction closely to ensure that the interfaces between lifts are intact and watertight.
- In areas where subbase and base may be clogged by fine subgrade soil brought up by a fluctuating water level, a filter layer is needed to protect the drainage layers.
- Close tolerance of subgrade grading should be achieved to prevent depressions that could trap water.

Proper drainage maintenance plays a vital role in preventing the occurrence of water-induced problems. Regularly scheduled inspection and maintenance of drainage features is a must. Timely maintenance and sealing of joints and cracks offer long-term benefits by cutting off possible inflows of water.

One of the cases presented in this paper suggested that paving a dense overlay on a porous wearing course would lead to water-induced pavement damage. This is particularly relevant in the tropics where many old road surfaces are badly stripped and eroded. If the cavities and voids in these weathered surfaces are not removed or filled before overlay construction, there is a high probability that infiltration water will eventually get trapped in the old weathered wearing course. It therefore makes good engineering sense in the tropics to investigate the drainage condition and permeability properties of an old pavement, in addition to the commonly performed structural evaluation, before constructing an overlay.

Poorly constructed utility trenches present a tremendous potential for the development of water-induced problems. Utility patches and surrounding pavement sections may be damaged by water intrusion from the boundary joints or by backfill that interrupts the subsurface drainage of the original system. Intrusion of water can be checked by sealing the edges of trench patches. Poor backfill can be avoided by proper supervision and control during construction.

CONCLUSIONS

The climate of wet tropical regions provides an environment that is conducive to the development of water-related distress in flexible pavement. Surface deterioration such as stripping and raveling is visible and can be easily detected. Another form of water-induced flexible pavement distress, which is caused by the presence of trapped water within the structural system of a flexible pavement, has been described in this paper. Detection of such distress is difficult until an advanced stage when an elaborate repair of the affected pavement is required.

Several cases of distress in Singapore and Malaysia have been presented to illustrate the circumstances in which such distress occurs. These cases were selected to reveal the various mechanisms by which water-induced problems could develop. An important lesson learned from the study of these cases is that there is a need for a thorough material permeability and drainage analysis to be carried out during the pavement design phase, and that it is equally important for site supervisors of construction work and pavement maintenance staff to be aware of the significance of providing proper drainage to suit actual ground conditions.

REFERENCES

1. *Bituminous Materials in Road Construction.* Road Research Laboratory, Department of Scientific and Industrial Research, London, England, 1962, pp. 70–87.
2. M. A. Taylor and N. P. Khosla. Stripping of Asphalt Pavement—State of the Art. In *Transportation Research Record 911*, TRB, National Research Council, Washington, D.C., 1983, pp. 150–158.
3. *Singapore Statistics 1983/84.* Singapore Department of Statistics, Singapore, 1984.
4. *Yearbook of Statistics, 1984.* Department of Statistics, Malaysia, 1984.
5. *Monthly Digest of Statistics.* Vol. 23, No. 7, Department of Statistics, Singapore, July 1984.

Publication of this paper sponsored by Committee on Strength and Deformation Characteristics of Pavement Sections.

An Evaluation of Design High-Water Clearances for Pavements

M. K. ELFINO AND J. L. DAVIDSON

In this paper is described a study to investigate the effect of capillary water presence on permanent deformation of four common Florida subgrade soils. Physical and engineering properties were first determined, with emphasis on developing soil-water retention characteristics. Repetitive triaxial load tests were then performed on the soils, under several different water conditions. These included at optimum, to represent the as-built condition, and at varied water retention conditions, to represent subgrade conditions in service (i.e., in equilibrium with the designated water table). Deformation characteristics of a subgrade fill, at different water conditions, were related to pavement rutting in accordance with the Shell Oil criteria. When a tolerable permanent deformation was obtained at a specified water condition, the specimen's location on the soil-water retention curve was determined. The height of the most economical subgrade fill could then be fixed.

The presence of excess water in highway pavement systems can accelerate deterioration and destruction of the pavement. Increases in moisture can be caused by the infusion of water from a number of different sources. Results of an investigation of one such source, capillary suction from an underlying water table, are presented.

To prevent capillary water rise into critical areas of a pavement system or to reduce its effects, some state departments of transportation have developed high-water clearance guidelines. In these guidelines the clearance (i.e., a minimum height between a groundwater level and a particular elevation within the pavement system) is specified. The Florida Department of Transportation (FDOT) has such guidelines. They state that the bottom of the pavement base should be located a specific height above a designated high-water level. Details are given in the following table.

Road	*Specification*
Four-lane primary and Interstate	3 ft above 50-year high water
Two-lane primary	2 ft above 50-year high water
Secondary	1 ft above 25-year high water

The policy has been applied uniformly statewide and is intended to satisfy two concerns:

1. That the required compaction and stability be achieved during construction operations and
2. That adequate pavement performance be provided.

M. K. Elfino, Virginia Department of Highways and Transportation, 1401 East Broad Street, Richmond, Va. 23219. J. L. Davidson, Civil Engineering Department, University of Florida, Gainesville, Fla. 32611.

The guidelines, however, do not address the critical factor of subgrade soil type. As a result, there have been locations where the specified clearance appeared excessive for the conditions encountered. However, with no other guidelines to follow, the policy was adhered to. The resulting high fill costs may not be justified. At the other extreme, situations may exist in which the specified clearance may be inadequate. This also leads to eventual waste of funds caused by construction problems or poor pavement performance.

Taking subgrade soil type into account in setting such guidelines requires a determination of which physical and mechanical soil properties influence behavior during construction and under the expected dynamic service loadings. It is also important that the water present in the subgrade be correctly modeled in any laboratory testing (i.e., correct water content and water pressure).

The purpose of the study reported in this paper was to investigate the soil-water retention behavior of four different Florida soils, to determine their deformation characteristics under repetitive loading at different water retention conditions, and to recommend the most economic subgrade height above the water table for each soil.

The research was planned in six phases. These are briefly listed for completeness, though not all are discussed in detail in this paper.

1. A questionnaire was sent to all state departments of transportation to ascertain if they used high-water clearance specifications and, if so, the basis for their criteria.
2. Physical and engineering properties were determined for the four soils. These included grain size distribution, Atterberg limits, specific gravity, permeability, soil mineralogy, density–water content relationships, cohesion, and internal friction angle.
3. Soil-water characteristic curves were obtained for the four soils in two ways: *(a)* using Tempe pressure cells and *(b)* using 4-ft-high compacted soil columns.
4. Repetitive axial loading triaxial tests were performed to obtain deformation characteristics of the four subgrade materials compacted at optimum water content. This represents the as-built pavement condition.
5. Repetitive axial loading triaxial tests were performed to obtain deformation characteristics of the four subgrade materials under different soil-water retention conditions. These represent the subgrade conditions at different depths in service (i.e., in equilibrium with the designated water table).
6. Recommendations for high-water clearances were developed for the four soils based on two procedures: *(a)* an

inspection of the soil-water characteristic curves and the engineering properties and *(b)* use of the Shell Oil criteria for rutting and strains from the laboratory testing and from multilayer elastic analyses.

In this paper, the results from Phase 2 are summarized in a single table. From Phase 3, only the characteristic curves obtained using Tempe cells, which are quite convenient to use, are included. Also, because of length restrictions, the Phase 4 as-built results are not included.

ENGINEERING PROPERTIES OF SOILS TESTED

The four soils tested in the study are representative of the most commonly used fill materials in the state of Florida. They came, respectively, from Polk, Baker, Washington, and Broward counties. Table 1 gives a summary of their physical and engineering properties.

SOIL-WATER RETENTION CHARACTERISTICS

The mechanical behavior of subgrade soils is affected by the presence of water and the development of capillary potential above the water table. It is therefore essential in any study to simulate field conditions for the subgrade soil as it exists, in-service, under the pavement, and in equilibrium with the designated water table. Soil-water characteristic curves provide the necessary parameters to achieve this simulation.

The soil-water retention characteristics of the project soils reported herein were determined using commercially available Tempe pressure cells and a procedure similar to that outlined by Janssen and Dempsey *(1)*. Figure 1 shows retention characteristic curves for all four soils compacted to standard Proctor (T-99). The soils with curves plotting from left to right in this figure have increasing percentages of fines (< 0.074 mm). From the shapes of the curves, those materials susceptible to large changes in the position of the water table are easily recognized.

In this study, only the more critical capillary retention case has been considered. At any elevation above a water table, the water content will be greater in the retention or draining case than in the wetting-up case.

REPETITIVE LOAD TESTING

Specimen Preparation and Conditioning

The water content at any location in a compacted subgrade soil will not remain at the optimum compacted value but will change until it comes into equilibrium with groundwater conditions. The samples for in-service repetitive loading triaxial testing were therefore prepared under optimum conditions, then conditioned to bring them to a desired water content and soil suction state representing some height above the water table.

Samples were compacted in 4-in.-diameter, 8-in.-high lucite molds. To these were fitted a perforated base with filter paper

TABLE 1 ENGINEERING PROPERTIES OF THE FOUR TEST SOILS

Property	Soil Number			
	1	2	3	4
Sand (0.074-4.76 mm)%	95.9	89.5	71.1	5.5
Silt (0.002-0.074 mm)%	4.1	6.5	7.0	73.5
Clay (< 0.002 mm)%	---	4.0	21.9	21.0
Liquid Limit (%)	NP	NP	31	52
Plasticity Index (%)	NP	NP	11	8
AASHTO Classification	A-3	A-2-4	A-2-6	A-5
Unified Classification	SP	SP-SM	SC	MH
Specific Gravity	2.61	2.62	2.68	2.55
Standard Proctor (T-99)				
Optimum Water Content (%)	15.6	13.3	11.8	36.4
Max. Dry Unit Weight (pcf)	102.2	104.9	120.5	73.2
Soil Mineralogy	---	kaolinite chlorite	chlorite	kaolinite montmorillonite
Permeability (cm/sec)	7.3×10^{-4}	1.1×10^{-5}	4.8×10^{-7}	6.4×10^{-6}

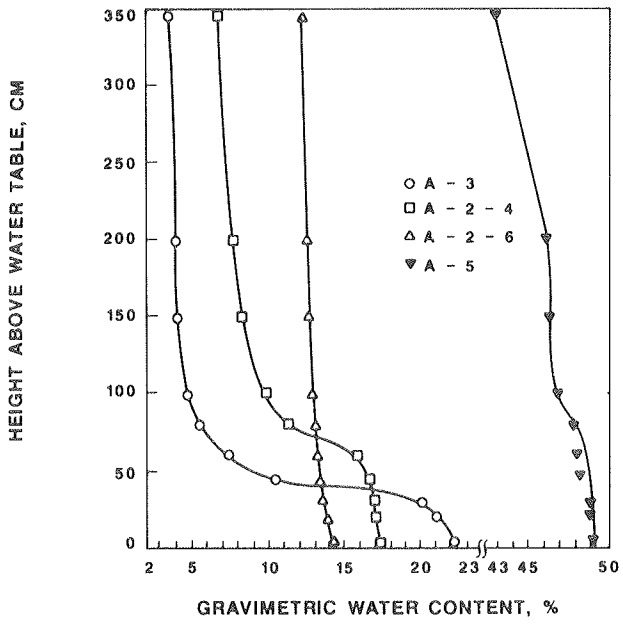

FIGURE 1 Retention characteristic curves for all project soils compacted to standard Proctor.

disc, a top collar, and connecting threaded rods. The assembled mold was then placed in a deep sink and the water level raised to the top of the mold and maintained at that level. Water could enter the specimen only from the bottom. Saturation was assumed when a glaze of water was observed on top of the specimen. The A-3 (sand) took only a few hours to saturate. On the other hand, the A-2-6 (clayey sand) took almost 8 days. After saturation, the water in the sink was allowed to drain slowly to simulate water drawdown in the field. The mold assembly was then lifted out of the sink, dismantled, and the mold weighed. Total unit weight, water content, and degree of saturation could then be calculated.

This provided assurance that the specimen was still saturated. When satisfactory saturation was achieved (S greater than 98 percent) the mold was fitted with a pressure plate (rated at 1 bar), a lucite cup with two drains, a small reservoir, and a water manometer. O-rings and silicon grease were used to seal any gaps between the mold and the lucite cup. The upper end of the mold was covered with a perforated lucite plate to allow air to enter the specimen. Connecting rods were used to hold the cup, mold, and cover together as one unit. This arrangement is essentially a large Tempe cell, except it uses a negative column rather than air pressure to condition the specimen. Figure 2 shows the components of the conditioning cup and Figure 3 a specimen during conditioning. When equilibrium is reached, the specimen is representative of a similar specimen, in the subgrade, at a height above the water table equal to the length of the negative column.

The mold assembly was then taken apart and the wet unit weight and water content of the specimen were determined. A check was then made to determine if the specimen had actually reached the target water content, as obtained from the soil-water characteristic curve. If so, the specimen was ready for repetitive load testing.

Because of the large size of the specimen and the limited distance above the water table to be investigated as a fill height,

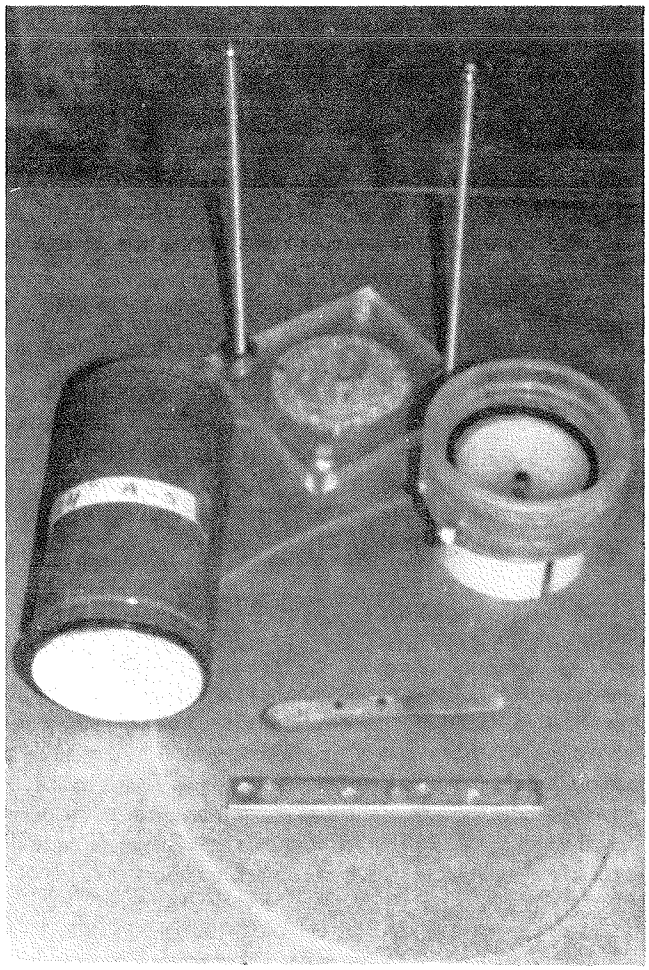

FIGURE 2 Components of the conditioning cup.

attaining the target water content throughout the entire specimen was impractical. For this reason, it was decided that if the water content of the middle 4 in. of the specimen was within 1 percent of the target value, the specimen would be considered acceptable. In some cases, achieving this required considerable time (up to 45 days).

Repetitive Loading Equipment

The repetitive loading equipment consisted of a triaxial chamber capable of accommodating a 4- by 8-in. specimen, vertical and lateral deformation measuring equipment, and a vertical loading source. The external loading source was a closed-loop electrohydraulic system manufactured by MTS Systems Corporation. An electronic load cell measured the axial forces. The axial and radial deformation measurements were made using two pairs of linear variable differential transformers (LVDTs). These were mounted on a pair of expandable clamps that contacted the specimen through four wide feet on each clamp. Air was used as the chamber fluid and was monitored with conventional pressure gauges. Signal excitation, conditioning, and recording equipment provided for simultaneous recording of the axial loads and deformations. The LVDTs were wired so that the average signal from each pair was recorded. Figure 4 shows an overall view of the equipment used.

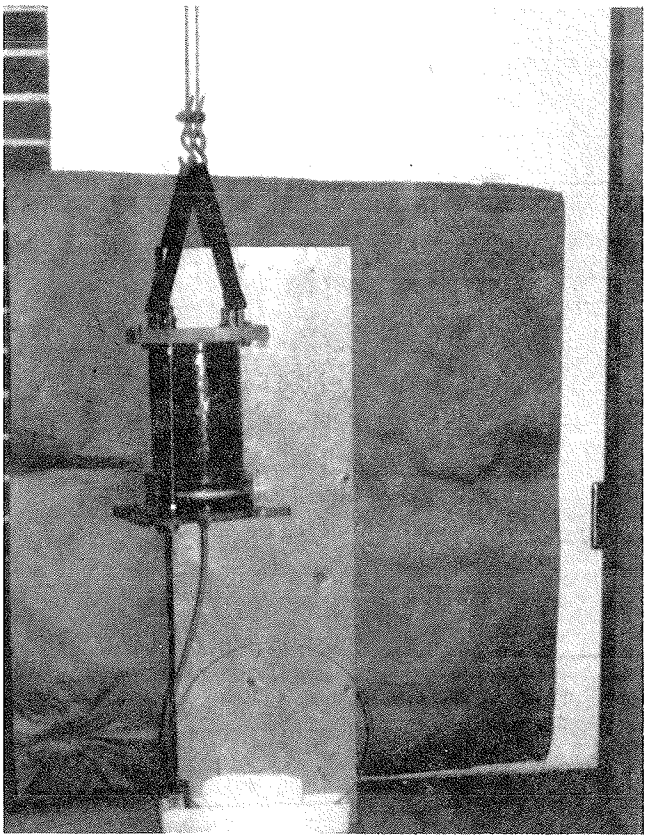

FIGURE 3 Specimen during conditioning.

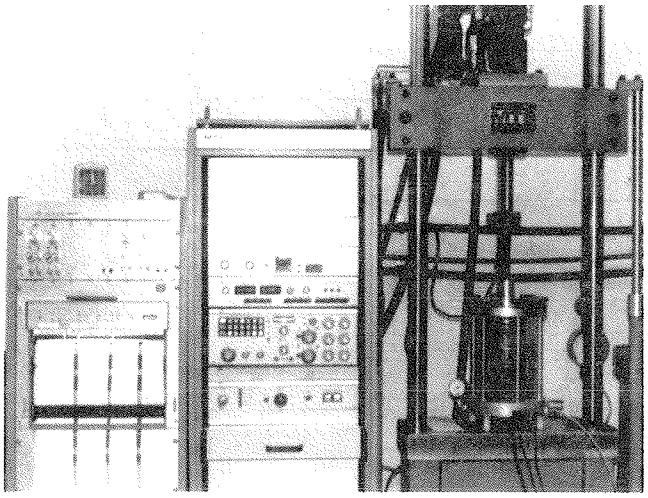

FIGURE 4 Overall view of the repetitive loading test equipment.

Testing Procedure

The objective of the repetitive load testing was to characterize the resilient and permanent strains of the project soils at different water retention conditions. The condition specimen was extruded from its mold and assembled in the triaxial chamber with top and bottom porous stones, surrounding rubber membrane, and the horizontal and vertical LVDT clamps at 2- and 6-in. heights. A confining pressure of 2 psi was first applied for 30 min under drained conditions.

The MTS controls were set to give a 0.1 sec load on and a 0.9 sec load off. The pulse wave was haversine. Because the specimen diameter and the stress desired were known, the load could be calculated and the controls set accordingly. The confining pressure was maintained at 2 psi in all tests. Dynamic conditioning of the specimen was performed to eliminate the end imperfection of the specimen, to allow for better seating of the porous stones, and to eliminate the effects of the interval between compaction and loading. This dynamic conditioning consisted of first applying 200 load repetitions of a 2-psi deviator stress ($\sigma_1 = 4$ psi and $\sigma_3 = 2$ psi). The axial load was then incremented by 2 psi after each 200 repetitions until a total axial load of 8 psi was applied, (deviator stress $\sigma_d = 6$ psi). Specimen testing was started at the end of 600 repetitions of conditioning with the same stress as the last 200 repetitions. The stress level of $\sigma_d = 6$ psi and $\sigma_3 = 2$ psi was considered representative of the stresses encountered in the field in the subgrade layer. All specimens were tested for 10,000 repetitions. Test data were recorded at or near the following repetition levels: 1; 10; 100; 200; 400; 600; 800; 1,000; then every 1,000 until the termination of the test. Test data monitored included axial load, axial deformation, and radial deformation. These were recorded on a strip chart recorder.

Testing Program

Table 2 gives the different water retention conditions tested. These were selected from the water retention curves of Figure 1 to model conditions in the subgrade at different heights above the water table. Average specimen dry densities were 103.2 pcf for the A-3, 107.9 pcf for the A-2-4, 119.5 pcf for the A-2-6, and 72.1 pcf for the A-5. These values are the averages of three specimens in each condition.

EXPERIMENTAL RESULTS

Results from the conditioned specimen repetitive load testing of the four subgrade soils were analyzed in terms of the permanent and resilient strains (ε_p^a and ε_r^a) and the resilient modulus (M_R).

The A-3 soil was tested by repetitive loading under three different water retention conditions (Table 2). Figure 5 shows a cumulative plot of axial permanent strain (ε_p^a) versus number of stress applications (N) for the three water retention conditions. The curves stack: the one representing 24 in. is at the bottom; the one representing 18 in. is in the middle; and the one representing 15 in. is at the top. For a certain number of stress applications, the bottom curve yields the lowest axial permanent deformation and the top curve the highest. A power function, of the form

$$\varepsilon_p^a = AN^B$$

where

ε_p^a = accumulated axial permanent strain;
N = number of stress applications; and
A, B = constants (which would represent intercept and slope terms, respectively, on a log-log plot)

TABLE 2 TEST PROGRAM OF PROJECT SOILS UNDER DIFFERENT WATER RETENTION CONDITIONS

Height Above	Soil Type			
Water Table	A-3	A-2-4	A-2-6	A-5
in inches	Water Content Percentage			
15	13.24			
18	10.53			
24	8.10			
30		11.70		
36		10.50		
48		8.70		
0			12.20	
36				44.40

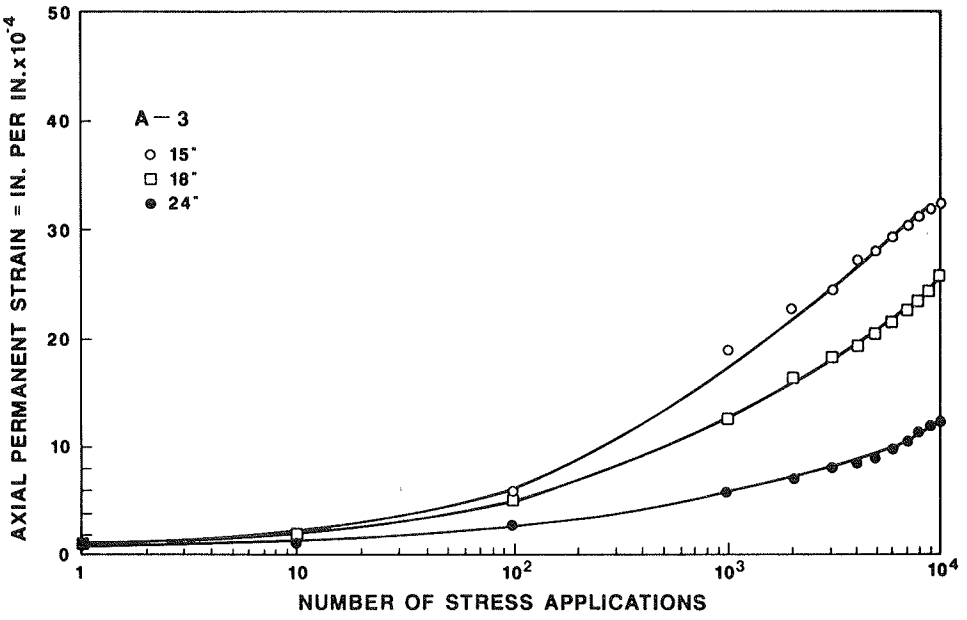

FIGURE 5 Accumulated axial permanent strain versus number of stress applications for A-3 soil at different water retention conditions.

was found to fit all the data points. Such a function was also reported by Monismith et al. *(2)* and was verified for up to 100,000 stress applications. The data are presented in semilog format to better show the change in permanent strain with the number of stress applications. These results are in general agreement with those of Shackel *(3)*, showing that the cumulative permanent (axial) strain decreases rapidly with increasing suction.

The A-2-4 soil was also tested under three different levels of water retention. Water contents chosen were 11.70, 10.50, and 8.7 percent, representing 30, 36, and 48 in. above the water table. Figure 6 shows the plots of ε_p^a versus N. Again, as expected, the plot representing the greatest distance, 48 in., was located at the bottom of the figure; that representing 36 in. was in the middle; and the 30-in. plot was on top. The A-2-4 soil showed behavior quite similar to that of the A-3 soil. Power functions again can be used to fit the data.

The A-2-6 and A-5 soils were each tested at only one selected water retention level. The A-2-6 specimen was prepared by soaking in water for 8 days. This procedure led to a water content of only 12.2 percent. This was considered as saturated as this specimen could be. The specimen was never placed under any capillary tension. The condition therefore represents the worst that might be encountered in the field.

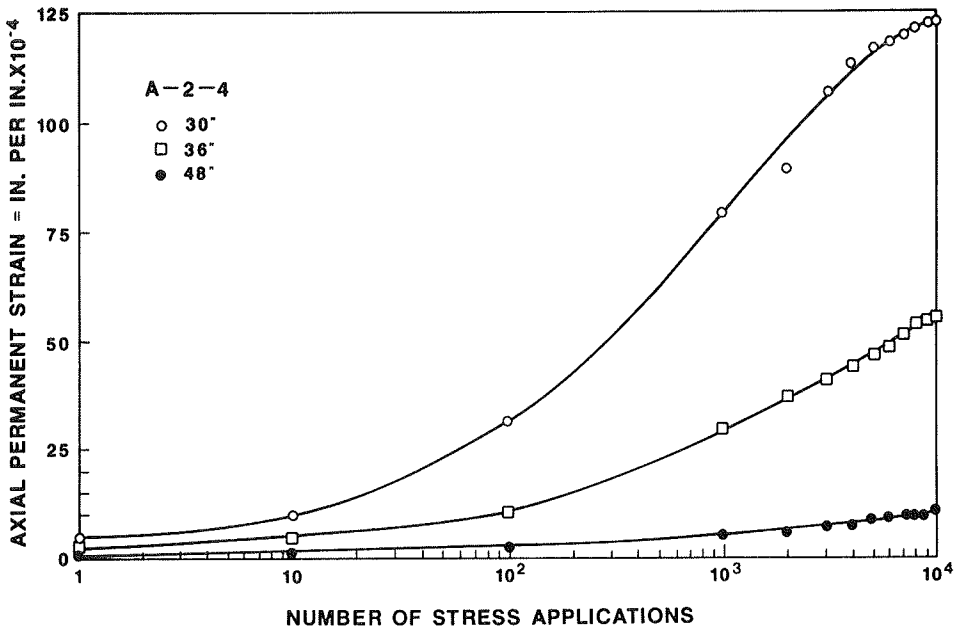

FIGURE 6 Accumulated axial permanent strain versus number of stress applications for A-2-4 soil at different water retention conditions.

The A-5 soil was placed under a capillary tension to represent a height of 36 in. above the water table. Its water content was 44.4 percent. Figures 7 and 8 show the plots of ε_p^a versus N. A power function was found to fit the data in the first stages up to 7,000 and 5,000 applications for the A-2-6 and A-5 soils, respectively. The second stage for both soils was a plateau where no increase in permanent strain was observed.

Table 3 includes a summary of M_R-values, the correlation equations and their coefficients, and the R^2 values for all four project soils at their different water retention conditions.

APPLICATION OF TEST RESULTS

The results obtained from both the engineering properties tests and the repeated load tests can be used in the following ways:

1. They will provide a data base on the essential engineering and physical properties of four common subgrade fill materials available in the state of Florida. This should help in making an economical decision about the selection of fill materials and the certification of borrow pits.

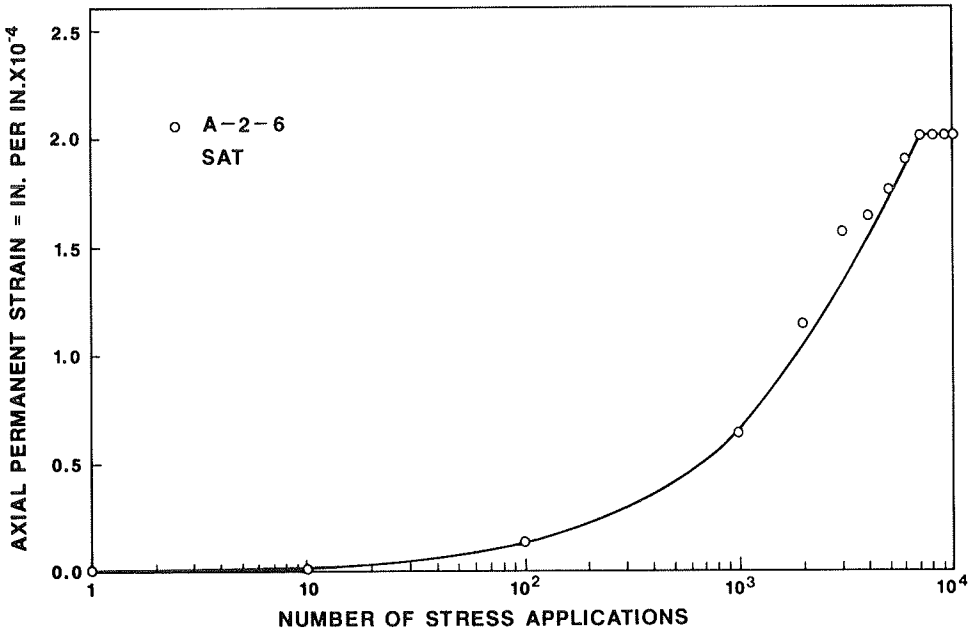

FIGURE 7 Accumulated axial permanent strain versus number of stress applications for A-2-6 soil at a single water retention condition.

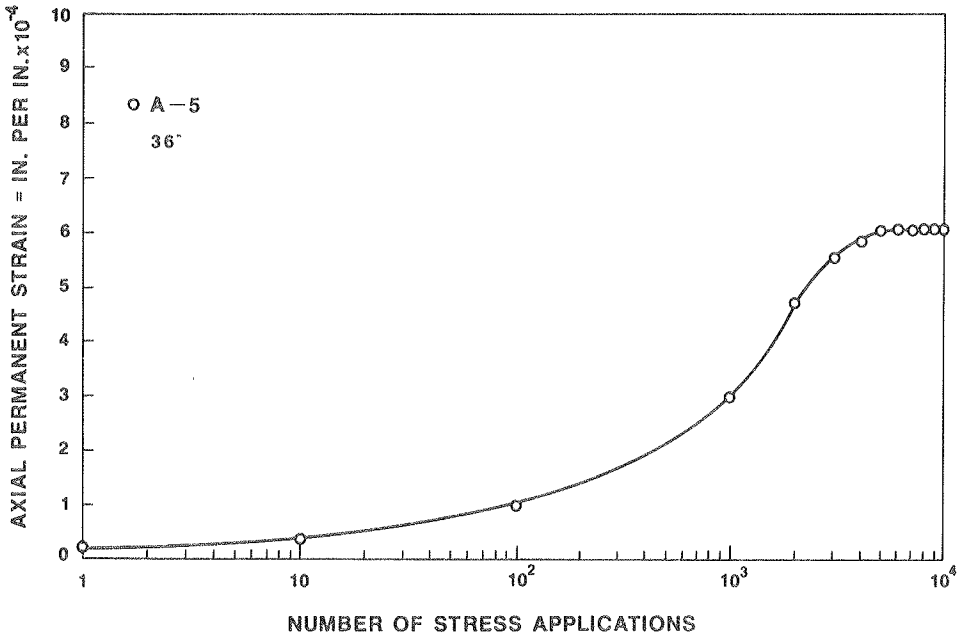

FIGURE 8 Accumulated axial permanent strain versus number of stress applications for A-5 soil at a single water retention condition.

2. The soil-water characteristic curves provide a realistic simulation of the water retention in a subgrade. Similar distributions have been found in field investigations reported by Kersten *(4)*, Russam *(5)*, and Janssen and Dempsey *(1)*. Instead of assuming full saturation, it is appropriate to estimate subgrade strength on the basis of such soil-water characteristic curves. This should be superior to simply assuming a regional (environmental) factor (1 for Florida) as is done in part of the AASHTO design procedures. From the soil-water characteristic curves, it can be seen that for a subgrade fill at a height that falls within the capillary fringe (almost fully saturated), water will have a detrimental effect on strength. This has been reported by Barber and Sawyer *(6)*. The minimum height of subgrade fill should therefore be greater than the height of the capillary fringe. Such a fill benefits from the strengthened effect caused by capillary suction and negative pore water pressures. This was demonstrated during repetitive load testing. Figures 5 and 6 show that the greatest axial permanent deformations occurred in the specimen representing the top of the capillary fringe, 15 in. in the A-3 soil and 30 in. in the A-2-4

TABLE 3 SUMMARY OF PREDICTION EQUATIONS AND M_R-VALUES FOR ALL PROJECT SOILS AT DIFFERENT WATER RETENTION CONDITIONS

Soil Type	Water Retention Condition %	Range of M_R psi	M_R at N = 1,000 psi	Number of Stress Applications N	Type of Function	Intercept A	Slope B	R^2
A-3	13.50	27,429-35,556	32,000	1-10,000	power	0.89	0.41	0.98
	10.53	33,103-56,471	35,553	1-10,000	power	0.90	0.37	1.00
	8.10	36,923-43,636	38,400	1-10,000	power	0.72	0.30	1.00
A-2-4	11.70	23,577-37,723	27,738	1-10,000	power	5.18	0.37	0.97
	10.50	26,667-35,556	28,235	1-10,000	power	2.18	0.36	0.99
	8.70	24,000-32,000	30,000	1-10,000	power	0.12	0.49	0.98
A-2-6	12.20	43,478-48485	43,478	1- 7,000	power	5.43×10^{-3}	0.68	0.97
		48,000	--	7,000-10,000	linear-flat	2.00	0	1.00
A-5	44.40	10,101-11,173	10,118	1-5,000	power	0.16	0.43	0.99
		11,152	--	5,000-10,000	linear-flat	6.06	0	1.00

soil. For the specimens representing heights above the capillary fringe, the axial permanent strains are greatly reduced.

A-3 subgrade fill could be built to a minimum height of 15 in. (see Figure 1). It is, however, recommended that A-3 subgrade fills be built up to 24 in. This provides a safety margin, introduced because of the soil's high permeability and the ease with which it might be saturated from some other moisture source.

For the A-2-4 soil, the minimum height is 30 in. A height of 36 in. is recommended, and this height is supported by the repetitive load testing results shown in Figure 6. A 48-in. height would not be justified.

For the A-2-6 soil, there is no distinguishing capillary fringe. Figure 1 shows a gradual uniform decrease in water content with height above the water table. The significant property of this soil is its well-graded nature and consequently its low void ratio. Because of this, the structure is strong even when the soil has been under water for 1 week. For the A-2-6 soil, a 12-in. height is suggested. Figure 7 shows the quite low permanent deformation and high resilient modulus of the A-2-6 soil.

The shape of the soil-water characteristic curve for the A-5 soil was found to be quite dependent on the method of compaction and voids formation (Figure 8). It is therefore difficult to assign a conclusive capillary fringe height. The soil remained near saturation up to 200 cm (6.5 ft) with the curves showing a break at 91 cm (3-ft). The water content loss at this break was approximately 2 percent. A specimen was saturated and placed under a 91-cm (3-ft) negative column. The water content obtained was 44.4 percent. This specimen was then tested under repetitive loading. Its resilient strain was high compared with that of the other three soils. In addition, swelling was observed at the end of the saturation stage. Such serious drawbacks must be carefully weighed against economics before it is decided to use the A-5 soil as subgrade fill. However, it is recognized that in some circumstances it will be the only material available within an economical hauling distance. In these cases, a height between 4 and 6 ft (5 ft average) is recommended as a reasonable fill height.

The recommendations in this section pertain only to the soils tested in this project. The capillary fringes reported were based on the draining case (retention condition) and a soil structure achieved by the mechanical compaction method. Figure 9 shows the recommended heights of subgrade fill for the project soils, based on the retention case capillary fringes.

3. The resilient modulus, obtained from laboratory testing of the project soils under a variety of water retention conditions, can be used as input in a multilayer elastic analysis. BISAR (BItumen Structures Analysis in Roads) is a general-purpose program for computing stresses, strains, and displacements in elastic multilayered systems subjected to a uniform load over a circular surface area. BISAR was introduced in 1972 by Koninlijke/Shell Laboratorium, Amsterdam *(7)*. Obtaining the stresses and strains from such an analysis will allow a comparison to be made with the Shell Oil Company criteria (Shell criteria) for limiting subgrade strain.

The following parameters were used in a series of BISAR program runs:

- Wheel load = 9,000 lb (18,000-lb axle load);
- Tire pressure = 100 psi;
- Radius of circular surface area = 5.35 in.;
- Poisson's ratio = 0.35;
- M_R, asphalt concrete (3 in.) = 171,000 psi;
- M_R, lime rock base (10 in.) = 84,000 psi; and
- M_R, stabilized subgrade (12 in.) = 60,000 psi.

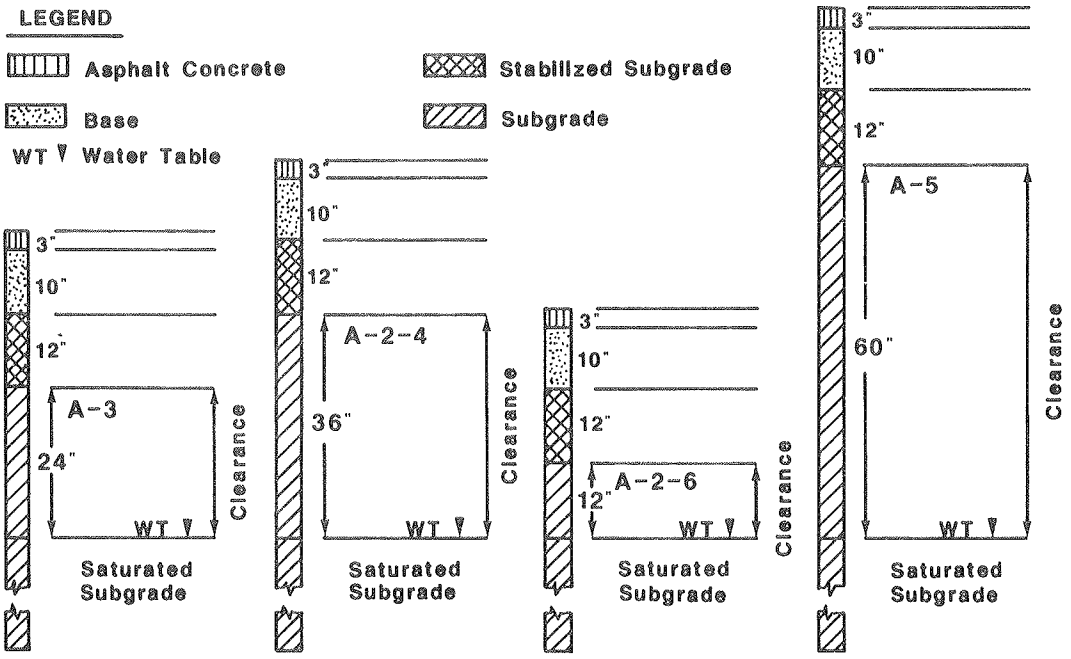

FIGURE 9 Recommended subgrade clearance heights for project soils based on capillary fringe (retention case).

Resilient moduli for the subgrade layers depend on the material and on its location above the water table. Table 4 gives values for the four project soils at 10,000 repetitions and the corresponding heights above the water table. The final layer, below the water table, was given a modulus value of 10,000 psi. This value was chosen because the weakest material at saturation, the A-5, had an M_R-value of 11,152 psi.

These parameters were also used as input in BISAR, with an overload of 30-kip axle load and 125-psi tire pressure (radius = 6.18 in.). Table 5 gives a summary of the strains at the top of the subgrade based on laboratory tests and BISAR's output at 18 and 30 kips. Table 6 gives the Shell criteria (i.e., limiting subgrade compressive strain values corresponding to different numbers of load applications). These criteria were established

TABLE 4 SUBGRADE RESILIENT MODULI USED AS INPUT IN BISAR PROGRAMS

Height Above Water Table in inches	Soil Type A-3	A-2-4	A-2-6	A-5
	M_R (Resilient Modulus, psi) at 10,000 Rep.			
15	28,235			
18	34,286			
24	40,000			
30		24,666		
36		30,968		
48		32,000		
0			48,000	
36				11,152

TABLE 5 SUMMARY OF STRAINS AT TOP OF SUBGRADE FROM LABORATORY TESTS AND FROM BISAR'S OUTPUT AT 18 AND 30 KIPS

Height Above Water Table	Soil Type A-3			A-2-4			A-2-6			A-5		
in inches	Lab.	18k	30k	Lab.	18k	30k	Lab.	18k	30k	Lab.	18k	30k
15	2.13	1.55	2.54									
18	1.75	1.38	2.25									
24	1.50	1.25	2.05									
30				2.43	1.70	2.83						
36				1.94	1.50	2.47						
48				1.88	1.45	2.44						
0							1.25	1.07	1.75			
36										5.38	2.61	4.28

Note: All strain values are in in/in x 10^{-4}

TABLE 6 SHELL CRITERIA—LIMITING SUBGRADE COMPRESSIVE STRAIN VALUES CORRESPONDING TO DIFFERENT LOAD APPLICATIONS

Load Repetitions	10^5	10^6	10^7	10^8
Axial Compressive strain in/in x 10^{-4}	10.5	6.5	4.2	2.6

by the Shell Oil Company in 1962 and were documented by Dormon and Metcalf *(8)*. The Shell criteria were developed from elastic analyses of pavements designed according to the California bearing ratio (CBR) procedure and from pavements in the AASHO Road Test. The Shell criteria ensure that permanent deformations in the subgrade will not lead to excessive rutting at the pavement surface. If the actual performance results from the AASHO Road Test are considered in terms of rut depth, the Shell criteria in Table 6 may be thought to be associated with an ultimate rut depth on the order of ¾ in.

The strain corresponding to 10^8 load applications in the Shell criteria was selected for comparison with the strains obtained from the laboratory tests and from the BISAR output for the 18- and 30-kip loads. The 10^8 load applications for a 20-year service life were recommended by the FDOT for the heavy traffic on an Interstate highway. From Table 6 a value of 2.6×10^4 in./in. strain is found to correspond to 10^8 load applications.

The comparisons show that, for the laboratory strains, all tested subgrade heights would qualify as adequate, except the A-5 at 36 in. For the strains output by BISAR for an 18-kip axle load, all heights qualify as adequate subgrade heights. For the BISAR 30-kip axle load, all heights qualify as adequate except the A-2-4 at 30 in. and the A-5 at 36 in. The BISAR program takes into account the relative stiffnesses of the pavement layers (i.e., the asphalt concrete, base, and stabilized subgrade). This leads to a reduction in the stresses and strains on top of the subgrade compared with the Boussinesq solution and the results of laboratory tests. The BISAR solution with the 30-kip axle load resulted in higher strains than did the laboratory testing, except in the A-5 soil. Because of this and to be on the safe side, the overloads have been considered in the comparisons to qualify certain subgrade heights above the water table. The comparisons were based on 10^8 load applications. Note that if 10^7 load applications were considered, the strain criterion would be 4.2×10^{-4} in./in. (from Table 6), and all heights of subgrade fill above the water table would qualify as adequate except the A-5. For 10^6 applications, the A-5 with a height of 36 in. would also be adequate. The Shell criterion strain for 10^6 load applications is 6.5×10^{-4} in./in. This strain level is about 30 percent higher than the strain for the A-5 soil under a 30-kip axle load. The 30 percent higher strain could be considered a safety margin for this particular condition. Figure 10 shows the recommended subgrade clearance heights above the water table, based on the overload of 30 kips for the project soils.

This analysis agrees well with that done using capillary fringe heights.

CONCLUSIONS

1. Soil gradation, the percent passing the No. 200 sieve, and the mineralogy of the subgrade soil influence soil-water retention characteristics to a great extent (Figure 1).

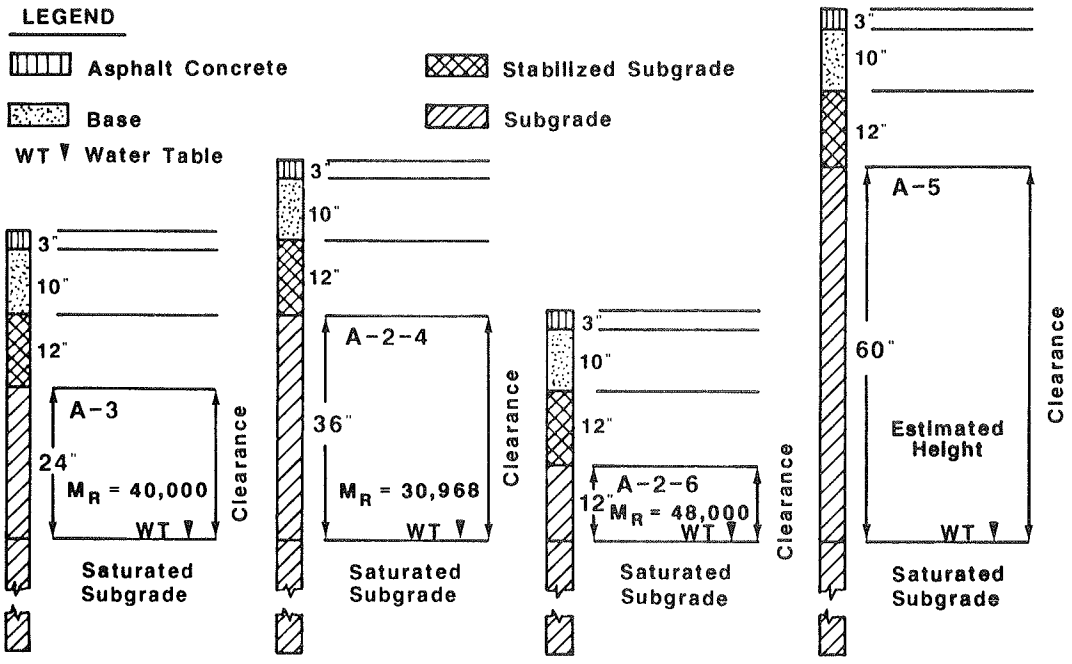

FIGURE 10 Recommended subgrade clearance heights based on a 30-kip axle load and 10^8 load applications for the project soils.

2. At different heights above the water table, the subgrade fill possesses different deformation characteristics. The greater this height, the stronger the fill (Figures 5 and 6).

3. The deformation characteristics of the subgrade soil (i.e., the plot of accumulated axial permanent strain versus number of stress applications at different water retention conditions) can be represented by a power function of the form

$$\varepsilon_p^a = AN^B$$

4. As a prospective subgrade fill, the A-2-6 soil tested in this research appears to be the best of the four project soils.

5. The A-5 soil has a tendency to swell because of its montmorillonite content. It also possesses very high resilient strain.

6. On the basis of the soil-water characteristics capillary fringe, an analysis using results from repetitive load testing, the BISAR computer program, and the Shell criteria, a subgrade fill of 24 in. is adequate for the A-3 soil, 36 in. is adequate for the A-2-4, and 12 in. is adequate for the A-2-6. If the A-5 soil must be used, a careful analysis should be undertaken. A fill thickness in the range of 4 to 6 ft is probably adequate for the A-5 soil.

7. The gradation of each soil can be related to its compaction characteristics. The well-graded A-2-6 soil showed the highest dry density at optimum. That in turn was reflected in the response of the soil during repeated load testing, when it experienced quite small permanent strain. On the other hand, the A-2-4 soil experienced high permanent strain and high elastic strain due to its uniform gradation and poor drainability.

8. Soil type is an important factor and should be considered in current guidelines for evaluating high-water clearances in pavements. This is based on the variation in deformation characteristics found in the different soils.

Note: The research study on which this paper is based is reported in detail by Elfino *(9)* and Davidson et al. *(10)*.

ACKNOWLEDGMENTS

This research study was sponsored by the Florida Department of Transportation as Project 99700-7311. Receipt of this research support and the assistance of many FDOT personnel are gratefully acknowledged.

REFERENCES

1. D. J. Janssen and B. J. Dempsey. Soil-Moisture Properties of Subgrade Soils. In *Transportation Research Record 790*, TRB, National Research Council, Washington, D.C., 1981, pp. 61–67.
2. C. L. Monismith, N. Ogawa, and C. R. Freeme. Permanent Deformation Characteristics of Subgrade Soils Due to Repeated Loading. In *Transportation Research Record 537*, TRB, National Research Council, Washington, D.C., 1975, pp. 1–17.
3. B. Shackel. Changes in Soil Suction in a Sand-Clay Subjected to Repeated Triaxial Loading. In *Highway Research Record 429*, HRB, National Research Council, Washington, D.C., 1973, pp. 29–39.
4. M. S. Kersten. Survey of Subgrade Moisture Conditions. *HRB Proc.*, Vol. 24, 1944, pp. 497–513.
5. K. Russam. Subgrade Moisture Studies by the British Road Research Laboratory. In *Highway Research Record 301*, HRB, National Research Council, Washington, D.C., 1970, pp. 5–17.
6. E. S. Barber and C. L. Sawyer. Highway Subdrainage. *HRB Proc.*, Vol. 31, 1952, pp. 643–666.
7. *BISAR Users Manual: Layered Systems Under Normal and Tangential Loads*. Koninlijke/Shell Laboratorium, Amsterdam, The Netherlands, July 1972.
8. G. M. Dormon and C. T. Metcalf. Design Curves for Flexible Pavements Based on Layered System Theory. In *Highway Research Record 71*, HRB, National Research Council, Washington, D.C., 1965, pp. 69–84.
9. M. K. Elfino. *An Evaluation of Design Highwater Clearances for Pavements*. Ph.D. dissertation. University of Florida, Gainesville, 1986.
10. J. L. Davidson, M. K. Elfino, and A. M. Gallet. *An Evaluation of Design Highwater Clearances for Pavements*. Final Report, Project 99700-7311. Florida Department of Transportation, Tallahassee, 1986.

Publication of this paper sponsored by Committee on Environmental Factors Except Frost.

Economic Impact of Pavement Subsurface Drainage

RAYMOND A. FORSYTH, GORDON K. WELLS, AND JAMES H. WOODSTROM

Even though road builders have recognized the role of water in pavement deterioration since the last century, with the development of the "rational" methods of pavement design evolved a strong reliance on the ability to build pavements stout enough to resist damage without the benefits of good drainage. Even today, most designers attempt to improve the strength and "quality" of the pavement and base layers used in road construction and neglect rapid drainage. Much of the water that falls on pavements penetrates the structural section through cracks, joints, and porous surfaces. Conventional slow-draining pavements are deteriorating more rapidly than is necessary because of the impacts of heavy vehicles on flooded structural sections. The most positive pavement drainage systems use an open-graded drainage layer under the full width of a roadbed with adequate collector pipes and outlet pipes. However, the California Department of Transportation has found that retrofit edge drains are greatly reducing the rate of step faulting of existing portland cement concrete pavements. The impact of positive rapid drainage features on the performance of a number of pavements is reviewed, with particular emphasis on the establishment of a cost-benefit relationship. The results of this evaluation indicate that the increased cost of effective pavement drainage is almost incidental to the savings realized through improved performance.

The ancient Romans, building their extensive road network, employed pavement sections that often enhanced pavement drainage. Before 1940, most pavement designers adhered to the belief that good drainage was essential for good performance. For example, Bruce *(1)* credits Tresaguet with one of the earliest improvements in pavement design circa 1764. In his pavement design, Tresaguet specified a base layer of large stone covered with a thin layer of smaller stone. Approximately 60 years later in England, Telford developed a similar design adding a thicker topping of fine stone and a crowned cross section, thereby providing better surface drainage. In 1816 McAdam began a study of stone-road construction. His design eliminated the heavy stone base used by Telford and Tresaguet and instead employed crushed stone of smaller size. Various types of macadam pavement have been used over the years. The first cement-bound pavement on record was built in Edinburgh, Scotland, in 1872, and was still in service in the 1930s.

Many macadam pavements were constructed with crushed rock placed over a thick layer of screenings, or rock chips, that served as a filter to prevent fine subgrade soils from working upward into the open-graded rock base. There is little doubt that good drainage provided by this construction technique improved pavement stability, thus enabling these pavements to provide service for many decades. In some cases, however, the open-graded rock was placed directly on fine-graded subgrade soils that gradually worked upward into the base, thereby diminishing its drainage capacity after a few years of service.

Not all road builders of McAdam's time believed in good drainage. In 1820 he warned *(2)* that "The erroneous opinion so long acted upon, and so tenaciously adhered to, that [by] placing a large quantity of stone under the roads, a remedy will be found for the sinking into wet clay, or other soft soils, or in other words, that a road may be made sufficiently strong, artificially, to carry heavy carriages though the sub-soil be in a wet state and by any such means to avert the inconvenience of the natural soil receiving water from rain, or other causes, has produced most of the defects of the roads of Great Britain."

A belief in good drainage generally prevailed among pavement designers until the late 1930s and early 1940s. Unfortunately, with the development of "modern" testing procedures to measure the strength of soils in a saturated state, there developed a belief that resistance to free water was built into pavement design.

UNDRAINED PAVEMENT PERFORMANCE

Free water that easily enters and collects in undrained pavements, and is acted on by traffic, is a primary cause of premature and continuing damage. In his 1820 report *(2)* McAdam stated: " . . . if water pass through a road and fill the native soil, the road whatever may be its thickness goes to pieces."

Because of the decision to live with the water that completely fills most pavements for weeks or months each year, most pavements have a built-in defect that is significantly reducing service life.

Faulting, frost damage, D-cracking, and pothole damage do not occur in the absence of free water. Several well-documented road tests made in the past 35 years or so demonstrate that, regardless of thickness or strength of pavements, rates of damage under flooded conditions (internally) can be up to hundreds, even thousands, of times greater than when little or no free water is present in the structural section.

The report of one of the earliest of the road tests, Road Test One-MD *(3)*, revealed that much greater damage occurred to 10-year-old concrete pavements in wet periods than in dry. The next major test road, the WASHO Road Test, produced rates of damage as much as 70,000 times greater during the spring thaw than in summer months when there was little or no free water in the sections *(4)*. Only a few years later, the most comprehensive of all road tests, the AASHO Road Test in Ottawa, Illinois

Office of Transportation Laboratory, California Department of Transportation, 5900 Folsom Boulevard, Sacramento, Calif. 95819.

(5), had damage rates for many of its pavements that were much greater in wet periods than in dry. W. J. Liddle, in a paper presented to the First International Conference on the Structural Design of Asphalt Pavements *(6)*, stated that the damaging actions of traffic were noticeably more severe in spring than in summer or fall. A chart of rates of loss of serviceability versus months of the year showed rates of damage up to 40 to 50 times greater in wet periods than in dry. Extensive discussions of the AASHO Road Test results were given in the Proceedings of this conference. One speaker, C. R. Foster, commented that

> the supposedly pervious shoulders did not provide adequate drainage and water was trapped in the base and subbase especially during critical periods. Pore pressures and resulting weakness developed in both of these materials. . . . we should take steps to provide better subbase drainage so as to obtain maximum benefits of our materials.

Little or no heed was paid to Foster's comments. The predominant view of those overseeing the AASHO Road Test and interpreting its results was that drainage was a low-priority item. Even though most of the severe damage to pavements of the AASHO Road Test was caused by pore pressures from impacts on undrained water, no criteria for improving roadbed drainage evolved from the AASHO Road Test and, as a consequence, the prevailing practice continued to be the design of "stout" pavements.

A few years after the AASHO Road Test, Barenberg and Thompson *(7)* employed the circular test track at the University of Illinois to evaluate some of the AC pavement designs of the AASHO Road Test. These investigators found that when free water was introduced into the test sections, after many load applications had been put on while bases were only moist or damp, the rates of damage per traffic impact were up to 200 times greater than the rate before water was added.

Despite these findings, and in addition to those of the prior road tests, no change in design practices occurred. As a result, nearly all important pavement built in the decade following the publication of these findings is of the undrained variety. Only in the past few years has there been a renewed interest in the importance of good drainage. A number of states are now specifying open-graded base drainage layers as one of their standard designs for important roads in order to achieve rapid removal of infiltrated surface water.

Cedergren *(8)* estimated that $217 billion of the $329 billion ($15 billion per year) in estimated repairs from 1976 to 1990 could be saved if all important pavements were constructed as well-drained systems. This estimate was made assuming that U.S. pavements on the average are exposed to internal flooding about 15 percent of the year, and that wet impacts cause 10 to 20 times more damage (per impact) than impacts on dry or well-drained pavements. Because many of the undrained pavements are kept in a flooded state much more than 15 percent of the time, and many have wet impact damage rates much greater than 10 or 20, the estimated $15 billion annual waste is believed conservative.

RECENT DEVELOPMENTS IN SUBSURFACE PAVEMENT DRAINAGE

The relatively recent movement toward subsurface pavement drainage is largely due to the development of improved and economical drainage materials along with greater awareness of the nature and extent of the problem resulting from the research of a number of individuals throughout the world. In the following section, what are believed to be a few of the milestones in this evolution are described.

Geotextiles

The problem of providing a drainage layer sufficiently permeable to remove excess water quickly and yet fine enough to preclude contamination from clogging by fines was largely solved with the development of Terzaghi's filter criterion and its subsequent modification by others. This practice has been developed to a high degree in earth dam construction in which, in some instances, up to five layers of graded materials are employed for filtration and drainage.

The use of a separate filtration layer for roadway structural section drainage, however, failed to gain wide acceptance, presumably because of the cost, complexity, and difficulties visualized in placing and compacting the open-graded drainage layer. The introduction of geotextiles to drainage applications enhanced the economical application of blanket drains in pavement drainage.

Geotextiles were first used for subsurface water drainage applications. The excellent filtration and separation characteristics associated with nonwoven geotextiles permitted the use of a single layer of a more economical drainage aggregate enveloped in a geotextile. Success with geotextiles in subdrainage in the late 1970s led to their application in pavement drainage for both groundwater and surface water infiltration. The thin geotextile filter/separator reduced excavation as well as the cost of a drained structural section. The tensile properties of geotextile filters permitted further cost reductions by facilitating the use of thin layers of open-graded stabilized drainage materials.

Asphalt-Treated Permeable Material

One of the early proponents of two-layer subsurface drainage in highway construction was W. R. Lovering who, as a District Materials Engineer for the California Division of Highways, had many occasions to observe the results of inadequate or clogged drains through the wet cuts common in northwestern California. In 1960 Lovering made specific proposals for the employment of two-layer subdrainage systems in highways. Recognizing the difficulties inherent in the construction of a firm working table using the single-sized aggregates necessary for the drainage layer, Lovering and Cedergren proposed in 1962 *(9)* the use of a lean asphalt mix of coarse single-sized material for the drainage layer. They reported on the effect on permeability of treatment of open-graded aggregate with 2 percent asphalt. These data revealed that the presence of asphalt binder did not significantly lower the permeability of the drainage layer (10,000 to 30,000 ft/day).

FHWA Study

In 1970 the FHWA authorized an in-depth study of the problems associated with water in state and Interstate highways

under a contract with the joint venture of H. R. Cedergren of Sacramento and Ken O'Brien & Associates of Long Beach, California *(10)*. After a thorough examination of all known literature on roadbed drainage, the interview team visited engineers in each of the nine FHWA regions to discuss pavement problems with FHWA and state engineers in design, construction, and maintenance. The team then examined several hundred miles of pavement in one state in each of the regions and selected a case study site to be drilled and tested to determine the causes of problems at each site.

This study concluded that traffic impacts on structural sections containing large amounts of free water are the root cause of most pavement deterioration. The consultants were asked to develop a subdrainage system that could largely eliminate extensive entrapment of free water in structural sections. The drainage system that evolved had the following key features: *(a)* a highly permeable open-graded base drainage layer under the full width of the roadway, *(b)* a base under the drainage layer designed using a filter criterion with subbases as needed for obtaining the total thickness needed for support of loads, *(c)* collector pipes along lower edges of the drainage layer, *(d)* outlet pipes suitably sized and spaced to rapidly remove all of the water entering the system, and *(e)* markers on posts at pipe outlets to flag their locations and protect them from damage from mowers and the like.

The FHWA report of this study *(10)* provided procedures for estimating inflows and designing drainage systems to quickly remove infiltrated surface water.

Evolution of Portland Cement Concrete Pavement Edge Drains

The primary distress mechanism of plain jointed concrete pavement, step faulting due to pumping of base and shoulder fines in the presence of free water, has been recognized and studied by pavement researchers since the 1940s. In 1952 the California Department of Transportation (Caltrans) adopted, as a standard, a cement-treated base for concrete pavements to provide a nonerodible support for the pavement slab and thus mitigate the problem of step faulting. The effect of this change was only a slowing of the faulting process. Beginning in the 1960s the faulting phenomena were studied in some depth by a number of agencies *(11–20)*. The faulting process was successfully modeled by Caltrans researchers in a laboratory environment in 1980 *(16)*. It was generally concluded in these studies that four conditions must be present for faulting to occur:

1. Heavy wheel loads,
2. Curled pavement slabs,
3. Source of fine materials, and
4. Free water and voids under and around the pavement slab.

It was concluded that if at least one of these elements could be eliminated, step faulting could be significantly arrested or stopped completely. Denying access to fines and the rapid removal of infiltrated surface water from the structural section were the logical candidates for successful mitigation of the problem because heavy wheel loads are considered inevitable and curling can only be partly reduced by the use of shortened slabs. Beginning in 1975, California, along with several other states, experimented with a number of edge drain designs from which evolved, in 1979, the present standard designs used for retrofit installations and new construction. The primary modifications made during this period were stabilization of the permeable material with cement or asphalt and elimination of the complete envelopment of the permeable material with filter fabric (Figure 1).

Current Status

A growing recognition of the importance of positive subsurface pavement drainage resulted from the FHWA study of 1970 *(10)* and the work of a number of researchers, some of whom are cited in this paper. Subsurface drainage of pavement is treated extensively in the AASHTO *Guide for the Design of Pavement Structures* published in 1986 and will be an integral part of the Strategic Highway Research Program (SHRP). The specific pavement studies portion of the Long-Term Pavement Performance Study will incorporate 96 test sections involving both plain jointed concrete pavement and jointed reinforced concrete pavement. The effect of three different subdrainage designs will be evaluated. Similarly, 32 flexible pavement test sections that incorporate two different subdrainage designs will be evaluated. The authors believe that this comprehensive and carefully controlled study of the effect of pavement subdrainage will produce extremely valuable data on the economics of pavement drainage and, indeed, is one of the key elements of the program.

CASE HISTORIES

Rigid Pavement

Edge drains for rapid removal of infiltrated surface water at the pavement-shoulder joint have been used by a number of entities since the mid-1970s with mixed, although often favorable, results. The Georgia DOT placed a moratorium on edge drains in 1978 *(21)* as a result of problems created by the migration of fines into the permeable material surrounding the collector pipe. Attempts to mitigate the problem by encapsulating the entire drainage element with filter fabric proved ineffective because of the buildup of fines on the fabric and the resultant loss of drainage capacity. The California DOT found that, even with the modifications described previously, edge drains were not effective and were possibly detrimental in those instances in which the slope of the longitudinal collector was less than 0.2 percent or the outlet was subject to inundation. In general, however, edge drains have resulted in a significant improvement in pavement performance. Darter et al. *(22)* reported in 1979 that the use of experimental edge drains on three different continuously reinforced concrete projects in Illinois reduced the number of punchouts an average of 24 percent. In 1984 Darter et al. *(23)* reported the results of a comprehensive six-state concrete pavement performance study in which various design features and environmental conditions were related to pavement performance. It was concluded that edge drains significantly increased the service life for jointed

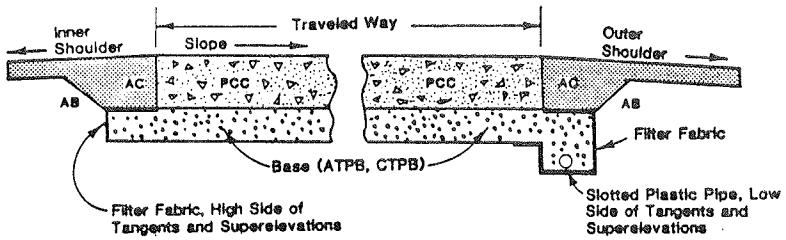

Rigid Pavement Permeable base detail

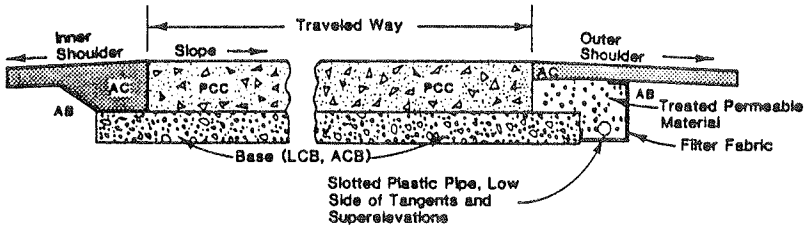

Rigid Pavement Non-permeable base-edge drain detail

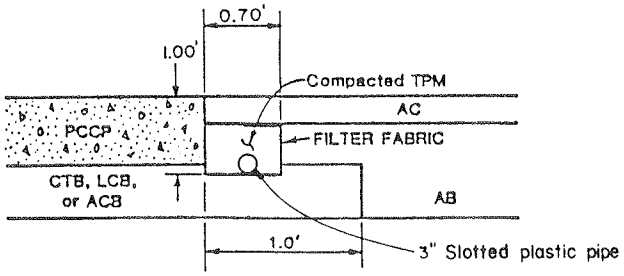

Retrofit Subgrade Drain Detail

FIGURE 1 Details of rigid pavement drainage.

concrete pavement and jointed reinforced concrete pavement. The use of edge drains on pavements susceptible to D-cracking resulted in a large decrease in joint deterioration and pumping. The Illinois results indicated that, in terms of the rate of joint deterioration, edge drains provided a 50 percent increase in service life.

The beneficial effect of edge drains on concrete pavement performance was also convincingly demonstrated in Spain on the Valencia-Tarragona Toll Road. This facility, constructed in 1974, consisted of plain jointed concrete slabs over cement-treated base with no provision for pavement drainage. By 1978 measurements of 85 randomly selected joints on the two projects indicated that step faulting was occurring. The decision was made to install a retrofit edge drain system to slow, or stop, the progression of faulting (Figure 2). The step-off was almost completely arrested from installation until 1985.

The results of a California research study of the effect of edge drains on pavement performance *(24)* indicated that, for undrained plain jointed concrete pavements, the average faulting rate was 0.006 in./year, whereas the average faulting rate for retrofit edge drains (installed some time after initial construction) was –0.0003 in./year. This reduction in faulting, attributable to the provision of drainage, should result in significantly improved performance of portland cement concrete pavements (PCCPs).

This study also included two contracts under which some projects were initially constructed with edge drains. The average faulting rate for the undrained portions was –0.002 in./year. In contrast, on the drained portions the faulting rate averaged a relatively insignificant 0.0005 in./year. This study also indicated that the rate of slab cracking was less in the drained pavements than in the undrained pavements.

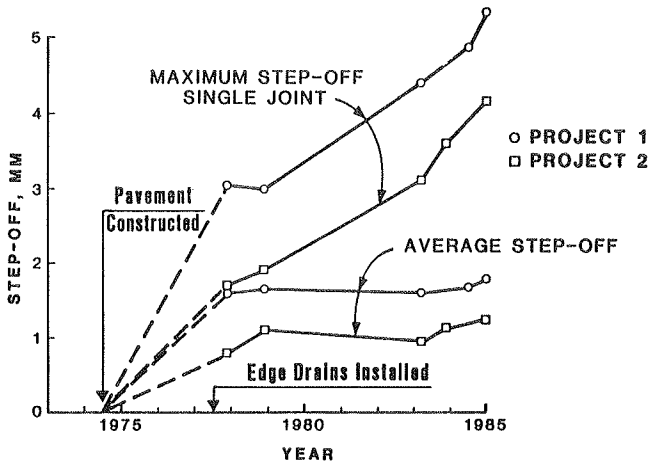

FIGURE 2 Effect of edge drains on pavement faulting.

Four additional projects on which drained PCCPs were used were reviewed for performance. The drained PCCPs consisted of

1. Edge drains placed during construction,
2. PCCP over an untreated permeable material (UPM),
3. PCCP over an asphalt-treated permeable base (ATPB), and
4. PCCP over a cement-treated permeable base (CTPB).

The performance of these pavements was analyzed by reviewing the Caltrans pavement management surveys that are performed every 2 years. These surveys rate all pavement for rideability and structural damage. Structural damage of PCCP is rated as a function of the type of cracking. Stages 1 and 2 (rated together) are nonintersecting cracks in the pavement slab. Third-stage cracks are intersecting cracks in the slab and are an indication of slab failure. Cracking is reported as the percentage of cracked slabs within the surveyed section.

The effect of positive drainage on the performance of these pavements (percentage of cracked slabs) is shown in Figure 3. With the exception of 7-LA-14, which has yet to show cracking in either the drained or the undrained sections, the drained sections manifest significantly lower rates of cracking. Overall, the percentage of cracked slabs in the undrained exceeds that in the drained sections by a ratio of 2.4 to 1.

Flexible Pavement

In 1982 Markow *(25)* reported the results of a pavement performance simulation using a Federal Highway Administration EAROMAR system aimed specifically at establishing the effect of positive rapid drainage of pavements. The results indicated that, in regions that receive annual rainfall of approximately 40 in., pavement life is extended by 4 years.

Relatively few systematic field evaluations of the benefits of rapid positive drainage of flexible pavement are found in the literature. In 1981 Barenberg and Brown *(26)* reported the results of a study for the New Jersey Department of Transportation on the use of open-graded drainage layers directly under a 5-in. asphalt concrete layer on the University of Illinois test track. The performance of a standard undrained design was compared with that of drained designs in terms of rut depth and deflection level. Subgrade was an A-6 clay with an unsoaked California bearing ratio (CBR) value of 6. The open-graded permeable layers were 2.5 in. thick and placed in both a stabilized and an unstabilized state. Permeabilities ranged from 2,000 to 6,000 ft/day. The test loadings were applied by two 10:25 × 20 tires inflated to 75 psi, each bearing 3,200 lb. Before loading, an initial series of tests was made to establish the drainage characteristics of the various test sections. Water was then introduced simultaneously with the application of wheel loads. Of particular interest were Section 1, the standard undrained section, and Sections 2 and 3, which were structurally equivalent according to California pavement design criteria but which included an open-graded drainage layer. A review of the results indicated a reduction of approximately 20 percent in deflection level for the two drained sections compared with the standard design.

Given the fatigue properties of 0.4-ft-thick California flexible pavements *(27)*, the effect of a reduction in deflection level of this magnitude on fatigue life would depend on initial deflection level, pavement thickness, and equivalent single axle load (ESAL), as shown in Figure 4. For example, a 0.4-ft-thick pavement with an initial deflection level of 0.025 in. would have its fatigue life extended by 90,000 ESALs with a 20 percent reduction in deflection level. At a lower level of initial deflection, say 0.013 in., the 20 percent reduction in deflection level would increase ESALs by 7 million. This extrapolation of the results of a study of admittedly limited scope, consisting of a single subgrade condition and surfacing thickness, is intended only to illustrate the potential improvement in fatigue performance of AC pavements in a severe (wet) environment. Under these conditions, results may be conservative in that they do

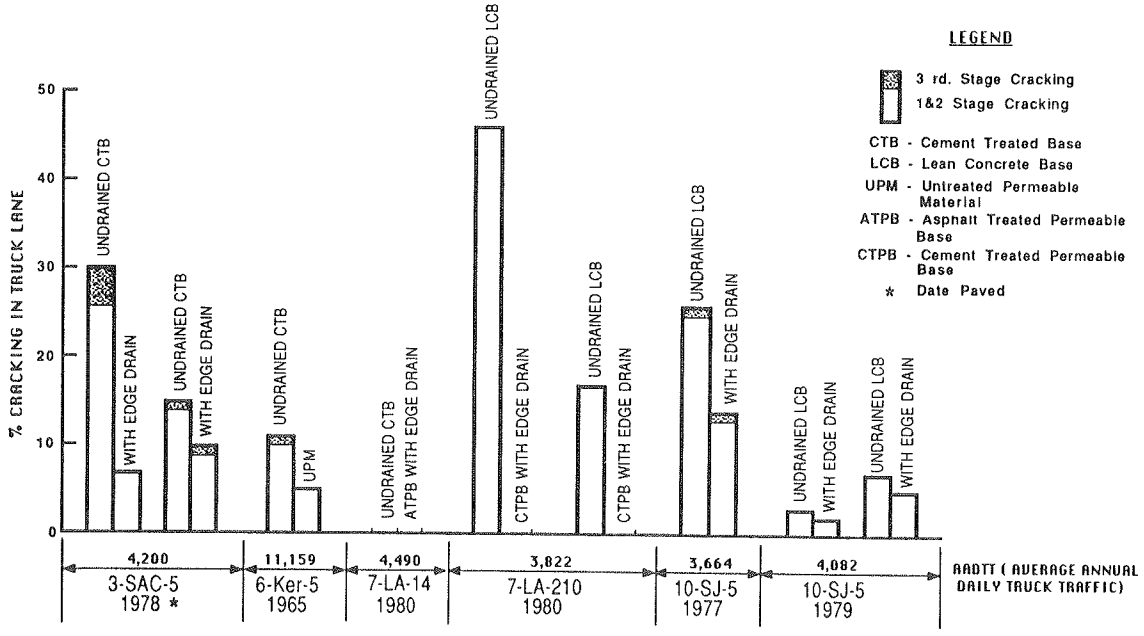

FIGURE 3 Comparison of cracking in undrained and drained PCCP.

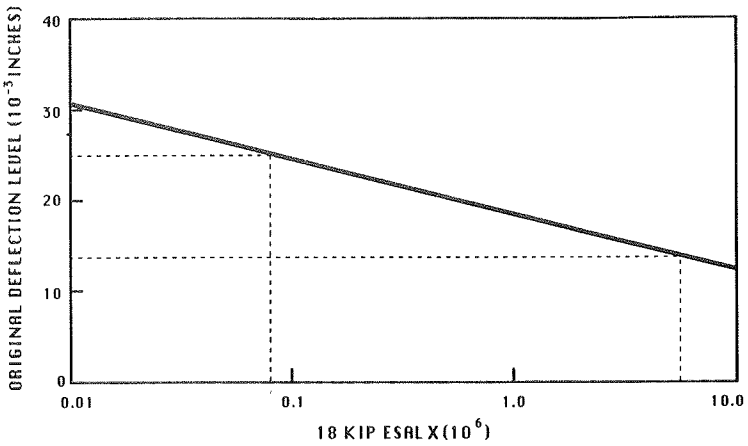

FIGURE 4 Potential increase in 0.4-in.-thick AC pavement fatigue life resulting from 20 percent reduction in deflection level.

not include the effects of the reduce rate of asphalt concrete oxidation, and thus embrittlement, that would result from the rapid removal of surface-infiltrated water from the drained pavement section.

In 1982 Caltrans adopted a policy of requiring the placement of asphalt-treated permeable material (ATPM) under the surfacing layer with collectors and outlets for new flexible pavement construction. The oldest pavements constructed using this drainage design have been in place only 3 years. Thus a definitive evaluation of the effect of this feature on performance is not yet possible. The earliest use of ATPM under the base layer in California was on Kneeland Road in Humboldt County, initially reported on by Cedergren *(28)*.

A 500-ft section of logging road was reconstructed by a county public works department in 1967 using a highly permeable open-graded base drainage layer after the road had failed twice in just a few years. The prior reconstructions had used the then-standard drainage materials specified by the California Division of Highways (now Caltrans), which contained several percent minus No. 200 fines that had permeabilities of perhaps 5 to 10 ft/day. Heavy logging trucks on flooded structural sections caused rapid failures in this water-abundant environment (40 to 80 in. of rain a year, plus inflows from springs etc.). The open-graded base drainage layer, graded from 3/4-in. to No. 4 sieve, was stabilized with 2.25 percent paving-grade asphalt. When tested as a case study site in the FHWA guidelines study, its permeability was found to be in the range of 10,000 to 30,000 ft/day. The two-layer drain consisted of a 0.33-ft filter layer and a 0.66-ft ATPM layer. The filter material contained more fines than would normally have been desirable, but it still met primary filter criteria. A recent (1986) field review of this 500-ft section revealed that the original pavement is still in excellent condition with no patching. As shown in Figure 5, the adjoining pavement has been extensively patched. The 19-year service life of this section (to date) is well beyond the normal 12-year life of AC pavements in California.

Gray et al. *(29)* reported on another two-layer drainage (ATPM) project on Route 299 between Arcata and Willow Creek. The experimental section consisted of 0.4 ft of ATPM underlaid by 0.3-ft Class 2 permeable material as the filter medium. The control section consisted of 0.7 ft of Class 2 permeable material.

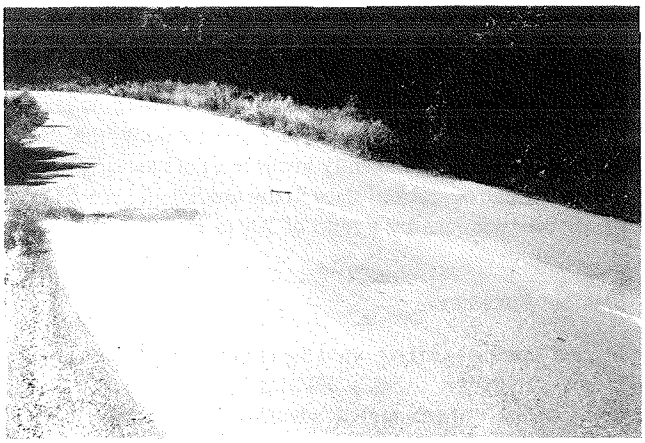

FIGURE 5 Kneeland Road, July 1986.

The results of in situ permeability tests revealed that the drainage capacity of the two-layer section was three to nine times that of the control section. This was not surprising because the coefficient of permeability of standard Class 2 permeable material ranges from 10 to 500 ft/day compared with 10,000 to 25,000 ft/day for ATPM. This section was not open to traffic until 1972. A recent field review indicated some fine alligator cracking of the surface in both drained sections, which have been chip sealed. However, the performance to date of this road in a severe environment (40 to 80 in. annual rainfall) under heavy logging truck traffic has exceeded the average performance of California flexible pavements.

Cedergren *(28)* cites a number of other instances of excellent performance of individual flexible pavements with positive rapid drainage.

ECONOMICS

Attempting to quantify the economic impact of positive rapid pavement drainage is difficult, to say the least, for a number of reasons. The literature contains few controlled experimental data on the effect of drainage on pavement service life, primarily because so little research on the subject has been conducted. What is available is extremely limited in terms of

variation in subgrade and environmental conditions and structural section design. Because this is the case, the authors have made what are believed to be extremely conservative assumptions about the increases in pavement service life.

With respect to flexible pavements, the work of Markow *(25)*, Barenberg and Brown *(26)*, and the case histories cited suggest a minimum increase of 4 years of service life with a drained system.

For rigid pavement, the work of Darter et al., the results of the California edge drain study, and the performance of the retrofit edge drain system on the Valencia-Tarragona Toll Road suggest a minimum 50 percent extension of service life of PCC pavements with an efficient functioning edge drain system.

To assess economic impact, a life-cycle cost analysis was not considered realistic because

1. An appropriate life cycle would be extremely difficult to establish and justify,
2. The extent and nature of required rehabilitation are uncertain, and
3. Realistic maintenance and user costs would be extremely difficult to establish.

The analysis therefore was done in terms of cost per square yard per year from construction to first rehabilitation. The assumed structural sections are equivalent in load-carrying capacity, differing only by the inclusion of rapid drainage capability in each of the two basic pavement types. Costs (in place) are from the Caltrans 1985 Construction Cost Index.

Rigid Pavement (undrained section)

	Thickness (ft)	*Cost in Place ($/yd³)*
Portland cement concrete	0.85	65.00
Lean concrete base	0.50	51.00
Aggregate subbase	0.70	11.00

Converting to a square yard basis and assuming a 20-year service life, the pavement cost is

$$\frac{\$29.49/yd^2}{20\ yr} = \$1.47/yd^2/yr$$

Rigid Pavement (drained section)

	Thickness (ft)	*Cost in Place ($)*
Portland cement concrete	0.85	65.00/yd³
Asphalt-treated permeable base	0.25	42.00/yd³
Aggregate subbase	1.05	11.00/yd³
Edge drains		0.70/linear foot
Edge drain outlets		3.50/linear foot

Converting to a square yard basis and assuming a 30-year service life, the pavement cost is

$$\frac{\$26.13/yd^2}{30\ yr} = \$0.87/yd^2/yr$$

This represents an annual savings of 41 percent in rigid pavement costs over the service life of the pavement due to its drainage features.

Flexible Pavement (undrained section)

	Thickness (ft)	*Cost in Place ($/yd³)*
Asphalt concrete	0.70	60.00
Aggregate base	1.00	19.00
Aggregate subbase	1.40	11.00

Converting to a square yard basis and assuming a 12-year service life, the pavement cost is

$$\frac{\$25.47/yd^2}{12\ yr} = \$2.12/yd^2/yr$$

Flexible Pavement (drained section)

	Thickness (ft)	*Cost in Place ($)*
Asphalt concrete	0.65	60.00/yd³
Asphalt-treated permeable base	0.25	42.00/yd³
Aggregate base	0.75	19.00/yd³
Aggregate subbase	1.40	11.00/yd³
Edge drains	–	0.70/linear foot
Edge drain outlets	–	3.50/linear foot

Converting to a square yard basis and assuming a 16-year service life, the pavement cost is

$$\frac{\$26.74/yd^2}{16\ yr} = \$1.67/yd^2/yr$$

representing an annual savings in pavement cost of 21 percent over the service life of the pavement, which does not include reduced maintenance or user costs.

Extrapolated Savings

California historically has constructed approximately 200 lane miles of new pavement (20 percent rigid and 80 percent flexible) annually (new alignments, widenings, lane additions, etc.). Extrapolating the annual cost savings for drained pavements to a program of this magnitude, the annual savings amount to

1. Rigid pavement. A savings of $0.60/yd²/year applied to 40 lane miles per year yields a savings of $168,960 per year. For the estimated 30-year service life, a total rigid pavement savings of $5,068,800 (present dollars) could be realized.
2. Flexible pavement. A savings of $0.45/yd²/year applied to 160 lane miles per year yields a savings of $506,880 per year. For the estimated 16-year service life, a total flexible pavement savings of $8,110,080 (present dollars) could be realized. Thus, for the annual 200 lane miles of new pavement, a total savings of $13,178,880 (or 36 percent of pavement costs) can be realized throughout the service life of the pavements constructed in any given year. This does not include the

savings due to increased service life from retrofit edge drains installed on in-service pavements or maintenance and user costs.

SUMMARY AND CONCLUSIONS

Even though the benefits of rapid positive drainage of pavements have been recognized for more than 160 years, the pavement design community has been painfully slow to incorporate it in pavement design. This is due to a number of factors, including resistance to change; a belief that resistance to free water is built into pavement design or that pavements can be effectively sealed; and, of course, the additional expense of drainage features.

In recent years the development of filter fabrics and treated permeable material, along with the evolution of slotted PVC pipe, has greatly simplified and reduced the cost of pavement drainage. Recent studies involving edge drains and the effect of permeable bases on the performance of PCC pavements, although limited in scope, provide convincing evidence that pavement service life can be significantly extended by positive drainage. On the basis of studies of Markow *(25)* and Barenberg and Brown *(26)* and individual case histories, an increase in service life of 4 years (33 percent in California) is believed to be a conservative estimate for flexible pavements. An extension of service life of this magnitude will reduce pavement costs by approximately 21 percent. Similarly, studies of the effect of retrofit edge drains on PCC pavement performance in California and Spain suggest an extension of service life of 10 years (50 percent), which equates into a cost reduction of 41 percent, not including user and maintenance costs. For the annual 200 lane miles of new construction in California, this amounts to more than $5 million for rigid pavements and $8 million for flexible pavements over the service life of pavements constructed during any given year (or 36 percent of pavement costs). Certainly one of the significant studies planned for the Long-Term Pavement Performance Study of the Strategic Highway Research Program is that portion of the study devoted to the quantification of the effect of positive rapid drainage on the performance of both flexible and rigid pavements. For this purpose 128 test sections will be dedicated throughout the United States.

ACKNOWLEDGMENT

The authors wish to acknowledge and thank Harry Cedergren for his review and input to the introductory portion of this paper and, more important, his lifelong efforts in the promotion of positive, rapid pavement drainage.

REFERENCES

1. A. G. Bruce. *Highway Design and Construction.* International Textbook Co., Scranton, Pa., 1934.
2. J. McAdam. *Report to the London Board of Agriculture*, 1820.
3. *Special Report 4: Road Test One-MD.* HRB, National Research Council, Washington, D.C., 1952.
4. *The WASHO Road Test, Part 2: Test Data, Analyses, and Findings.* HRB, National Research Council, Washington, D.C., 1955.
5. *Special Report 61G: The AASHO Road Test, Report 7: Summary Report.* HRB, National Research Council, Washington, D.C., 1962.
6. W. J. Liddle. Application of AASHO Road Test Results to the Design of Flexible Pavement Structures. *Proc., International Conference on the Structural Design of Asphalt Pavements*, University of Michigan, Ann Arbor, 1962.
7. *Behavior and Performance of Flexible Pavements Evaluated in the University of Illinois Test Track.* Highway Engineering Series 36, Cooperative Highway Research Program Series 108. Urbana, Ill., 1970.
8. H. R. Cedergren. Poor Pavement Drainage Could Cost $15 Billion Yearly. *Engineering News Record*, June 8, 1978.
9. W. R. Lovering and H. R. Cedergren. Structural Section Drainage. *Proc., International Conference on the Structural Design of Asphalt Pavements*, University of Michigan, Ann Arbor, 1962, pp. 773–784.
10. H. R. Cedergren, K. H. O'Brien, and J. A. Arman. *Guidelines for the Design of Subsurface Drainage Systems for Highway Structural Sections.* Report FHWA-RD-72-30. FHWA, U.S. Department of Transportation, 1972.
11. D. L. Spellman, J. . R. Stoker, and B. F. Neal. *California Pavement Faulting Study.* California Division of Highways, Sacramento, Jan. 1970.
12. D. L. Spellman, J. H. Woodstrom, and B. F. Neal. Faulting of Portland Cement Concrete Pavements. In *Highway Research Record 407*, HRB, National Research Council, Washington, D.C., 1972, pp. 1–9.
13. W. Gulden. *Extent and Severity of Pavement Faulting in Georgia.* Georgia Department of Transportation, Atlanta, Aug. 1972.
14. W. Gulden. *Investigation into the Causes of Pavement Faulting on the Georgia Interstate System.* Georgia Department of Transportation, Atlanta, Jan. 1974.
15. B. F. Neal and J. H. Woodstrom. *Faulting of Portland Cement Concrete Pavements.* FHWA-CA-TL-5107-20. California Department of Transportation, Sacramento, July 1977.
16. B. F. Neal. *Model Slab Faulting Study.* FHWA-CA-TL-80-23. California Department of Transportation, Sacramento, June 1980.
17. *NCHRP Synthesis of Highway Practice 56: Joint-Related Distress in PCC Pavement: Cause, Prevention and Rehabilitation.* TRB, National Research Council, Washington, D.C., 1979.
18. W. Gulden. *Pavement Faulting Study.* Research Project 7104, Final Report. Georgia Department of Transportation, Atlanta, May 1975.
19. C. P. Nguyen, M. Ray, and J. F. Griselin. Concrete Pavements—Problems Raised by the Presence of Water in Their Structure. *Bulletin de Liaison des Laboratoires des Ponts et Chaussées*, Special No. VIII, July 1979.
20. L. H. Moore. Drainage Considerations for Rehabilitation of Portland Cement Concrete Pavements. Presented at TRB National Seminar on PCC Pavement Recycling and Rehabilitation, Sept. 1981.
21. W. Gulden. Experience in Georgia with Drainage of Jointed Concrete Pavements. *Proc., International Seminar on Drainage and Erodibility at the Concrete Slab-Subbase Shoulder Interface*, Paris, France, 1983.
22. M. I. Darter, S. A. LaCoursiere, and S. A. Smiley. Structural Distress Mechanisms in Continuously Reinforced Concrete Pavement. In *Transportation Research Record 715*, TRB, National Research Council, Washington, D.C., 1979, pp. 1–7.
23. M. I. Darter and J. M. Becker. *Concrete Pavement Evaluation Systems (COPES).* Vol. 1, Final Report. NCHRP, TRB, National Research Council, Washington, D.C., 1984.
24. G. K. Wells. *Evaluation of Edge Drain Performance.* Report FHWA/CA/TL-85-15. California Department of Transportation, Sacramento, 1985.
25. M. J. Markow. Simulating Pavement Performance Under Various Moisture Conditions. In *Transportation Research Record 849*, TRB, National Research Council, Washington, D.C., 1982, pp. 24–29.

26. E. J. Barenberg and D. Brown. *Modeling Effects of Moisture and Drainage of NJDOT Flexible Pavement Systems.* Department of Civil Engineering, University of Illinois, Champaign, 1981.
27. California Test 356: Methods of Test to Determine Overlay Requirements by Pavement Deflection Measurements. In *Manual of Test*, Vol. 2, California Department of Transportation, Sacramento, 1981.
28. H. R. Cedergren. *Drainage of Highway and Airfield Pavements.* John Wiley and Sons, Inc., New York, 1974.
29. W. C. Gray, J. B. Hannon, and R. A. Forsyth. *Performance of Two Layer Asphalt Stabilized Drainage Blankets for Highway Subdrainage.* Caltrans Report CA-DOT-TL-2618-1-74-25. California Department of Transportation, Sacramento, 1974.

Publication of this paper sponsored by Committee on Subsurface Drainage.

Use of Open-Graded, Free-Draining Layers in Pavement Systems: A National Synthesis Report

JOHN S. BALDWIN

The effects of excessive and uncontrolled water entrapped in the various components of a paving system are known or suspected to have been responsible for unsatisfactory performance and outright failures of both portland cement concrete and asphaltic concrete pavements. To eliminate or at least reduce the detriment, almost half of the highway and transportation agencies across the nation have been addressing the problem by designing and constructing free-draining pavement systems. In an effort to ascertain just how much and what kind of attention is being given free-draining pavements on a national scale and to gain some insight into the performance characteristics of such systems designed to date, the Transportation Research Board's Committee on Subsurface Drainage prepared a questionnaire for national distribution in the fall of 1985. This paper is an attempt to summarize the responses to that questionnaire.

The effects of excessive and uncontrolled water entrapped in the various components of a paving system are known or suspected to have been responsible for unsatisfactory performance and outright failures of both portland cement concrete and asphaltic concrete pavements. In general, the adverse effects are manifested in premature rutting, cracking, faulting, increased roughness, and a relative decrease in the level of serviceability.

For several years, notable highway engineers such as Cedegren, Moulton, and others have advocated pavement designs that emphasize rapid and effective drainage of the pavement structure in order to eliminate or at least reduce the detriment caused by entrapped water. Because it is virtually impossible to keep water out of pavements for anything but a relatively short time and prohibitively expensive to build pavements strong enough to withstand the detriment of entrapped water, almost half of the highway and transportation agencies across the nation have been giving serious attention to the free-draining approach.

In an effort to ascertain just how much and what kind of attention is being given free-draining pavements on a national scale and to gain some insight into the performance characteristics of such systems designed to date, the Transportation Research Board's Committee on Subsurface Drainage prepared a questionnaire for national distribution in the fall of 1985. This paper is an attempt to summarize the response to that questionnaire.

Responses indicated that the term "free-draining pavement system" does not necessarily have the same meaning for everyone. In this discussion, a free-draining pavement is one that has been constructed with a full-width open-graded layer somewhere beneath the surface of the pavement but above the subgrade. This layer is normally outlet by some sort of underdrain system or by simply daylighting the free-draining layer to the surface drainage just past the shoulder.

West Virginia Department of Highways, 1900 Washington Street, East, Charleston, W. Va. 25305.

QUESTIONNAIRE RESPONSE

General

Of the 49 agencies that responded to the questionnaire, 25 indicated that they had not used free-draining layers, and 24 indicated that they had used or do use the free-draining concept in their pavement designs. Although there is apparently quite a bit of experimental work still being done with free-draining pavement systems, 15 agencies (or more than 62 percent of those using the concept) indicated that the free-draining approach is being used routinely and that anticipated future use would be on Interstates and high-volume secondary roads.

Response to the question about agency experience (Figure 1) indicated not only that a considerable number of lane miles have been constructed to date by some agencies (one agency reported 1,000 lane miles) but also that some agencies have been working with free-draining pavements for quite some time.

Design and Construction

In theory, the designed thickness of a free-draining pavement layer should be based largely on the amount of expected inflow into the pavement structure. Because most pavement systems are quite dense and, by design, have usually been constructed in an effort to keep water out, infiltration calculations are extremely difficult. Responses to the question about design thickness indicated that a variety of thicknesses of the free-draining layer have been used. The three most popular thicknesses appear to be 6 in. (7 states, 22 percent); 3 in. (3 states, 11 percent); and 12 in. (2 states, 7 percent). The thinnest free-draining layer was reported to be 2 in. and from 18 to 24 in. was reportedly used by one state agency.

The location of the free-draining layer within the pavement structure has been a subject of some controversy. Although cases have been made for putting the free-draining layer between the base and the subgrade, there are apparently equally

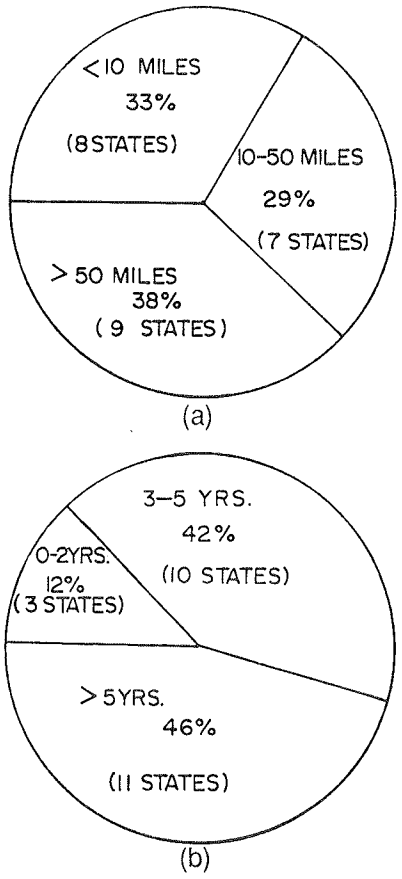

FIGURE 1 Agency experience: *(a)* lane miles of free-draining pavement (percentage of agencies) and *(b)* years of experience with free-draining pavement systems (percentage of agencies).

good reasons for placing the layer immediately beneath the surface of the pavement or in the middle of the pavement structure. Questionnaire responses indicated that the two most popular locations for free-draining layers were between the base and subgrade (44 percent) and immediately below the pavement surface and above the base material (40 percent).

The aggregate gradations specified for use in free-draining layers by responding agencies exhibited quite a bit of variability. Of all of the gradings received, only two were used by more than one responding agency. It is apparent from reviewing gradation specifications that some are considerably more permeable than others. Figure 2 shows the variability in the degree of openness indicated in the responses. (One state reported using 6 to 3/4 in.). Although the goal may be the same, the approach, at least in terms of gradation, is quite different.

Aggregate properties that relate specifically to the permeability or structural stability, or both, of the free-draining layers were of interest. Although the majority of the responses to the aggregate inquiry related more to various quality characteristics such as Los Angeles abrasion and soundness, the single most popular aggregate property listed was face fracture or crushed particle content. Nine states responded that this particular property was important but individually specified crushed particle percentages ranging from 50 to 100 percent. Although the various quality aspects of a particular aggregate can have a bearing on permeability and stability, the only other specified property that appears to be directly related is the coefficient of uniformity (two states).

Stabilization of the free-draining layer solely by compaction appears to be the most popular construction technique. This category received 16 of 29 responses (55 percent) and the next most popular (41 percent) stabilizing technique used bitumen. Completed questionnaires indicated that an approximate average of 2 percent bitumen was used, but actual responses ranged from 2 to 5 percent. Only one response indicated that portland cement was used as a stabilizer and that state reported that they used 282 lb/yd^3 and a 0.37 water-to-cement ratio. Eighty-five percent of all responses indicated that the choice of stabilizer was not optional.

For any free-draining system to be effective, one of the primary requirements is that the free-draining layer be highly permeable. Questionnaire responses concerning permeability indicated that some states are doing better than others with this aspect. Three states responded to the lowest permeability category on the questionnaire (100 to 500 ft/day), and four states responded that permeabilities of from 500 to 1,000 ft/day had been achieved. The majority of the responses (six states or 33 percent) was to the 1,000 to 5,000 ft/day category, and five states responded to the "other" category with one of those states indicating that permeabilities of 10,000 ft/day had been achieved.

The responding state agencies reported several ways in which permeability values were derived. According to the questionnaire responses, falling-head and constant-head measurements were the two most popular methods accounting for nearly 29 percent of the responses each. The only other method used by more than one state was the FPTD, an experimental field instrument developed by Moulton of West Virginia University. Two states indicated that they used the FPTD to make permeability measurements, and one of those states indicated that the permeability exceeded the limits of the device.

Questionnaire responses to the inquiry about compaction of the free-draining layer were for the most part ambiguous. Most states answering this question used phrases such as "to the satisfaction of the engineer" or "enough to seat the stone." No matter how it is accomplished, stabilization is important and has to be given consideration. What might be adequate for a free-draining layer in one location in the pavement system might not be satisfactory in another. The base should be compacted so as to not lose its free-draining character or to the point that the aggregate is crushed. Although generalized compaction requirements may suffice, two states specify a certain percentage of the solid volume density.

Varied responses were given about the type of compaction equipment specified. Most detailed responses indicated that steel-wheeled rollers were used. Those rollers appeared to be generally around 8 tons but ranged from as light as 3 tons to as heavy as 20 tons.

Surface tolerance of the free-draining layer can be an important consideration, especially when different phases of the construction process, involving different materials, are subcontracted to separate contractors. Unless specified grade tolerances can be maintained, significant problems with quantities can arise. There were more responses (five states) indicating a

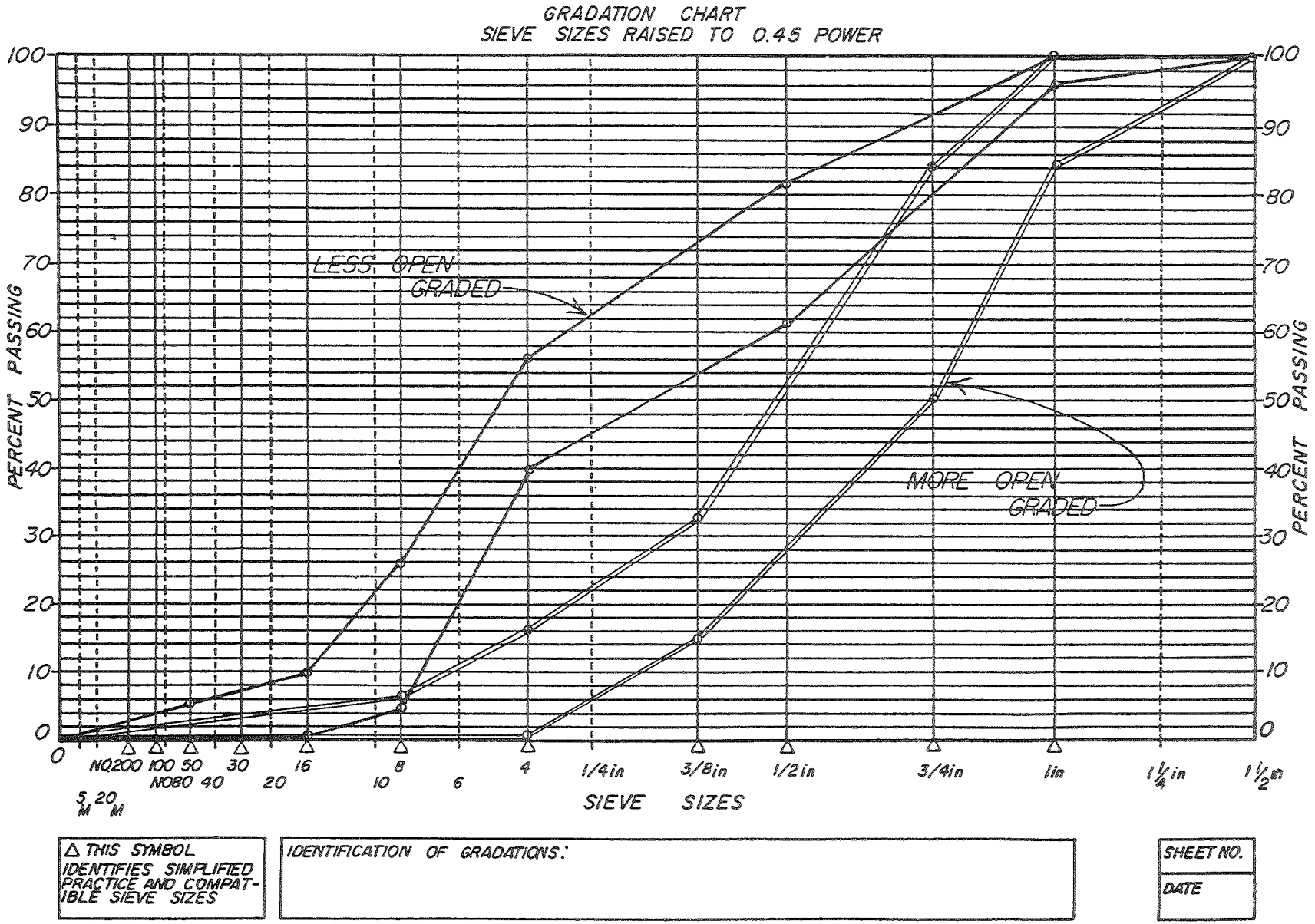

FIGURE 2 Variability in degree of openness indicated in responses.

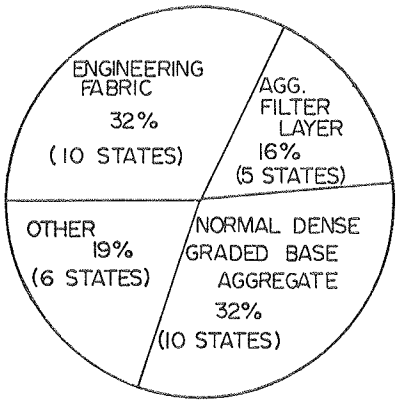

FIGURE 3 Protection of free-draining layer against intrusion of fine particles.

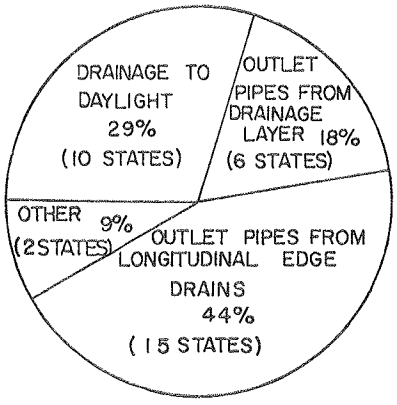

FIGURE 4 Outletting water.

± 0.25-in. tolerance than any other. All other tolerances specified were greater than 1/4 in., and two states allow as much as ± 1.2 in.

The next questionnaire inquiry involved structural determinations and the assigning of structural values to free-draining layers. Forty-seven percent of the responses indicated that a structural value of 0.14 was used for the free-draining layer. No other single value reported was used by more than one state. Those values ranged from 0.08 to 0.80 and, except for a few ambiguous answers, no two states agreed on the method of determining the value assigned.

Protection of the open-graded layer against the intrusion of fine particles is worthy of special consideration if that layer is to function as intended for the normal design life of the pavement. As is evident in Figure 3, as many states are using engineering fabric for this application as consider the normal dense-graded base aggregate sufficient.

Getting the water out of the drainage layer and away from the pavement is critical to satisfactory performance. As shown in Figure 4, there are three basic methods that have been used by the responding states to accomplish this.

The appropriate spacing between outlets is highly dependent on the amount of inflow into the pavement system, which is influenced in part by the amount and duration of rainfall. When the variety of climatic conditions associated with the different regions of the United States is considered, it is not surprising to find a variety of responses to the inquiry about outlet spacing. Three states (17 percent) indicated that spacing intervals of 500 ft were used, and four states (22 percent) indicated that a 300-ft spacing was used. All other responses were unique and ranged from as close as 100 ft to as far as 1,500 ft per outlet.

Ten state agencies or 43 percent of the responses indicated that their outlet spacing is determined by hydraulic design, and six agencies or 26 percent of the respondents used standard (state) specifications. All other responses (seven) were too generalized to be definitive.

Protection of the outlets through which water exits the system is an important consideration. No matter how adequately a free-draining system is designed, if the outlets become restricted or blocked, the effectiveness of the entire system could be eliminated. This could lead to problems even greater than those that free-draining pavements are designed to correct. One of the more effective protective measures would appear to be the construction of concrete headwalls, an approach indicated by 50 percent of the responding state agencies. One of these agencies indicated that they went one step further by including bars, presumably to prohibit animals from nesting within the outlet. One other state used rock backfill around the outlet, and most of the remaining responses had to do with using markers to identify where the outlets were located or using grates or flaps on the outlets.

Because of the physical characteristics of most free-draining pavement layers, a little more care or caution needs to be exercised during construction in order to meet grade tolerances and to keep the material free draining. According to the questionnaire responses, shoving or rutting of the free-draining layer during construction is the single most troublesome problem as indicated by 35 percent of the responses (eight states). The only other problem common to more than one state (three states or 13 percent of responses) has to do with maintaining traffic during construction of the free-draining layer. The remaining 12 states (52 percent of responding agencies) indicated varied individual problems not shared or indicated by any other state. These problems ranged from problems with the overdensification of the material to problems with meeting the grade tolerance of the layer.

SUMMARY

In an effort to prolong pavement life, a significant number of highway agencies across the nation are taking positive steps to provide rapid internal drainage of their pavements through the incorporation of a free-draining layer. Although several states are still experimenting, the majority of the states that have tried the free-draining approach are now using the concept routinely in pavement design.

As is evident from the responses to this questionnaire, there is considerable variability in design of free-draining pavements among the various states. Because of the relative newness of most of the free-drainage projects constructed nationally, a valid overall performance evaluation or assessment may not be possible for a number of years. On the sole basis of performance to date of such pavement systems, however, the overwhelming majority (78 percent) of the respondents rated their systems as either excellent or good.

Publication of this paper sponsored by Committee on Subsurface Drainage.